

ABSTRACT

Title of Document: C-DI-GMP SIGNALLING IN BACTERIA-
NEW OPPORTUNITIES FOR THE
DEVELOPMENT OF ANTI-BIOFILM DRUGS

Jie Zhou, Doctor of Philosophy, 2014

Directed By: Professor Dr. Herman O. Sintim
Department of Chemistry and Biochemistry

Bacterial infections are becoming more difficult to treat, due to the emergence of resistance strains to almost every antibiotic. Most bacteria that infect humans to cause diseases are biofilm forming bacteria and it has been shown that most antibiotics that are in clinical use today are not very effective against bacteria in a biofilm. Despite the difficulty in eradicating bacterial biofilms, there is no anti-biofilm drug in clinical use today. Cyclic diguanylate (c-di-GMP) is a second messenger in bacteria and it that is synthesized in the cytosol, in response to a changing bacterial environment to regulate bacterial physiology. Due to the central role that c-di-GMP plays in bacteria, there are interests in understanding c-di-GMP signaling with the hope that detailed understanding of c-di-GMP signaling would provide avenues to design small molecules that could be used to inhibit bacterial virulence and biofilm formation, which c-di-GMP regulates. We aim to understand the determinants of c-di-GMP binding to receptor proteins and RNA riboswitches, using c-di-GMP analogs. We

designed a concise synthetic strategy to make c-di-GMP and analogs. These analogs were used to study the structure-activity-relationship (SAR) of c-di-GMP. The polymorphisms of the synthesized analogs were studied using a panel of spectroscopic techniques. It was discovered that one analog of c-di-GMP, namely 2'-F-c-di-GMP, which had a high propensity to exist in the closed conformation could potentially inhibit c-di-GMP synthesis by c-di-GMP synthases. Since c-di-GMP promotes biofilm formation in bacteria, these analogs represent good starting points to design anti-biofilm agents to treat persistent bacterial infections.

C-di-AMP was recently discovered as another important bacterial signaling molecule and it is mostly found in Gram-positive bacteria. C-di-AMP controls many processes in bacteria, including growth, cell wall synthesis, ion transport, and sporulation. Many of the receptor or effector proteins that mediate c-di-AMP signaling remain to be characterized and there is lack of knowledge regarding how environmental factors regulate c-di-AMP metabolism. We developed a new fluorescent probe for the “real-time” detection of c-di-AMP. This assay could be used to find inhibitors of c-di-AMP signaling as well as studying the enzymatic proficiencies of c-di-AMP metabolism proteins.

C-DI-GMP SIGNALLING IN BACTERIA-NEW OPPORTUNITIES FOR THE
DEVELOPMENT OF ANTI-BIOFILM DRUGS

By

Jie Zhou

Dissertation submitted to the Faculty of the Graduate School of the
University of Maryland, College Park, in partial fulfillment
of the requirements for the degree of
Doctor of Philosophy
2014

Advisory Committee:
Associate Professor Herman O. Sintim, Chair
Professor Jeffery Davis
Adjunct Professor Steven Rokita
Professor Lyle Isaacs
Professor Wade C. Winkler

© Copyright by
Jie Zhou
2014

Dedication

To mom, dad, grandparents and Hao Tang

Acknowledgements

Firstly, I would like to express my deepest appreciation to my dissertation advisor, Dr. Herman Sintim, not only for teaching, but also providing numerous helpful directions, pieces of advice (regarding both research and career choices) and encouragement during the past four and half years. I would also like to thank Prof. Jeffery Davis for helpful suggestions for my research and my career development. I also thank my dissertation committee members Prof. Steven Rokita, Prof. Lyle Isaacs and Dr. Wade Winkler for helpful discussions and suggestions.

I would like to thank Dr. Vincent Lee and his student, Ms. Sarah Watt, for help with the expression of WspR, RocR and Alg44 and also help with the determination of half maximal inhibitory concentration (IC_{50}) of my compounds against these proteins, which are discussed in Chapter 2 of this thesis.

I would also like to thank Dr. Nicole LaRonde, for training and allowing me to do radiolabeling experiments in her laboratory.

I also owe much gratitude to Mr. David Sayre, a very talented undergraduate who worked with me on the synthesis, purification and fluorescence studies of c-di-GMP and c-di-AMP analogs used in chapters 2, 3 and 4.

I would like to thank my old colleagues, Dr. Jingxin Wang, for carefully training me to synthesize c-di-GMP and analogs; Dr. Shizuka Nakayama, for training me to

operate UV, fluorometer, circular dichroism spectrophotometers, HPLC instrument and DNA/RNA synthesizer. I also thank Dr. Yiling Luo for making RNA for me and training me to do equilibrium microdialysis experiments. I also thank Dr. Dayie, a collaborator of Dr. Sintim and also a co-advisor of Dr. Luo for his intellectual input regarding experiments related to RNA and the wonderful collaborative papers that I have published with him.

I am grateful to my colleague and best friend, Ms. Yue Zheng, for making proteins, DisA and YybT used for the c-di-AMP detection project and for training me, with much patience, to do bacterial cell culture, protein purification and biofilm culture.

I also would like to thank my colleagues, Mr. Benjamin Roembke, Ms. Lauretee Bernard and Dr. Marialuisa Micco, for helping me with the preparation and HPLC purifications of c-di-GMP analogs.

I would like to thank Mr. Min Guo for training me to operate mass spectrometer and always helping me with synthesis obstacles I encountered.

I am also very grateful for the help of Dr. Yiu-fai Lam, Dr. Yinde Wang and Dr. Daoning Zhang for the helpful discussions on NMR. I would like to thank Dr. Yue Li for his help in mass spectrometry.

Last but not least, I thank the National Science Foundation (CHE 0746446 and CHE 1307218), American Heart Association (11PRE7890040) and University of Maryland Graduate Dean's Dissertation Fellowship for the generous financial support.

Table of Contents

Dedication	ii
Acknowledgements	iii
Table of Contents	vi
List of Tables	viii
List of Figures	ix
List of Schemes	xiii
List of Abbreviations	xiv
Chapter 1. C-di-GMP and c-di-AMP Signaling in Bacteria.....	1
1.1 Introduction.....	1
1.2 C-di-GMP, a ubiquitous bacterial signaling molecule.....	4
1.2.1 Diguanylate cyclases.....	6
1.2.2 Phosphodiesterases	7
1.2.3 C-di-GMP binding to effector proteins.....	10
1.2.4 Detection of c-di-GMP	14
1.2.5 Inhibitors of c-di-GMP receptors.....	17
1.2.6 Polymorphism of c-di-GMP	20
1.3 C-di-AMP, another ubiquitous and important signaling molecule.....	23
Chapter 2. Potent suppression of c-di-GMP synthesis via I-site allosteric inhibition of diguanylate cyclases with 2'-F-c-di-GMP	30
2.1 2'-modified analogs of c-di-GMP.....	30
2.1.1 Introduction.....	30
2.1.2 Synthesis of c-di-GMP analogs	33
2.2 Effect of 2'-modification on binding to proteins	42
2.2.1 Theoretical analysis of c-di-GMP binding proteins.....	42
2.2.2 IC ₅₀ s against c-di-GMP binding proteins and analogs.....	43
2.2.3 2'-F-c-di-GMP is a potent inhibitor of c-di-GMP synthase WspR.....	46
2.3 Conclusion	50
Chapter 3. Binding studies between c-di-GMP analogs and c-di-GMP riboswitch -	54
3.1 Synthesis and polymorphism of endo-S-c-di-GMP analogs.....	54
3.1.1 Introduction.....	54
3.1.2 Synthesis of endo-S-c-di-GMP analogs.....	55

3.1.3 Polymorphism of endo-S-c-di-GMP analogs.....	56
3.2 Binding Studies between endo-S-c-di-GMP analogs and Class I riboswitch...	65
3.3 Conclusion	69
Chapter 4. Unexpected Complex Formation between Coralyne and Cyclic Diadenosine Monophosphate Providing a Simple Fluorescent Turn-on Assay to Detect This Bacterial Second Messenger	72
4.1 A simple and selective detection of c-di-AMP by coralyne	72
4.1.1 Introduction.....	72
4.1.2 The quenching study of coralyne by halide ion.....	75
4.1.3 The complex formation between coralyne and c-di-AMP.....	84
4.1.4 The biological application of coralyne assay.....	92
4.1.5 Conclusion	95
4.2 Synthesis of c-di-AMP.....	97
Chapter 5. Conclusion and Future Directions	101
Chapter 6. Experimental Section	106
6.1 General procedure.....	106
6.1.1 General reaction conditions	106
6.1.2 Preparation of dry solvents	106
6.1.3 Reagents.....	106
6.1.4 Instruments.....	107
6.2 Synthetic protocols for compounds in Chapter 2-4	110
6.2.1 Synthesis of 2'-modified c-di-GMP analogs in Chapter 2.....	110
6.2.2 Synthesis of endo-S-c-di-GMP analogs in Chapter 3	112
6.2.3 Synthesis of c-di-AMP in Chapter 4.....	112
6.3 Computational data.....	114
6.4 Biophysical data.....	115
6.4.1 Sample preparation for spectrometric and optical measurements in Chapter 2.....	115
6.4.2 Sample preparation for spectrometric and optical measurements in Chapter 3.....	115
6.4.3 Sample preparation for spectrometric and optical measurements in Chapter 4.....	115
6.5 Biological data	117
6.5.1 Enzymatic Assay in Chapter 2.....	117
6.5.2 Enzymatic Assay in Chapter 4.....	119
Appendices.....	121

List of Tables

Table 1.1 Summary of small molecules identified as DGC inhibitors.....	18
Table 2.1 Calculations of the radii of c-di-GMP and analogs (2.2 and 2.3) in their different aggregation states.	41
Table 2.2 IC ₅₀ value against protein (WspR, RocR and Alg44) by c-di-GMP and analogs (2.1 to 2.4).....	44
Table 2.3 Sugar pucker ring mode of c-di-GMP and analogs (2.1 to 2.3).....	46
Table 2.4 Effect of c-di-GMP and 2'-F-c-di-GMP on WspR enzyme kinetics.	49
Table 3.1 Computed energy difference between “open” and “closed” forms of c-di-GMP (3.1) and analogs (3.2 to 3.5).	59
Table 4.1 Fluorescence quenching of coralyne with KBr.a ex. 445 nm, em 480/30 nm.	82

List of Figures

Figure 1.1 Examples of biofilms from various bacteria. a) <i>Staphylococcus aureus</i> biofilm on a vascular prosthesis. ⁸ b) <i>Escherichia coli</i> biofilm in the calyx area of an inoculated golden delicious apple. ⁹ c) <i>Pseudomonas aeruginosa</i> strain PA14 biofilm carrying Green fluorescent protein (GFP). ¹⁰	2
Figure 1.2 Structures of c-di-GMP and c-di-AMP, bacterial second messengers.	3
Figure 1.3 Overview of c-di-GMP regulations in bacteria. ¹¹ Reproduced by permission of The Royal Society of Chemistry	5
Figure 1.4 Crystal structure of WspR where c-di-GMP is bound to I-site (PDB code: 3I5A ⁴⁸).	6
Figure 1.5 (a) crystal structure of c-di-GMP PDE YahA (PDB code: 4LJ3 ⁵⁹); (b) crystal structure of c-di-GMP PDE TBD 1265 (PDB code: 3N3T ⁵⁸).....	8
Figure 1.6 (a) GMP as hydrolysis product, bound to PmGH; (b) c-di-GMP as substrate, bound to PmGH; (c) surface representation of c-di-GMP bound to PmGH; (d) superposition of the structures of PmGH bound to cyclic di-GMP and GMP (PDB code: 4ME4 ⁵²). Reproduced with permission from John Wiley & Sons Ltd. ⁵²	9
Figure 1.7 Crystal structures of several PilZ domain proteins bound with c-di-GMP and c-di-GMP modulation modes. (a) Crystal structure of PA4608 (PDB code: 2L74 ⁷⁷); (b) crystal structure of VCA0042 (PDB code: 2RDE ⁷⁶); (c) crystal structure of PP4397 (PDB code: 3KYF ⁷⁵); (d) Different modulation modes in changes in conformation or aggregation of PilZ domain proteins when bound to c-di-GMP; YcgR-N domain is in blue color and PilZ domain is in green color. Reproduced by permission of The Royal Society of Chemistry. ¹¹	11
Figure 1.8 FleQ binds to c-di-GMP to inhibit the flagella gene expression. Reproduced by permission of The Royal Society of Chemistry. ¹¹	13
Figure 1.9 (a) Colorimetric and (b) fluorescent detection of c-di-GMP utilizing aggregation strategy. Reproduced by permission of The Royal Society of Chemistry. ¹¹	15
Figure 1.10 Nanomolar detection of c-di-GMP using an aptamer tethered to a Spinach RNA.	17

Figure 1.11 Structures of small molecules identified as DGC inhibitors. ⁸⁷⁻⁹³	18
Figure 1.12 Proposed model of polymorphism of c-di-GMP in presence of cations or intercalators. Reproduced by permission of The Royal Society of Chemistry. ¹¹	21
Figure 1.13 Structure of endo-S-c-di-GMP.	22
Figure 1.14 Overview of c-di-AMP functions in bacteria.	23
Figure 1.15 Schematic illustration of detection of c-di-AMP by coralyne assay. Reprinted with permission from ref 105. Copyright (2014) American Chemical Society.....	24
Figure 2.1 2'-modified analogs of c-di-GMP designed and synthesized.....	33
Figure 2.2 HPLC chromatography of c-di-GMP analogs (2.2 and 2.3).....	35
Figure 2.3 ¹ HNMR stacked spectra of 3.0 mM analog 2.2 in D ₂ O.....	38
Figure 2.4 ¹ HNMR stacked spectra of 3.0 mM analog 2.3 in D ₂ O.....	39
Figure 2.5 C-di-GMP is shown in sticks and colored by atom (oxygen in red, nitrogen in blue, carbon in green and phosphorus in orange); amino acid residues are shown in blue sticks. a) dimeric c-di-GMP bound to WspR (DGC domain; PDB code 3I5C). b) Monomeric c-di-GMP bound to LapD (EAL domain; PDB code 3PJT). c) Dimeric c-di-GMP bound to PP4397 (PilZdomain; PDB code 3KYF). d) Monomeric c-di-GMP bound to VCA0042 (PilZ domain; PDB code 2RDE).....	42
Figure 2.6 a) and b) Inhibition of c-di-GMP synthesis by WspR and PA1107 with guanine-containing nucleotides. c) and d) Inhibition of c-di-GMP hydrolysis by RocR and PvrR with guanine-containing nucleotides. Measurements were done in triplicate.	47
Figure 2.7 Inhibition of c-di-GMP synthesis by different concentrations of c-di-GMP or 2'-F-c-di-GMP. Measurements were done in triplicate.....	48
Figure 3.1 Family of dual-modified c-di-GMP analogs (endo-S-c-di-GMP analogs) synthesized.....	55
Figure 3.2 ¹ HNMR stacked spectra of 3.0 mM analog 3.3 in D ₂ O.....	62
Figure 3.3 ¹ HNMR stacked spectra of 3.0 mM analog 3.4 in D ₂ O.....	63
Figure 3.4 ¹ HNMR stacked spectra of 3.0 mM analog 3.5 in D ₂ O.....	64
Figure 3.5 Co-crystal structure of c-di-GMP bound to Vc2 RNA (PDB code: 3IRW). C-di-GMP is shown in sticks and colored by atom (oxygen in red, nitrogen in blue,	

carbon in green and phosphorus in orange). Vc2 RNA is shown as surface and colored by atom (oxygen in red, nitrogen in blue and carbon in yellow).	66
Figure 3.6 C-di-GMP fluorescent riboswitch.	67
Figure 3.7 Fluorescent c-di-GMP sensor screening for c-di-GMP and analogs (3.2 to 3.5).	68
Figure 4.1 Structures of c-di-AMP, c-di-GMP, pApA and coralyne.	75
Figure 4.2 Fluorescence (a) and UV (b) profiles of coralyne in the presence of various nucleotides.....	77
Figure 4.3 The fold fluorescence of coralyne in the presence of c-di-AMP. In the absence of a halogen quencher the unbound coralyne is also fluorescent and therefore changes in fluorescence intensity in the presence of different concentrations of c-di-AMP are not large. For example, the fluorescence fold changes for 10 μ M c-di-AMP and 20 μ M c-di-AMP or 20 μ M and 40 μ M are almost similar. The addition of bromide or iodide improves the discrimination between different c-di-AMP concentrations (see Figure 4.10).	78
Figure 4.4 (a) KBr quenching of coralyne in 50 mM Tris-H ₃ PO ₄ Buffer (pH 7.5) at 25 °C. The squares show the values of relative intensity and circles of lifetimes. (b) Modified Stern-Volmer plot for quenching of Coralyne with KBr.	80
Figure 4.5 KBr quenching of coralyne in presence of 40 μ M of c-d-AMP at 25 °C. Buffer: 50 mM Tris-H ₃ PO ₄ (pH 7.5). Squares are intensity and circles are lifetime data.	81
Figure 4.6 KI quenching of coralyne fluorescence in absence (a) and presence of 40 μ M c-d-AMP (b) at 25 °C.	84
Figure 4.7 KI quenching in the absence of c-di-AMP or in the presence of c-di-AMP at 60 °C.....	85
Figure 4.8 KI quenching in the absence of c-di-AMP or in the presence of c-di-AMP at 10 °C.....	86
Figure 4.9 Fold fluorescence profiles of coralyne in the presence of c-di-AMP at different pHs.	87
Figure 4.10 The fluorescence of coralyne is proportional to the concentration of c-di-AMP.....	87

Figure 4.11 CD of coralyne-c-di-AMP or pApA complex.	89
Figure 4.12 CD of coralyne-c-di-AMP or pApA complex (220-700 nm).	89
Figure 4.13 Job plot of coralyne and c-di-AMP interaction. [coralyne] + [c-di-AMP] was fixed at 50 μ M. The experiment was done in triplicate and plotted together on the graphs.	90
Figure 4.14 Job plot. [coralyne] + [c-di-AMP] was fixed at 50 μ M. The experiment was done in triplicate and plotted together on the graphs.	91
Figure 4.15 ^1H NMR spectra of c-di-AMP with (a) or without (b) coralyne. Addition of coralyne (0.1 equiv.) to c-di-AMP caused complete disappearance of the c-di-AMP peaks in the ^1H NMR spectrum (spectrum a).	92
Figure 4.16 (a) Conversion of ATP into c-di-AMP by DisA. DisA (10 μ M) was added to ATP (100 μ M) in 200 mM Tris-HCl, pH 7.5, 100 mM NaCl and 10 mM MgCl_2 at 30 $^\circ\text{C}$. Reactions were stopped at 1 min, 2 min, 5 min, 7 min, 10 min, 15 min, 20 min and 30 min and incubated with conditions stated in the experimental part. The fluorescence was subsequently measured; (b) Cleavage of c-di-AMP by YybT and SVPD. YybT (10 μ M) in 100 mM Tris-HCl, pH 8.3, 20 mM KCl, 500 μ M MnCl_2 , 1 mM DTT or SVPD (1 mg/mL) in 50 mM Tris-HCl, pH 8.8 and 15 mM MgCl_2 were used to cleave c-di-AMP (100 μ M) at 37 $^\circ\text{C}$. Reactions were stopped at 1 min and 30 min and incubated with conditions stated in the experimental part. Fluorescence measurements were taken after 1 min and 30 min.	94

List of Schemes

Scheme 2.1 Synthesis of compounds 2.2 and 2.3 via solution phase synthesis. Modified conditions of reported synthesis ²² were used: (a) pyridinium trifluoroacetate, H ₂ O, then <i>t</i> -BuNH ₂ . (b) dichloroacetic acid, then quenched with pyridine. (c) compound 2.5 or 2.6 . (d) <i>t</i> -BuOOH. (e) dichloroacetic acid, then quenched with pyridine. (f) 5,5-dimethyl-2-oxo-2-chloro-1,3,2-dioxaphosphinane (DMOCP). (g) I ₂ , H ₂ O, then HPLC purification. (h) 30% NH ₄ OH, then HPLC purification.....	33
Scheme 2.2 Solid-phase synthesis strategy of c-di-GMP and/or analogs.	34
Scheme 3.1 Synthesis of endo-S-c-di-GMP analogs (3.3 to 3.5). <i>Reagents and conditions</i> : a) programmed DNA synthesizer; b) methyltriphenoxyphosphonium iodide, 2,6-lutidine, anhydrous DMF, rt, 1h; c) 30% NH ₄ OH, 40 °C, 12h.	56
Scheme 4.1 Synthesis scheme of c-di-AMP.....	97
Scheme 5.1 Proposed “caging” strategy on c-di-GMP or 2'-F-c-di-GMP.....	103

List of Abbreviations

BBI	broadband inverse
cAMP	cyclic adenosine monophosphate
CD	circular dichroism
C-di-AMP	cyclic diadenosine monophosphate
C-di-GMP	cyclic diguanylate monophosphate
COSY	correlation spectroscopy
CPG	controlled-pore glass
DAC	diadenyl cyclase
DFHBI	3,5-difluoro-4-hydroxybenzylidene imidazolinone
DGC	diguanylate cyclase
DMF	dimethylformamide
DMOCP	5,5-Dimethyl-2-oxo-2-chloro-1,3,2-dioxaphosphinane
DMT	dimethoxyltrityl
DNA	deoxyribonucleic acid
DOSY	diffusion ordered spectroscopy
ETT	5-ethylthio-1H-tetrazole
FLIM	fluorescence lifetime imaging microscope
GTP	guanosine triphosphate
HPLC	high-performance liquid chromatography
IC ₅₀	half maximal inhibitory concentration
I-site	inhibitory site
MS	mass spectrometry

MSNT	1-mesitylenesulfonyl-3-nitro-1, 2, 4-triazole
NMR	nuclear magnetic resonance
PDB	protein databank
PDE	phosphodiesterase
PEI	polyethylenimine-modified
pApA	5'-phosphoguanylyl-(3'-5')-adenosine
pGpG	5'-phosphoguanylyl-(3'-5')-guanosine
RNA	ribonucleic acid
SAR	structure-activity relationship
SVPD	snake venom phosphodiesterase
TBS	tert-butyldimethylsilyl
TEA	triethylammonium
TEAA	triethylammonium acetate
TLC	thin Layer Chromatography
UV	ultraviolet
WHO	World Health Organization

Chapter 1. C-di-GMP and c-di-AMP Signaling in Bacteria

1.1 Introduction

According to the report from World Health Organization (WHO), 80% of human bacterial infections are caused by biofilm-forming bacteria such as *Pseudomonas aeruginosa*, *Staphylococcus aureus* and *Escherichia coli*.¹ Biofilm is a microbial derived sessile community characterized by cells that are attached to a substratum or interface or to each other, are embedded in a matrix of extracellular polymeric substances that they have produced, (see **Figure 1.1** for examples of biofilm) and exhibit an altered phenotype with respect to growth rate and gene transcription.² Biofilms are difficult to diagnose and are resistant to antibiotic treatment.³ It is believed that the physical barrier provided by the extracellular biofilm matrix partially accounts for the enhanced survival in the biofilm environment.^{1,4-7}

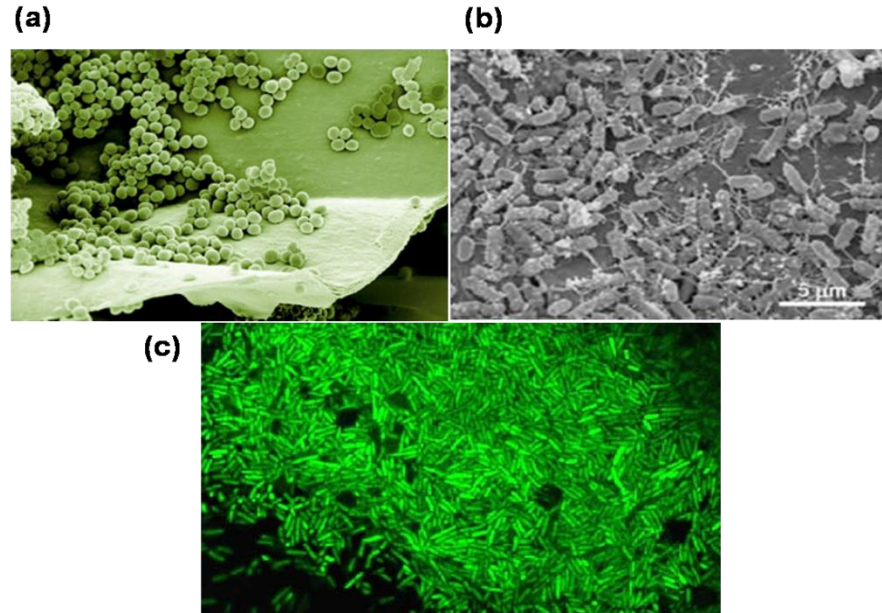


Figure 1.1 Examples of biofilms from various bacteria. a) *Staphylococcus aureus* biofilm on a vascular prosthesis.⁸ b) *Escherichia coli* biofilm in the calyx area of an inoculated golden delicious apple.⁹ c) *Pseudomonas aeruginosa* strain PA14 biofilm carrying Green fluorescent protein (GFP).¹⁰

In bacteria, the cyclic dinucleotides, c-di-GMP and c-di-AMP (see **Figure 1.2** for structures), have emerged as important second messengers involved in the regulation of processes that regulate virulence factor production or biofilm formation.^{1,11} Understanding how bacteria integrate signals from various environmental factors to regulate the metabolism of various dinucleotide second messengers, which control several key processes required for adaptation is key for efforts to develop agents to curb bacterial infections.

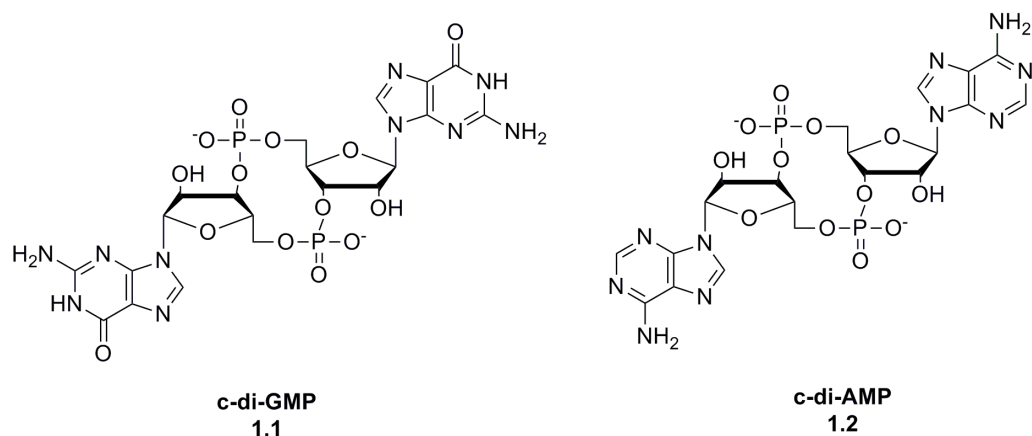


Figure 1.2 Structures of c-di-GMP and c-di-AMP, bacterial second messengers.

In general, scientists would like to control the intracellular concentrations of second messengers in order to prevent/disperse biofilm formation.¹ Common approaches that could be used to perturb second messengers signaling pathways involve, inhibiting the synthesis of second messengers by suppressing the synthases and/or stimulating the hydrolysis of c-di-NMP via the activation of phosphodiesterases,¹²⁻¹⁴ inhibiting receptors that bind to c-di-G(A)MP, called c-di-G(A)MP effectors, using small molecules¹⁵⁻¹⁸ or sequestration of the receptors with designed macromolecules^{19,20}. The Sintim group has suggested that the sequestration of c-di-G(A)MP with small molecules via supramolecular aggregate formation could also be a viable approach to inhibit c-di-G(A)MP signaling.^{21,22} Last but not least, others have also shown that small diffusible signals, such as NO, can perturb c-di-G(A)MP concentrations and therefore small molecules that release NO and related signals could be used to disperse bacterial biofilms.²³⁻²⁵

1.2 C-di-GMP, a ubiquitous bacterial signaling molecule

C-di-GMP was first discovered by Benziman and co-workers more than two decades ago.²⁶ C-di-GMP was discovered in *Acetobacter xylinum*²⁷⁻²⁹ and it is now appreciated that c-di-GMP affects many processes in other bacteria, including the synthesis of biopolymers that are components of bacterial biofilms^{29,30} and the expression of virulence-associated genes.^{31,32} Because c-di-GMP plays a central role in bacteria, there are interests in understanding c-di-GMP signaling with the hope that detailed understanding of c-di-GMP signaling would provide avenues to design small molecules that could be used to inhibit bacterial virulence and biofilm formation, which c-di-GMP regulates.¹¹ C-di-GMP binding proteins (effectors), such as PilZ domain proteins³³, transcriptional factors, such as VpsT³⁴, FleQ³⁵ and c-di-GMP riboswitches^{36,37}, which are involved in the regulation of bacterial biofilms and virulence have been characterized (see Figure 1.3 for a overview of c-di-GMP regulations).^{11,38}

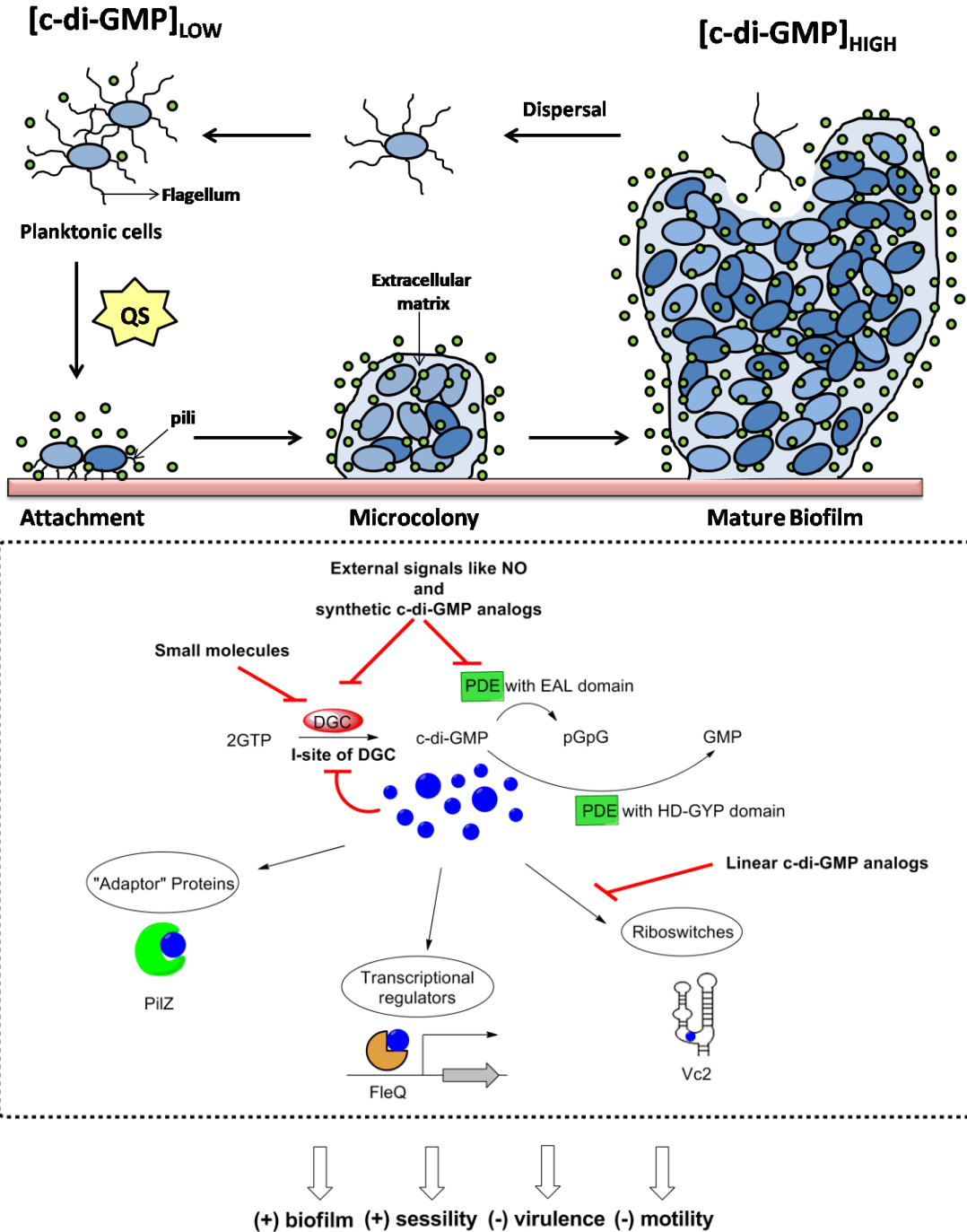


Figure 1.3 Overview of c-di-GMP regulations in bacteria.¹¹ Reproduced by permission of The Royal Society of Chemistry

1.2.1 Diguanylate cyclases

C-di-GMP is produced from two guanosine triphosphate (GTP) molecules by diguanylate cyclases (DGCs), which contain the common protein domain GGDEF (Gly-Gly-Asp-Glu-Phe) or GGEEF (Gly-Gly-Glu-Glu-Phe).³⁹⁻⁴¹ A DGC with AGDEF domain that is catalytically active has also been demonstrated in *Vibrio cholerae*.⁴² DGC proteins often contain an inhibitory site (I-site) with an RxxD motif (x: any amino acid). C-di-GMP synthesis is allosterically inhibited when c-di-GMP is bound to the I-site of some DGCs.⁴³ Examples of DGCs with I-site include WspR from *P. aeruginosa*⁴⁴ (see **Figure 1.4** for a crystal structure of WspR) whereby c-di-GMP is bound to both the active site (A-site) and allosteric site (I-site), PleD from *Caulobacter crescentus*⁴⁵ and DgcA from *Rhodobacter sphaeroides*⁴⁶. Some DGCs, such as XCC4471GGDEF from *Xanthomonas campestris*, do not possess an I-site and it is unclear how c-di-GMP productions are regulated in such proteins.⁴⁷

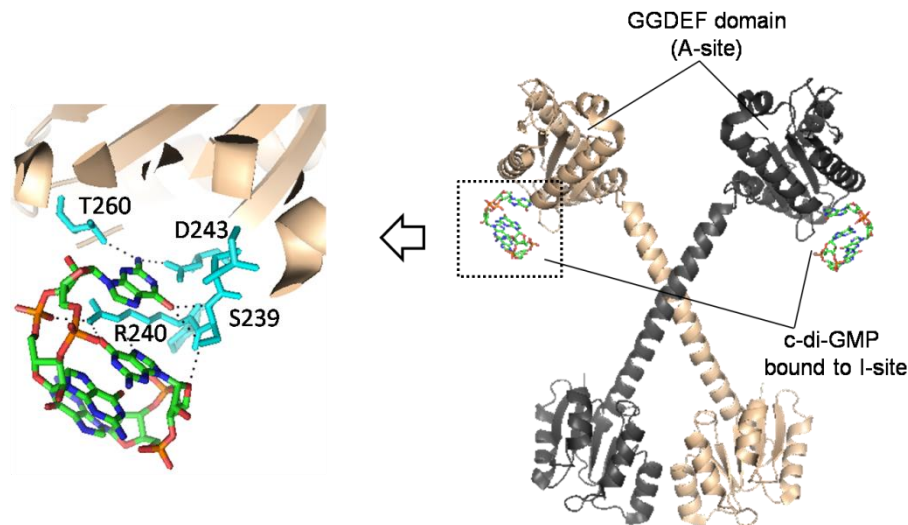


Figure 1.4 Crystal structure of WspR where c-di-GMP is bound to I-site (PDB code: 3I5A⁴⁸).

1.2.2 Phosphodiesterases

C-di-GMP is broken down into 5'-phosphoguanylyl-(3'-5')-guanosine (pGpG) by specific phosphodiesterases (PDEs), characterized with the EAL domain.⁴⁹ pGpG is then degraded further into GMP by phosphodiesterases⁴⁹ or nano RNAses⁵⁰. C-di-GMP can also be cleaved directly into GMP by PDE with HD-GYP domain.^{51,52}

PDEs containing the EAL domain^{44,53,54} use either Mg^{2+} or Mn^{2+} for catalysis^{55,56} and these enzymes are inhibited by Ca^{2+} , Ni^{2+} , Fe^{2+} and Zn^{2+} .^{49,53,57} Although several crystal structures of PDE enzymes have now been solved (see **Figure 1.5** for a few examples),^{58,59} the cleavage mechanisms of EAL containing PDEs have not been fully elucidated because crystal structures only give static pictures. HD-GYP-containing PDEs have proven difficult to crystallize and hence there is a paucity of high resolution HD-GYP PDE crystal structures.^{60,61} The crystal structure of a catalytically inactive HD-GYP containing PDE, BD1817 from *Bdellovibrio bacteriovorus*, has been solved.^{60,61} In this structure, a binuclear Fe^{2+} or Mn^{2+} center is found in the active site.⁶⁰ Recently, the crystal structure of a catalytically active HD-GYP domain protein from *Persephonella marina* (PmGH) was revealed.⁵² Bellini *et al.* demonstrated a novel trinuclear iron arranged in a triangular geometry in the binding site of the HD-GYP domain from *P. marina* with a single and “closed” form of c-di-GMP. C-di-GMP interacts with the central Fe ion in PmGH via one of the exocyclic phosphate oxygens. The other exocyclic phosphate oxygen is involved in hydrogen bonding with a tyrosine residue. The c-di-GMP nucleobase also makes key interactions with lysine and arginine residues (see **Figure 1.6**). Interestingly, the replacement of G, Y and P residues by alanine in PmGH did not affect the catalytic

proficiency of the enzyme and so it is unclear if these residues play any role during catalysis.^{52,61} It would have been instructive if the authors of the PmGH paper had investigated the selectivity of the PmGH mutants with other cyclic dinucleotides, such as c-di-AMP to find out if the GYP motif served as a selectivity motif.

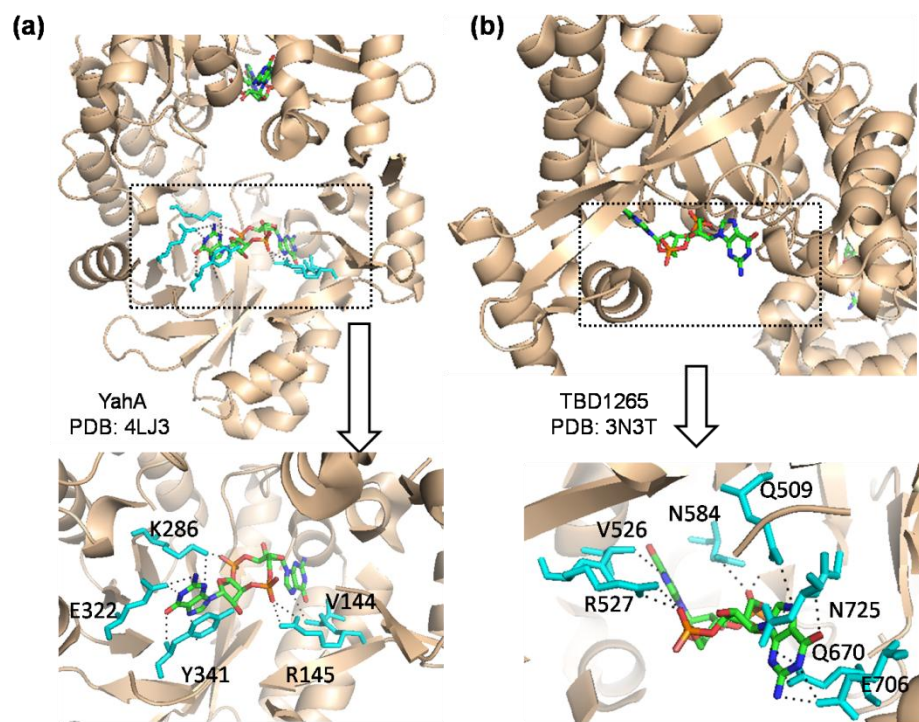


Figure 1.5 (a) crystal structure of c-di-GMP PDE YahA (PDB code: 4LJ3⁵⁹); (b) crystal structure of c-di-GMP PDE TBD 1265 (PDB code: 3N3T⁵⁸).

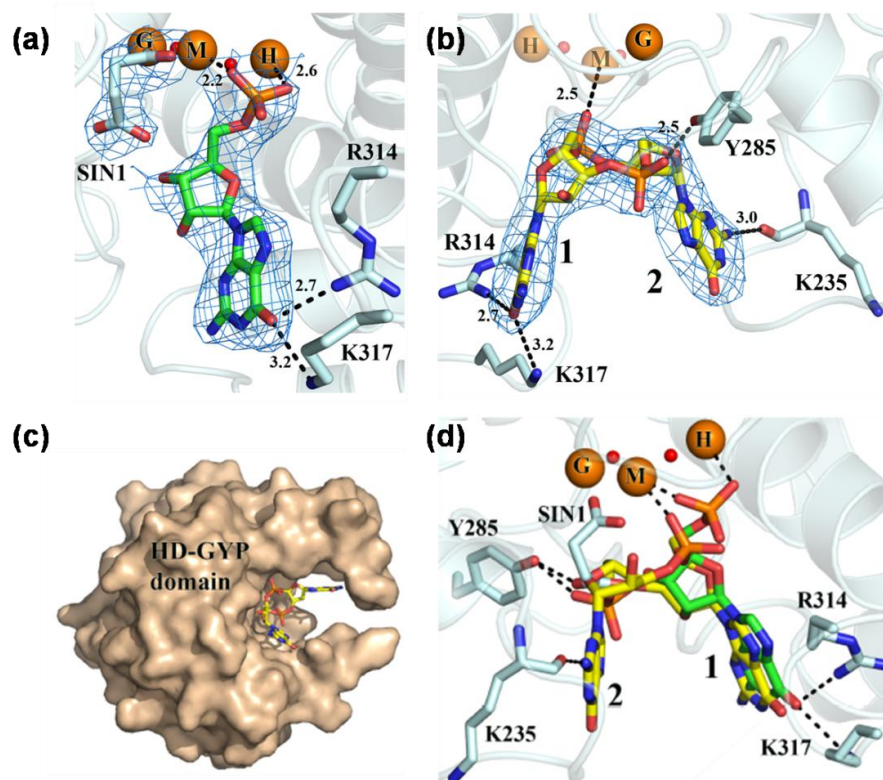


Figure 1.6 (a) GMP as hydrolysis product, bound to PmGH; (b) c-di-GMP as substrate, bound to PmGH; (c) surface representation of c-di-GMP bound to PmGH; (d) superposition of the structures of PmGH bound to cyclic di-GMP and GMP (PDB code: 4ME4⁵²). Reproduced with permission from John Wiley & Sons Ltd.⁵²

The activity of some c-di-GMP phosphodiesterases can be modulated by environmental factors.^{55,62,63} For example, Jenal has shown that the PDE CC3396, characterized with GGDEF-EAL domain, can be regulated by GTP. When the concentration of GTP is elevated, an allosteric site in CC3396 becomes occupied with GTP and further activates the EAL domain for phosphodiesterase activity.⁵⁵

1.2.3 C-di-GMP binding to effector proteins

As a second messenger, the major function of c-di-GMP is to relay signals by binding to different receptors in order to regulate functions like biofilm formation.^{1,11} C-di-GMP receptors can be categorized^{11,64} into four groups: a) PilZ domain proteins, which was the first c-di-GMP receptor protein identified and later proved to exist in various bacterial species^{32,65,66}; b) I-site on DGCs^{67,68} or inactive PDEs with EAL^{44,69} or HY-GDP⁵⁴ domain or proteins with degenerate GGDEF-EAL domain^{34,67,68,70,71}; c) transcription factors like FleQ, VpsT and Clp, which binds c-di-GMP binds and affect gene expression^{35,72,73} and d) riboswitches, which regulate transcription⁷⁴ or translation^{36,37} upon binding to c-di-GMP.

PilZ domain protein was first identified in *P. aeruginosa* as a protein that regulates pilus formation.³³ Several crystal structures of PilZ domain proteins (VCA004280, PP439781 and PA460882) have now been carefully examined to demonstrate different binding modes between c-di-GMP and the PilZ domains (**Figure 1.7a-c**). PP4397, a prototypical PilZ domain protein undergoes a dimeric to monomeric transition upon binding to c-di-GMP (**Figure 1.7d(i)**).⁷⁵ In another PilZ domain protein, VCA0042, the binding of c-di-GMP causes protein conformational change. (**Figure 1.7d(ii)**)⁷⁶ When c-di-GMP binds to PA4608, a PilZ domain protein found in *P. aeruginosa*, the protein undergoes a conformational change, leading to charge partition on the surface of the protein. Hence, the protein's surface becomes negatively charged and presumably interacts with positively charged downstream signaling proteins (**Figure 1.7d(iii)**).⁷⁷

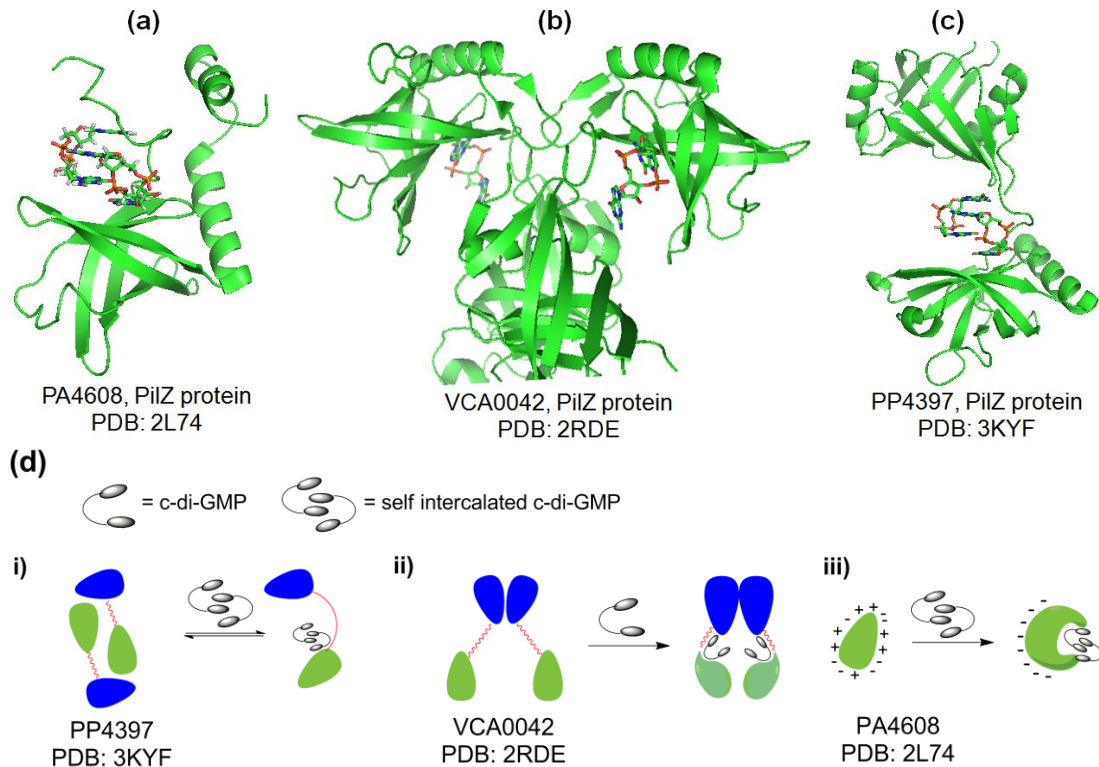


Figure 1.7 Crystal structures of several PilZ domain proteins bound with c-di-GMP and c-di-GMP modulation modes. (a) Crystal structure of PA4608 (PDB code: 2L74⁷⁷); (b) crystal structure of VCA0042 (PDB code: 2RDE⁷⁶); (c) crystal structure of PP4397 (PDB code: 3KYF⁷⁵); (d) Different modulation modes in changes in conformation or aggregation of PilZ domain proteins when bound to c-di-GMP; YcgR-N domain is in blue color and PilZ domain is in green color. Reproduced by permission of The Royal Society of Chemistry.¹¹

FimX is one of the typical examples of c-di-GMP receptors with degenerate GGDEF-EAL domains, controlling twitching motility as identified in *P. aeruginosa*.⁴⁴ Although FimX contains PDE (EAL) and DGC (GGDEF) domains, it can neither synthesize nor hydrolyze c-di-GMP but yet it binds c-di-GMP with high affinity ($K_d=104.2$ nM).⁴⁴

Recently, He and co-workers characterized a new FimX type protein, called Filp in *Xanthomonas oryzae* pv. *oryzae* (Xoo), commonly found as bacteria in rice. They also showed that this new FimX family protein interacted with a PilZ-domain protein PXO_02715 from the same bacteria.⁷¹

The third type of c-di-GMP receptors are transcription factors, which activate the expression of downstream genes in response to environmental triggers. FleQ was the first characterized c-di-GMP transcriptional regulator found in *P. aeruginosa*.³⁵ FleQ was shown to activate flagella gene expression in the absence of c-di-GMP. Upon binding to c-di-GMP, FleQ no longer activates flagella genes.⁷⁸ Recently, Harwood demonstrated that c-di-GMP also inhibited the ATPase activity of c-di-GMP (see **Figure 1.8**).⁷⁹ However, more work is needed to clarify the link between the ATPase activity of FleQ and bacterial physiology.

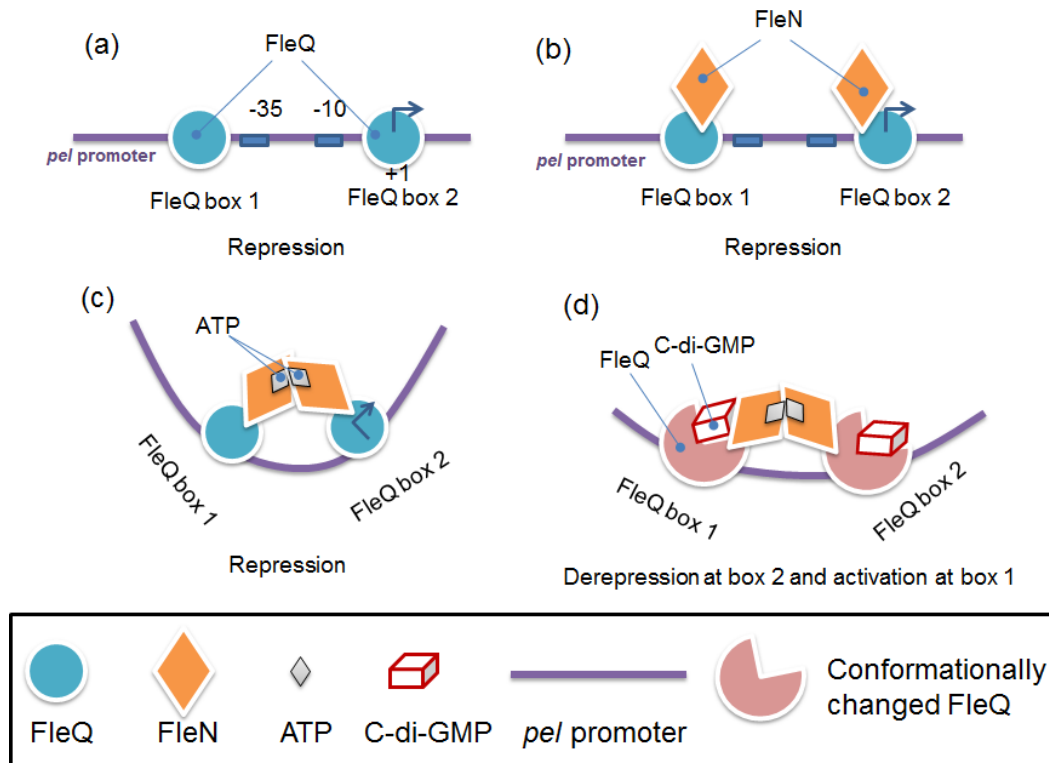
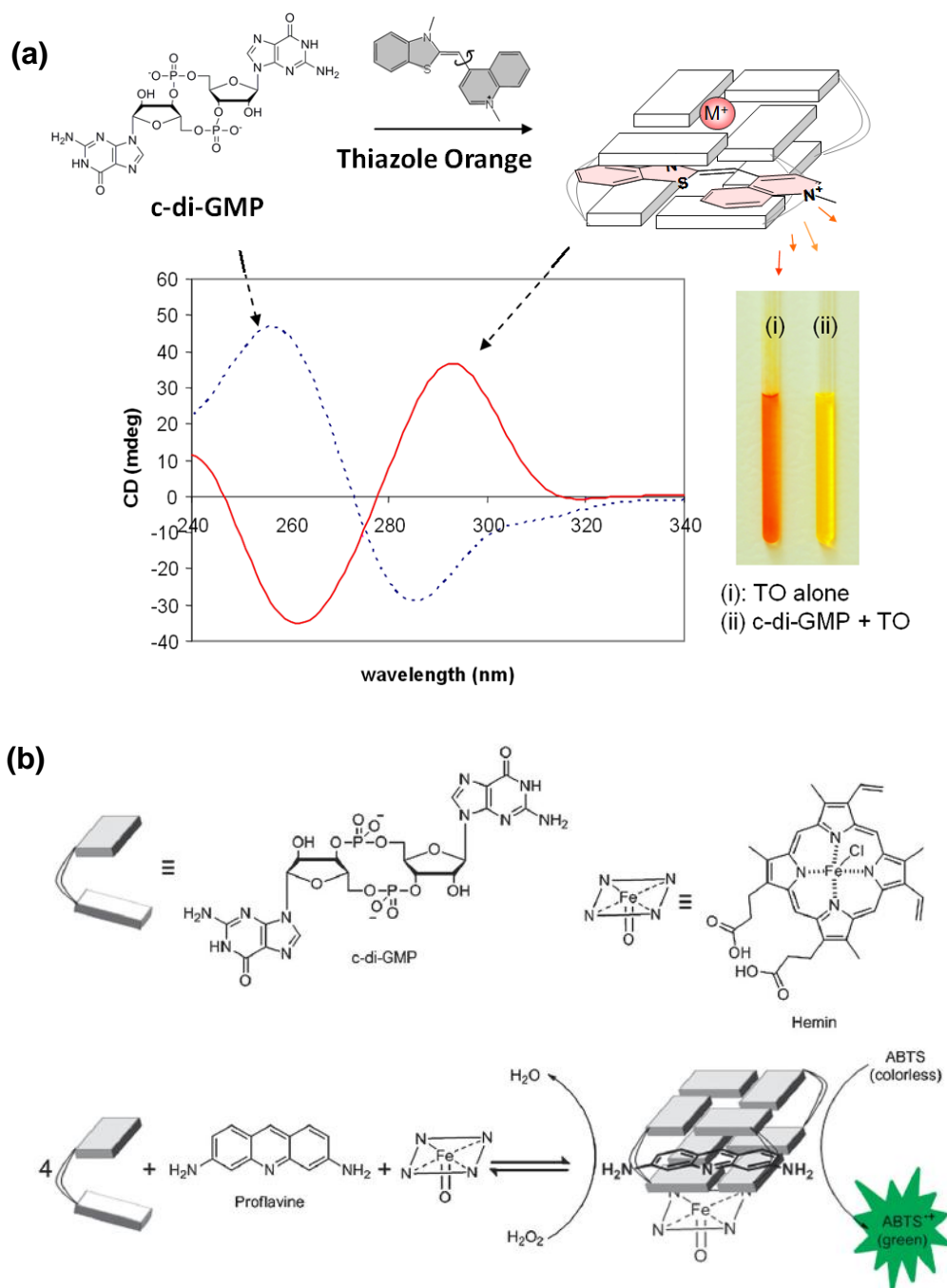


Figure 1.8 FleQ binds to c-di-GMP to inhibit the flagella gene expression. Reproduced by permission of The Royal Society of Chemistry.¹¹

Apart from proteins, c-di-GMP also binds to RNA structures called riboswitches.^{36,80,81} Riboswitches are RNAs aptamer domains that bind with small molecule ligands to control downstream signals. There have been over 20 different riboswitch classes reported for specific binding with amino acids, nucleobases, sugars, vitamins and coenzymes.⁸¹ However, there are only two different classes of c-di-GMP riboswitches reported by Breaker and co-workers.^{36,37}

1.2.4 Detection of c-di-GMP

The ability of small intercalators to aggregate c-di-GMP has been investigated by the Sintim group to provide various detection assays that have the potential to be used in high-throughput screenings to discover inhibitors of c-di-GMP metabolism proteins. For example, c-di-GMP can aggregate into supramolecular structures when thiazole orange (TO) is present.²² TO is entrapped in a cavity (presumably G-quadruplex) created by c-di-GMP, leading to fluorescence enhancement (see **Figure 1.9a**). The entrapment of TO reduces the rotational freedom of this molecule and this accounts for the fluorescence enhancement. In another rendition of c-di-GMP aggregate formation facilitated by intercalators, the Sintim group demonstrated that a G-quadruplex that form from c-di-GMP/proflavine associations can enhance the peroxidation proficiency of hemin, see **Figure 1.9b**.⁸² Sen and co-workers showed in the late 90's that DNA G-quadruplexes can act peroxidase mimics and these are referred as peroxidase DANzymes.⁸³ In analogy to DNAzymes, Sintim et al. referred to a c-di-GMP/proflavine hemin complex as a nucleotidezyme.⁸² The formation of a c-di-GMP nucleotidezyme facilitates a colorimetric detection of c-di-GMP using ABTS and H₂O₂.^{82,84,85}



A sensitive detection of c-di-GMP (nanomolar) using conditioned aptamer strategy has also been disclosed by the Sintim group (see **Figure 1.10**).⁸⁶ In this approach, an aptamer module that binds to the fluorogenic small molecule 3,5-difluoro-4-hydroxybenzylidene imidazolinone (DFHBI), also called Spinach, was fused to a c-di-GMP binding module. Binding of c-di-GMP to its aptamer module facilitated the binding of spinach to its aptamer module, leading to the enhancement of the fluorescence of spinach.⁸⁶

The various detection assays for c-di-GMP are currently being used by the Sintim group to study how environmental factors affect the intracellular concentrations of c-di-GMP in bacteria. Additionally, these assays are being utilized by others to discover inhibitors of c-di-GMP metabolism proteins.⁸⁷

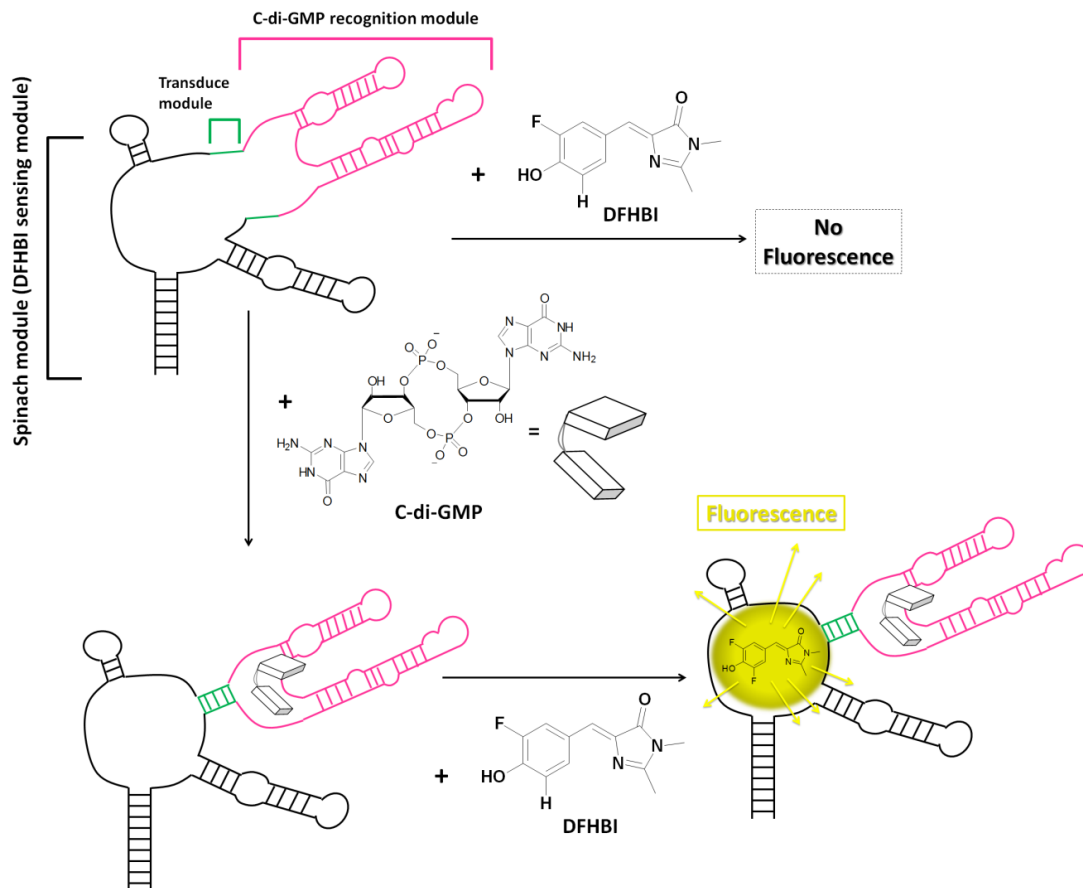


Figure 1.10 Nanomolar detection of c-di-GMP using an aptamer tethered to a Spinach RNA.

1.2.5 Inhibitors of c-di-GMP receptors

C-di-GMP is crucial in biofilms formation and hence there have been efforts to develop/discover small molecules that inhibit c-di-GMP signaling. So far, efforts have mainly been focused on the inhibition of c-di-GMP synthase DGC (see **Figure 1.11** and **Table 1.1**).⁸⁷⁻⁹³

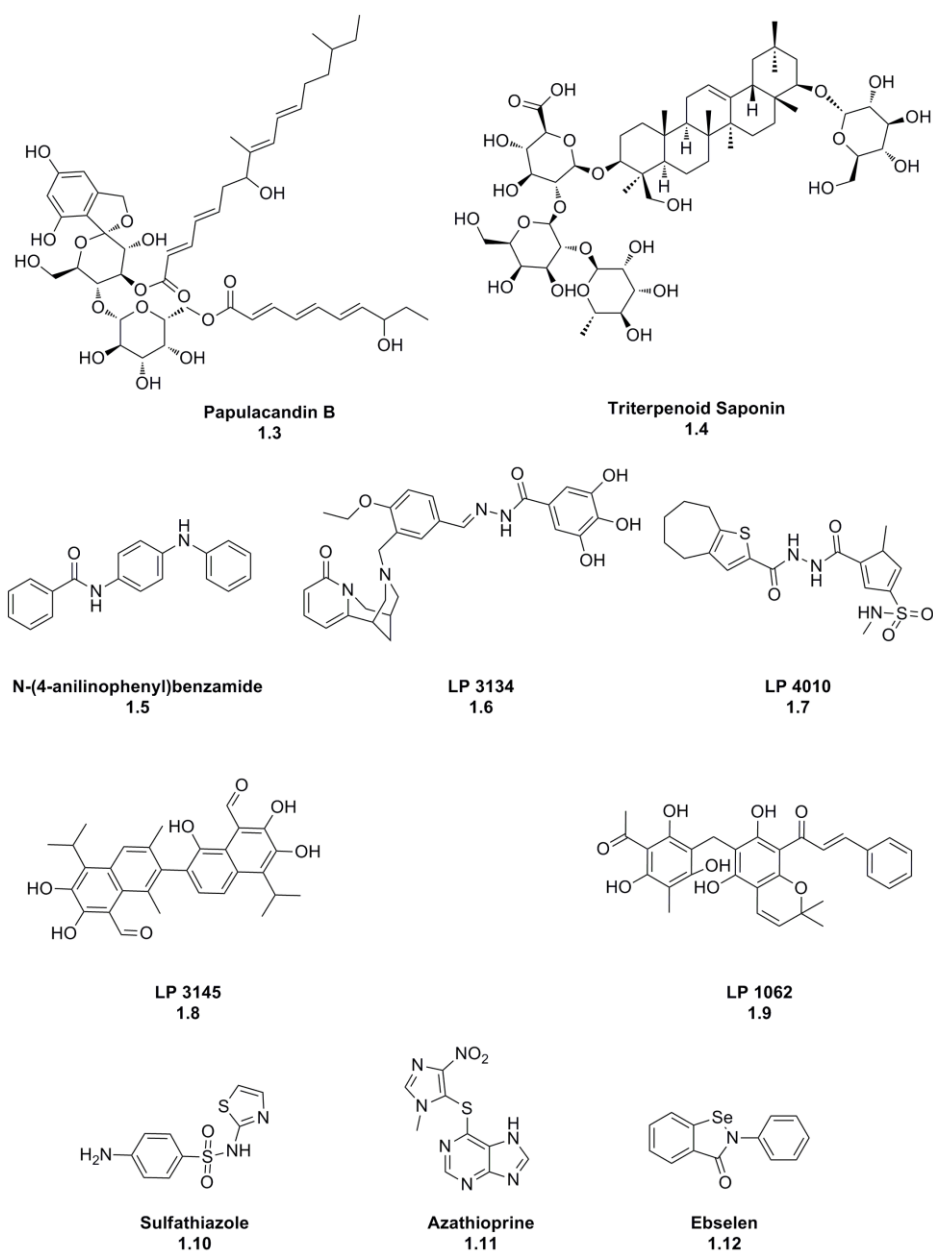


Figure 1.11 Structures of small molecules identified as DGC inhibitors.⁸⁷⁻⁹³

Table 1.1 Summary of small molecules identified as DGC inhibitors.

<i>Inhibitors</i>	<i>Functions</i>	<i>IC₅₀ or K_i[*]</i> <i>(μM)</i>	<i>Ref</i>
c-di-GMP (1.1)	Allosterically inhibit c-di-GMP production	48.9/15.42 [*]	16
2'-F-c-di-GMP (Chapter 2, 2.3)	Inhibit DGC (WspR)	11/12.6 [*]	16

Papulacandin B (1.3)	Inhibit DGC (<i>A. xylinum dgc</i>)	70*	88
Glycosidic triterpenoid saponin (GTS) (1.4)	Inhibit DGC (<i>A. xylinum dgc</i>)	5*	89
N-(4-anilinophenyl)benzamide (1.5)	Inhibit DGC (VC2370)	1	90
	Inhibit DGC (WspR)	17.8	90
LP-3134 (1.6)		44.9	91
LP-3145 (1.7)		70.9	91
LP-4010 (1.8)	Inhibit DGC (WspR)	102.4	91
LP-1062 (1.9)		73.1	91
Sulfathiazole (1.10)	Inhibit DGC (WspR)	5.8	92
Azathioprine (1.11)	Inhibit DGC (WspR)	40	93
	Inhibit DGC (YdaM)	270	93
Ebselen (1.12)	Inhibit DGC (WspR)	13.6	87
	Inhibit DGC (PelD)	5	87

In 1998, Benziman and co-workers identified two glycosylated triterpenoid saponins (GTS) as specific inhibitors of diguanylate cyclase in *Acetobacter xylinum*. However, these triterpenoid molecules are relatively large and not drug-like molecules. No antibiofilm studies have been performed with these DGCs inhibitors.^{88,89}

After over two decades, Waters and co-workers reported several small molecules, including N-(4-anilinophenyl)benzamide and LP-3145 as potential DGC inhibitors to prevent biofilm formation in *P. aeruginosa*.^{90,91}

Landini and co-workers also found that sulfathiazole⁹² and azathioprine⁹³ reduced *E. coli* biofilm via the inhibition of DGC (WspR), which leads to a lowering of intracellular c-di-GMP. Of note, azathioprine is used as anti-inflammatory drug in the treatment of Crohn's disease and rheumatoid arthritis. Therefore, its toxicity profile has already been known and could become a safe anti-biofilm drug to use in clinic. Recently, Lee and co-workers reported that ebselen inhibits DGC (WspR), via covalent modification of a cystein group near the active site.⁸⁷ Ebselen is however an alkylating agent as well as a planar aromatic molecule which may not be an ideal drug candidate due to the potential toxicity.⁹⁴

1.2.6 Polymorphism of c-di-GMP

Almost a decade ago, Jones and co-workers showed that in solution phase, millimolar c-di-GMP could readily form dimers, tetraplexes and higher aggregates in the presence of cations.^{95,96} Divalent cations such as magnesium promote dimer formation in c-di-GMP whereas monovalent cations such as potassium promote the formation of tetraplexes and octaplexes in c-di-GMP^{95,96} (see **Figure 1.12**). We have shown that a conservative change to the structure of c-di-GMP by replacing an endocyclic oxygen with sulfur to give an analog called endo-S-c-di-GMP (see **Figure 1.13**) dramatically diminishes the propensity to form G-quadruplexes or higher aggregation, implying that c-di-GMP is finely poised to respond to environmental changes via changes in polymorphism.¹⁵ The intracellular concentration of c-di-GMP is however up to 10 μM but even at 100 μM , c-di-GMP mainly exists as a monomer/dimer mixture.⁹⁷ Therefore, the biological relevance of a higher aggregate

of c-di-GMP was questioned by the Sintim group.^{15,21,22,98} Between 2011-2012, Sintim and co-workers published a series of papers that demonstrated that at physiological relevant concentrations of c-di-GMP (as low as 5 μM), c-di-GMP could form higher order aggregates when certain aromatic compounds, such as acridines and cyanines were present.^{21,22,98} This propensity of c-di-GMP to form tetraplexes or octaplexes (G-quadruplexes) or even higher order structures at micromolar concentrations in the presence of cations, such as K^+ or Na^+ , which are found *in vivo* is intriguing as simple nucleotides (such as GTP or pGpG) do not readily form G-quadruplex structures at micromolar concentrations. Plausibly, the facile interconversion of c-di-GMP into different aggregation states could be a means whereby bacteria regulate biofilms formation in the presence of different metals.

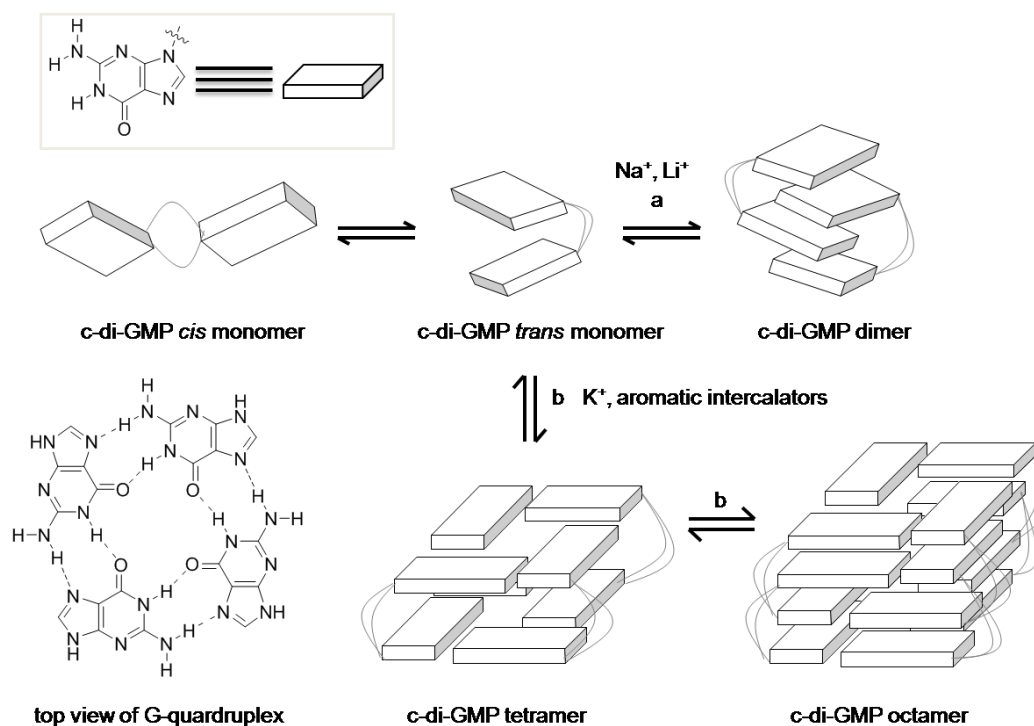
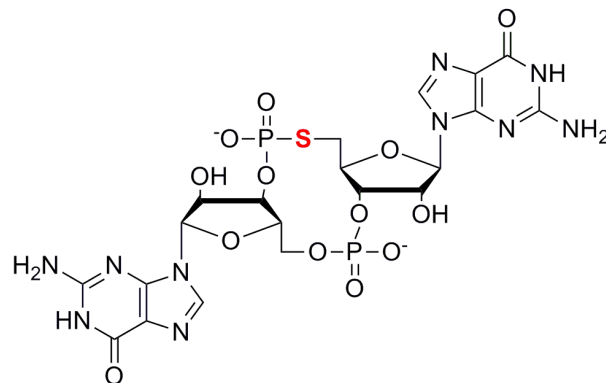


Figure 1.12 Proposed model of polymorphism of c-di-GMP in presence of cations or intercalators. Reproduced by permission of The Royal Society of Chemistry.¹¹



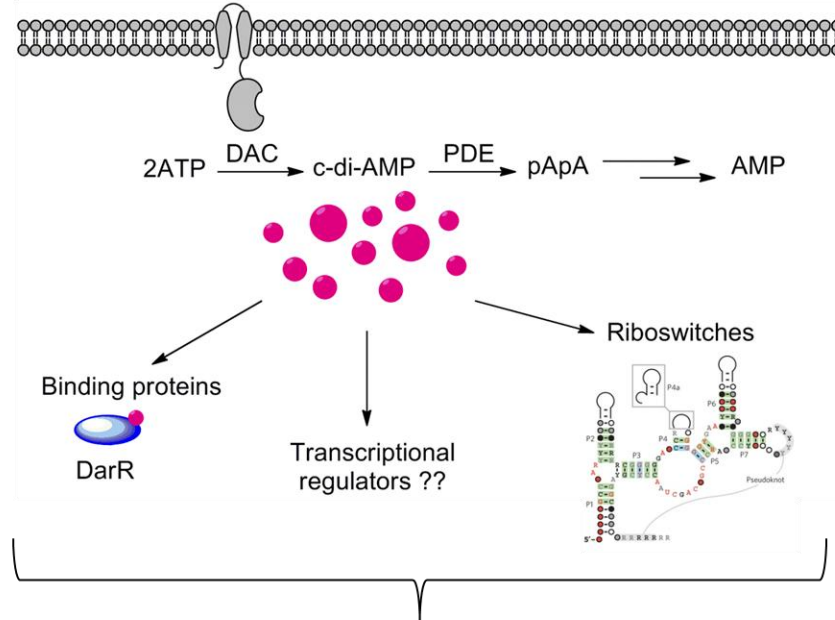
endo-S-c-di-GMP
1.13

Figure 1.13 Structure of endo-S-c-di-GMP.

During my PhD, I was interested in understanding or deciphering the moieties on c-di-GMP that are important for binding to different receptors. In Chapter 2, my published manuscript describing 2'-modified analogs of c-di-GMP and binding to protein receptors is presented. In Chapter 3, my published manuscript describing both the phosphate and 2'-modified c-di-GMP analogs and binding to RNA riboswitches is presented.

1.3 C-di-AMP, another ubiquitous and important signaling molecule

Cyclic-di-adenosine monophosphate (c-di-AMP) is a recently discovered bacterial signaling molecule. It was originally discovered during the structural elucidation of the *Bacillus subtilis* sporulation checkpoint protein, DisA, by Hopfner and co-workers.⁹⁹ C-di-AMP has now been shown to be involved in regulating cell size¹⁰⁰, controlling bacterial cell growth¹⁰¹ and homeostasis¹⁰² and sensing the DNA damage¹⁰³ (see **Figure 1.14**). Recent studies have suggested that c-di-AMP is as ubiquitous in Gram-positive bacteria as c-di-GMP in Gram-negative bacteria.^{99,104}



Output: Cell wall homeostasis; DNA integrity; Sporulation-related processes

Figure 1.14 Overview of c-di-AMP functions in bacteria.

Although the metabolism proteins and “adaptor/effector” proteins for c-di-AMP remain largely uncharacterized, efforts towards the quantitative detection of c-di-AMP *in vitro* and *in vivo* would aid the characterization of c-di-AMP receptors would help delineate the details of c-di-AMP signaling in bacteria.

In Chapter 4, I described a new assay that I developed to detect c-di-AMP in real time (see **Figure 1.15**). This new assay for detecting c-di-AMP has the potential to facilitate the discovery of inhibitors of c-di-AMP metabolism proteins.¹⁰⁵

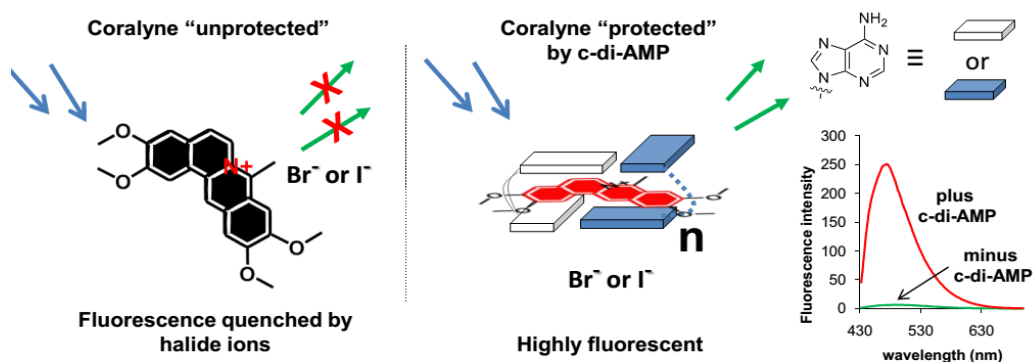


Figure 1.15 Schematic illustration of detection of c-di-AMP by coralyne assay. Reprinted with permission from ref 105. Copyright (2014) American Chemical Society.

References and Notes

- 1 Rönling, U.; Balsalobre, C. *J. Intern. Med.* **2012**, *272*, 541.
- 2 Donlan, R. M.; Costerton, J. W. *Clin. Microbiol. Rev.* **2002**, *15*, 167.
- 3 Sintim, H. O.; Al Smith, J.; Wang, J.; Nakayama, S.; Yan, L. *Future Med. Chem.* **2010**, *2*, 1005.
- 4 Duguid, I. G.; Evans, E.; Brown, M. R.; Gilbert, P. *J. Antimicrob. Chemother.* **1992**, *30*, 803.
- 5 Hoyle, B. D.; Wong, C. K.; Costerton, J. W. *Can. J. Microbiol.* **1992**, *38*, 1214.
- 6 Suci, P. A.; Mittelman, M. W.; Yu, F. P.; Geesey, G. G. *Antimicrob. Agents. Chemother.* **1994**, *38*, 2125.
- 7 Musk, D. J.; Hergenrother, P. J. *Curr. Med. Chem.* **2006**, *13*, 2163.
- 8 <http://www2.cnrs.fr/en/760.htm>, accessed on Apr 17th, 2014.
- 9 <http://www.ift.org/Knowledge-Center/Read-IFT-Publications/Science-Reports/Scientific-Status-Summaries/Quorum-Sensing-in-Biofilms.aspx>, accessed on Apr 17th, 2014.
- 10 <http://ausubellab.mgh.harvard.edu/picturehtml/pic20.html>, accessed on Apr 17th, 2014.
- 11 Kalia, D.; Merey, G.; Nakayama, S.; Zheng, Y.; Zhou, J.; Luo, Y.; Guo, M.; Roembke, B. T.; Sintim, H. O. *Chem. Soc. Rev.* **2013**, *42*, 305.
- 12 Purcell, E. B.; McKee, R. W.; McBride, S. M.; Waters, C. M.; Tamayo, R. *J. Bacteriol.* **2012**, *194*, 3307.
- 13 An, S.; Wu, J.; Zhang, L. H. *Appl. Environ. Microbiol.* **2010**, *76*, 8160.
- 14 Roy, A. B.; Petrova, O. E.; Sauer, K. *J. Bacteriol.* **2012**, *194*, 2904.
- 15 Wang, J.; Zhou, J.; Donaldson, G. P.; Nakayama, S.; Yan, L.; Lam, Y.-f.; Lee, V. T.; Sintim, H. O. *J. Am. Chem. Soc.* **2011**, *133*, 9320.
- 16 Zhou, J.; Watt, S.; Wang, J.; Nakayama, S.; Sayre, D. A.; Lam, Y. F.; Lee, V. T.; Sintim, H. O. *Bioorg. Med. Chem.* **2013**, *21*, 4396.
- 17 Kumagai, Y.; Matsuo, J.; Hayakawa, Y.; Rikihisa, Y. *J. Bacteriol.* **2010**, *192*, 4122.
- 18 Shanahan, C. A.; Gaffney, B. L.; Jones, R. A.; Strobel, S. A. *Biochemistry* **2013**, *52*, 365.
- 19 Ma, Q.; Yang, Z.; Pu, M.; Peti, W.; Wood, T. K. *Environ. Microbiol.* **2011**, *13*, 631.
- 20 Wexselblatt, E.; Katzhendler, J.; Saleem-Batcha, R.; Hansen, G.; Hilgenfeld, R.; Glaser, G.; Vidavski, R. R. *Bioorg. Med. Chem.* **2010**, *18*, 4485.
- 21 Nakayama, S.; Kelsey, I.; Wang, J. X.; Sintim, H. O. *Chem. Comm.* **2011**, *47*, 4766.
- 22 Nakayama, S.; Kelsey, I.; Wang, J.; Roelofs, K.; Stefane, B.; Luo, Y.; Lee, V. T.; Sintim, H. O. *J. Am. Chem. Soc.* **2011**, *133*, 4856.
- 23 Barraud, N.; Storey, M. V.; Moore, Z. P.; Webb, J. S.; Rice, S. A.; Kjelleberg, S. *Microb. Biotechnol.* **2009**, *2*, 370.
- 24 Carlson, H. K.; Vance, R. E.; Marletta, M. A. *Mol. Microbiol.* **2010**.
- 25 Liu, N.; Xu, Y.; Hossain, S.; Huang, N.; Coursolle, D.; Gralnick, J. A.; Boon, E. M. *Biochemistry* **2012**, *51*, 2087.

- 26 Ross, P.; Weinhouse, H.; Aloni, Y.; Michaeli, D.; Weinberger-Ohana, P.; Mayer, R.; Braun, S.; de Vroom, E.; van der Marel, G. A.; van Boom, H. H.; Benziman, M. *Nature* **1987**, *325*, 279.
- 27 Römling, U.; Gomelsky, M.; Galperin, M. Y. *Mol. Microbiol.* **2005**, *57*, 629.
- 28 Sondermann, H.; Shikuma, N. J.; Yildiz, F. H. *Curr. Opin. Microbiol.* **2012**, *15*, 140.
- 29 Hengge, R. *Nat. Rev. Drug Discov.* **2009**, *7*, 263.
- 30 Wolfe, A. J.; Visick, K. L. *J. Bacteriol.* **2008**, *190*, 463.
- 31 Tamayo, R.; Pratt, J. T.; Camilli, A. *Annu. Rev. Microbiol.* **2007**, *61*, 131.
- 32 Pratt, J. T.; Tamayo, R.; Tischler, A. D.; Camilli, A. *J. Biol. Chem.* **2007**, *282*, 12860.
- 33 Alm, R. A.; Boderer, A. J.; Free, P. D.; Mattick, J. S. *J. Bacteriol.* **1996**, *178*, 46.
- 34 Krasteva, P. V.; Fong, J. C.; Shikuma, N. J.; Beyhan, S.; Navarro, M. V.; Yildiz, F. H.; Sondermann, H. *Science* **2010**, *327*, 866.
- 35 Hickman, J. W.; Harwood, C. S. *Mol. Microbiol.* **2008**, *69*, 376.
- 36 Sudarsan, N.; Lee, E. R.; Weinberg, Z.; Moy, R. H.; Kim, J. N.; Link, K. H.; Breaker, R. R. *Science* **2008**, *321*, 411.
- 37 Lee, E. R.; Baker, J. L.; Weinberg, Z.; Sudarsan, N.; Breaker, R. R. *Science* **2010**, *329*, 845.
- 38 Yan, H.; Chen, W. *Chem. Soc. Rev.* **2010**, *39*.
- 39 Ausmees, N.; Mayer, R.; Weinhouse, H.; Volman, G.; Amikam, D.; Benziman, M.; Lindberg, M. *FEMS Microbiol. Lett.* **2001**, *204*, 163.
- 40 Paul, R.; Weiser, S.; Amiot, N. C.; Chan, C.; Schirmer, T.; Giese, B.; Jenal, U. *Genes Dev.* **2004**, *18*, 715.
- 41 Paul, R.; Abel, S.; Wassmann, P.; Beck, A.; Heerklotz, H.; Jenal, U. *J. Biol. Chem.* **2007**, *282*, 29170.
- 42 Hunter, J. L.; Severin, G. B.; Koestler, B. J.; Waters, C. M. *BMC Microbiol.* **2014**, *14*, 22.
- 43 Christen, B.; Christen, M.; Paul, R.; Schmid, F.; Folcher, M.; Jenoe, P.; Meuwly, M.; Jenal, U. *J. Biol. Chem.* **2006**, *281*, 32015.
- 44 Navarro, M. V.; De, N.; Bae, N.; Wang, Q.; Sondermann, H. *Structure* **2009**, *17*, 1104.
- 45 Chan, C.; Paul, R.; Samoray, D.; Amiot, N. C.; Giese, B.; Jenal, U.; Schirmer, T. *Proc. Natl. Acad. Sci. U. S. A.* **2004**, *101*, 17084.
- 46 Ryjenkov, D. A.; Tarutina, M.; Moskvina, O. V.; Gomelsky, M. *J. Bacteriol.* **2005**, *187*, 1792.
- 47 Yang, C. Y.; Chin, K. H.; Chuah, M. L.; Liang, Z. X.; Wang, A. H.; Chou, S. H. *Acta Crystallogr. D Biol. Crystallogr.* **2011**, *67*, 997.
- 48 De, N.; Pirruccello, M.; Krasteva, P. V.; Bae, N.; Raghavan, R. V.; Sondermann, H. *PLoS Biol.* **2008**, *6*, e67.
- 49 Schmidt, A. J.; Ryjenkov, D. A.; Gomelsky, M. *J. Bacteriol.* **2005**, *187*, 4774.
- 50 Suzuki, K.; Babitzke, P.; Kushner, S. R.; Romeo, T. *Genes Dev.* **2006**, *20*, 2605.

- 51 Ryan, R. P.; Fouhy, Y.; Lucey, J. F.; Crossman, L. C.; Spiro, S.; He, Y. W.; Zhang, L. H.; Heeb, S.; Camara, M.; Williams, P.; Dow, J. M. *Proc. Natl. Acad. Sci. U. S. A.* **2006**, *103*, 6712.
- 52 Bellini, D.; Caly, D. L.; McCarthy, Y.; Bumann, M.; An, S. Q.; Dow, J. M.; Ryan, R. P.; Walsh, M. A. *Mol. Microbiol.* **2014**, *91*, 26.
- 53 Barends, T. R.; Hartmann, E.; Griese, J. J.; Beitlich, T.; Kirienko, N. V.; Ryjenkov, D. A.; Reinstein, J.; Shoeman, R. L.; Gomelsky, M.; Schlichting, I. *Nature* **2009**, *459*, 1015.
- 54 Minasov, G.; Padavattan, S.; Shuvalova, L.; Brunzelle, J. S.; Miller, D. J.; Baslé, A.; Massa, C.; Collart, F. R.; Schirmer, T.; Anderson, W. F. *J. Biol. Chem.* **2009**, *284*, 13174.
- 55 Christen, M.; Christen, B.; Folcher, M.; Schauerte, A.; Jenal, U. *J. Biol. Chem.* **2005**, *280*, 30829.
- 56 Salter, E. A.; Wierzbicki, A. *J. Phys. Chem. B* **2007**, *111*, 4547.
- 57 Tamayo, R.; Tischler, A. D.; Camilli, A. *J. Biol. Chem.* **2005**, *280*, 33324.
- 58 Tchigvintsev, A.; Xu, X.; Singer, A.; Chang, C.; Brown, G.; Proudfoot, M.; Cui, H.; Flick, R.; Anderson, W. F.; Joachimiak, A.; Galperin, M. Y.; Savchenko, A.; Yakunin, A. F. *J. Mol. Biol.* **2010**, *402*, 524.
- 59 Sundriyal, A.; Massa, C.; Samoray, D.; Zehender, F.; Sharpe, T.; Jenal, U.; Schirmer, T. *J. Biol. Chem.* **2014**.
- 60 Lovering, A. L.; Capeness, M. J.; Lambert, C.; Hobley, L.; Sockett, R. E. *mBio* **2011**, *2*.
- 61 Wigren, E.; Liang, Z. X.; Römling, U. *Mol. Microbiol.* **2014**, *91*, 1.
- 62 Lindenberg, S.; Klauck, G.; Pesavento, C.; Klauck, E.; Hengge, R. *EMBO J.* **2013**, *32*, 2001.
- 63 Hengge, R. *Nat. Rev. Micro.* **2009**, *7*, 263.
- 64 Römling, U.; Galperin, M. Y.; Gomelsky, M. *Microbiol. Mol. Biol. Rev.* **2013**, *77*, 1.
- 65 Ryjenkov, D. A.; Simm, R.; Römling, U.; Gomelsky, M. *J. Biol. Chem.* **2006**, *281*, 30310.
- 66 Amikam, D.; Galperin, M. Y. *Bioinformatics* **2006**, *22*, 3.
- 67 Duerig, A.; Abel, S.; Folcher, M.; Nicollier, M.; Schwede, T.; Amiot, N.; Giese, B.; Jenal, U. *Genes Dev.* **2009**, *23*, 93.
- 68 Petters, T.; Zhang, X.; Nesper, J.; Treuner-Lange, A.; Gomez-Santos, N.; Hoppert, M.; Jenal, U.; Søgaard-Andersen, L. *Mol. Microbiol.* **2012**, *84*, 147.
- 69 Newell, P. D.; Monds, R. D.; O'Toole, G. A. *Proc. Natl. Acad. Sci. U. S. A.* **2009**, *106*, 3461.
- 70 Rakshe, S.; Leff, M.; Spormann, A. M. *Appl. Environ. Microbiol.* **2011**, *77*, 2196.
- 71 Yang, F.; Tian, F.; Li, X.; Fan, S.; Chen, H.; Wu, M.; Yang, C. H.; He, C. *Mol. Plant Microbe. Interact.* **2014**, DOI: 10.1094/MPMI-12-13-0371-R.
- 72 Chin, K. H.; Lee, Y. C.; Tu, Z. L.; Chen, C. H.; Tseng, Y. H.; Yang, J. M.; Ryan, R. P.; McCarthy, Y.; Dow, J. M.; Wang, A. H.; Chou, S. H. *J. Mol. Biol.* **2010**, *396*, 646.
- 73 Leduc, J. L.; Roberts, G. P. *J. Bacteriol.* **2009**, *191*, 7121.

- 74 Wilksch, J. J.; Yang, J.; Clements, A.; Gabbe, J. L.; Short, K. R.; Cao, H.; Cavaliere, R.; James, C. E.; Whitchurch, C. B.; Schembri, M. A.; Chuah, M. L.; Liang, Z. X.; Wijburg, O. L.; Jenney, A. W.; Lithgow, T.; Strugnell, R. A. *PLoS Pathog.* **2011**, *7*, e1002204.
- 75 Ko, J.; Ryu, K. S.; Kim, H.; Shin, J. S.; Lee, J. O.; Cheong, C.; Choi, B. S. *J. Mol. Biol.* **2010**, *398*, 97.
- 76 Benach, J.; Swaminathan, S. S.; Tamayo, R.; Handelsman, S. K.; Foltá-Stogniew, E.; Ramos, J. E.; Forouhar, F.; Neely, H.; Seetharaman, J.; Camilli, A.; Hunt, J. F. *EMBO J.* **2007**, *26*, 5153.
- 77 Habazettl, J.; Allan, M. G.; Jenal, U.; Grzesiek, S. *J. Biol. Chem.* **2011**, *286*, 14304.
- 78 Baraquet, C.; Murakami, K.; Parsek, M. R.; Harwood, C. S. *Nucleic Acids Res.* **2012**.
- 79 Baraquet, C.; Harwood, C. S. *Proc. Natl. Acad. Sci. U. S. A.* **2013**, *110*, 18478.
- 80 Smith, K. D.; Lipchock, S. V.; Ames, T. D.; Wang, J.; Breaker, R. R.; Strobel, S. A. *Nat. Struct. Mol. Biol.* **2009**, *16*, 1218.
- 81 Shanahan, C. A.; Strobel, S. A. *Org. Biomol. Chem.* **2012**, *10*, 9113.
- 82 Nakayama, S.; Roelofs, K.; Lee, V. T.; Sintim, H. O. *Mol. Biosyst.* **2012**, *8*, 726.
- 83 Travascio, P.; Li, Y.; Sen, D. *Chem. Biol.* **1998**, *5*, 505.
- 84 Roembke, B. T.; Nakayama, S.; Sintim, H. O. *Methods* **2013**, *64*, 185.
- 85 Roembke, B.; Wang, J.; Nakayama, S.; Zhou, J.; Sintim, H. *RSC Advances* **2013**, *3*, 6305.
- 86 Nakayama, S.; Luo, Y.; Zhou, J.; Dayie, T. K.; Sintim, H. O. *Chem. Commun. (Camb)* **2012**, *48*, 9059.
- 87 Lieberman, O. J.; Orr, M. W.; Wang, Y.; Lee, V. T. *ACS Chem. Biol.* **2014**, *9*, 183.
- 88 Ohana, P.; Delmer, D.; Volman, G.; Benziman, M. *Plant Cell Physiol.* **1998**, *39*, 153.
- 89 Ohana, P.; Delmer, D. P.; Carlson, R. W.; Glushka, J.; Azadi, P.; Bacic, T.; Benziman, M. *Plant Cell Physiol.* **1998**, *39*, 144.
- 90 Sambanthamoorthy, K.; Sloup, R. E.; Parashar, V.; Smith, J. M.; Kim, E. E.; Semmelhack, M. F.; Neiditch, M. B.; Waters, C. M. *Antimicrob. Agents Chemother.* **2012**, *56*, 5202.
- 91 Sambanthamoorthy, K.; Luo, C.; Pattabiraman, N.; Feng, X.; Koestler, B.; Waters, C. M.; Palys, T. J. *Biofouling* **2014**, *30*, 17.
- 92 Antoniani, D.; Bocci, P.; Maciag, A.; Raffaelli, N.; Landini, P. *Appl. Microbiol. Biotechnol.* **2010**, *85*, 1095.
- 93 Antoniani, D.; Rossi, E.; Rinaldo, S.; Bocci, P.; Lolicato, M.; Paiardini, A.; Raffaelli, N.; Cutruzzolà F.; Landini, P. *Appl. Microbiol. Biotechnol.* **2013**, *97*, 7325.
- 94 Schewe, T. *Gen. Pharmacol.* **1995**, *26*, 1153.
- 95 Zhang, Z.; Gaffney, B. L.; Jones, R. A. *J. Am. Chem. Soc.* **2004**, *126*, 16700.
- 96 Zhang, Z.; Kim, S.; Gaffney, B. L.; Jones, R. A. *J. Am. Chem. Soc.* **2006**, *128*, 7015.

- 97 Gentner, M.; Allan, M. G.; Zaehring, F.; Schirmer, T.; Grzesiek, S. *J. Am. Chem. Soc.* **2012**, *134*, 1019.
- 98 Kelsey, I.; Nakayama, S.; Sintim, H. O. *Bioorg. Med. Chem. Lett.* **2012**, *22*, 881.
- 99 Witte, G.; Hartung, S.; Büttner, K.; Hopfner, K. P. *Mol. Cell.* **2008**, *30*, 167.
- 100 Corrigan, R. M.; Abbott, J. C.; Burhenne, H.; Kaefer, V.; Gründling, A. *PLoS Pathog.* **2011**, *7*, e1002217.
- 101 Mehne, F. M.; Gunka, K.; Eilers, H.; Herzberg, C.; Kaefer, V.; Stülke, J. *J. Biol. Chem.* **2013**, *288*, 2004.
- 102 Luo, Y.; Helmann, J. D. *Mol. Microbiol.* **2012**, *83*, 623.
- 103 Witte, C. E.; Whiteley, A. T.; Burke, T. P.; Sauer, J. D.; Portnoy, D. A.; Woodward, J. J. *mBio* **2013**, *4*, e00282.
- 104 Gomelsky, M. *Mol. Microbiol.* **2011**, *79*, 562.
- 105 Zhou, J.; Sayre, D. A.; Zheng, Y.; Szmanski, H.; Sintim, H. O. *Anal. Chem.* **2014**, *86*, 2412.

Chapter 2. Potent suppression of c-di-GMP synthesis via I-site allosteric inhibition of diguanylate cyclases with 2'-F-c-di-GMP

(This chapter was published in Zhou et al. Bioorg. Med. Chem. 2013, 21, 4396)

2.1 2'-modified analogs of c-di-GMP

2.1.1 Introduction

Cyclic diguanylic monophosphate, c-di-GMP, was discovered in the late 80s as an allosteric modulator of cellulose synthase in bacteria,¹ but it was not until almost two decades later that c-di-GMP was established as a second messenger and its central role in biofilm formation and the regulation of virulence-related factors in diverse bacteria was discovered.²⁻⁷ C-di-GMP is produced from two guanosine triphosphate (GTP) molecules by diguanylate cyclases (DGCs), and is further broken down into 5'-phosphoguanylyl-(3'-5')-guanosine (pGpG) by specific phosphodiesterases (PDEs).⁸⁻¹¹ Generally, increased concentration of c-di-GMP in most bacteria leads to increased biofilm formation.¹²⁻¹⁴ Most DGCs that synthesize c-di-GMP have an inhibitory site (I-site), where c-di-GMP binds and allosterically inhibits product formation.^{9,15} Small molecules that can bind to the I-site of DGCs to inhibit c-di-GMP synthesis could potentially modulate biofilm formation and virulence factor production in a variety of bacteria. The identification of the structural features on c-di-GMP that confer specific binding to DGCs as well as other c-di-GMP binding proteins would provide important design principles for the preparation of c-di-GMP-

like molecules that could be used to perturb bacterial physiology. Thus far, the majority of c-di-GMP analogs synthesized have been tested for binding to riboswitches^{16,17} and only a handful of analogs (phosphate-^{18,19} and base-modified²⁰) have been tested for binding to proteins. Analyses of the crystal structures of over 20 c-di-GMP binding proteins reveal that the majority of these proteins make numerous contacts (via hydrogen bonding, π - π stacking or salt bridges) with the phosphate and guanine nucleobase of c-di-GMP. It is therefore not surprising that the analogs tested to date have displayed reduced affinity for c-di-GMP effector proteins.¹⁸⁻²⁰ On the other hand, analyses of over 20 c-di-GMP binding proteins revealed that some proteins have H-bonding interactions between the 2'-OH moiety of c-di-GMP and protein residues whereas in other proteins no polar interactions between the 2'-OH of c-di-GMP and protein residues were seen. Additionally, in some proteins one or both of the 2'-OH groups were either fully or partially buried inside the protein whereas for others, this moiety was solvent exposed. We therefore rationalized that the 2'-position of c-di-GMP is a prime position to modify in order to prepare ligands that could selectively bind to some c-di-GMP binding proteins and not others. In this paper, we investigated the modification of the 2'-position of c-di-GMP with hydrogen, fluorine or methoxy groups (see **Figure 2.1**). The replacement of the hydroxyl group at the 2'-position in riboses not only eliminates the potential for both H-bonding donation or acceptance but could also affect the sugar puckering of the ribose, which could affect the relative orientation of the guanine bases of c-di-GMP and possibly affect binding interactions that are remote from the 2'-OH site. Both fluorine and methoxy substitution are known to preserve the native sugar pucker,

however the methoxy substitution adds steric hindrance. Although fluorine is a good isostere of the OH group, it cannot act as a H-bond donor. Hence 2'-F-c-di-GMP could be used to tease out the importance of hydrogen bonding donation at the 2'-position of c-di-GMP. Interestingly, we have discovered that the replacement of the 2'-OH of c-di-GMP with fluorine affords an analog that binds to several c-di-GMP-binding proteins with similar or even better affinity than c-di-GMP. We recently revealed that small changes to the phosphodiester backbone of c-di-GMP (**2.1**) give endo-S-c-di-GMP remarkably decreased propensity to form G-quadruplexes and to bind c-di-GMP receptors.¹⁸ In order to determine the structural features of c-di-GMP that are important for polymorphism and binding to effector proteins, we prepared and studied 2'-modified analogs of c-di-GMP (2'-F-c-di-GMP (**2.2**) and 2'-H-c-di-GMP (**2.3**) following the strategy shown in **Scheme 2.1**.

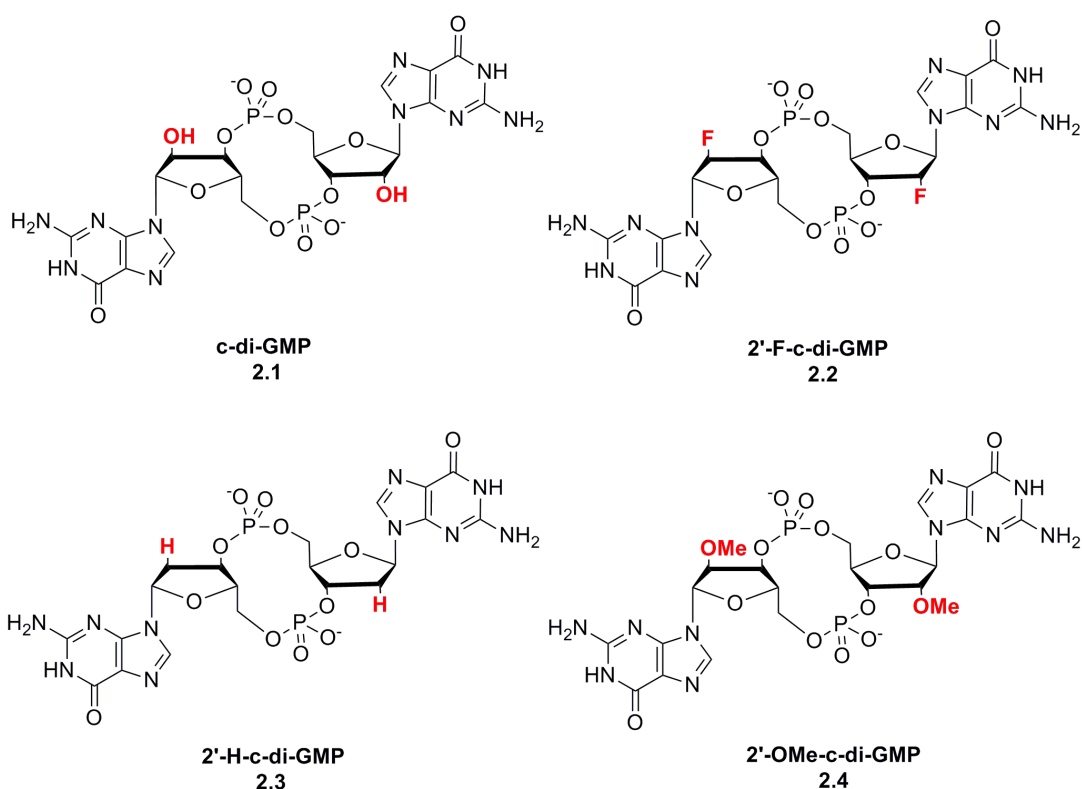
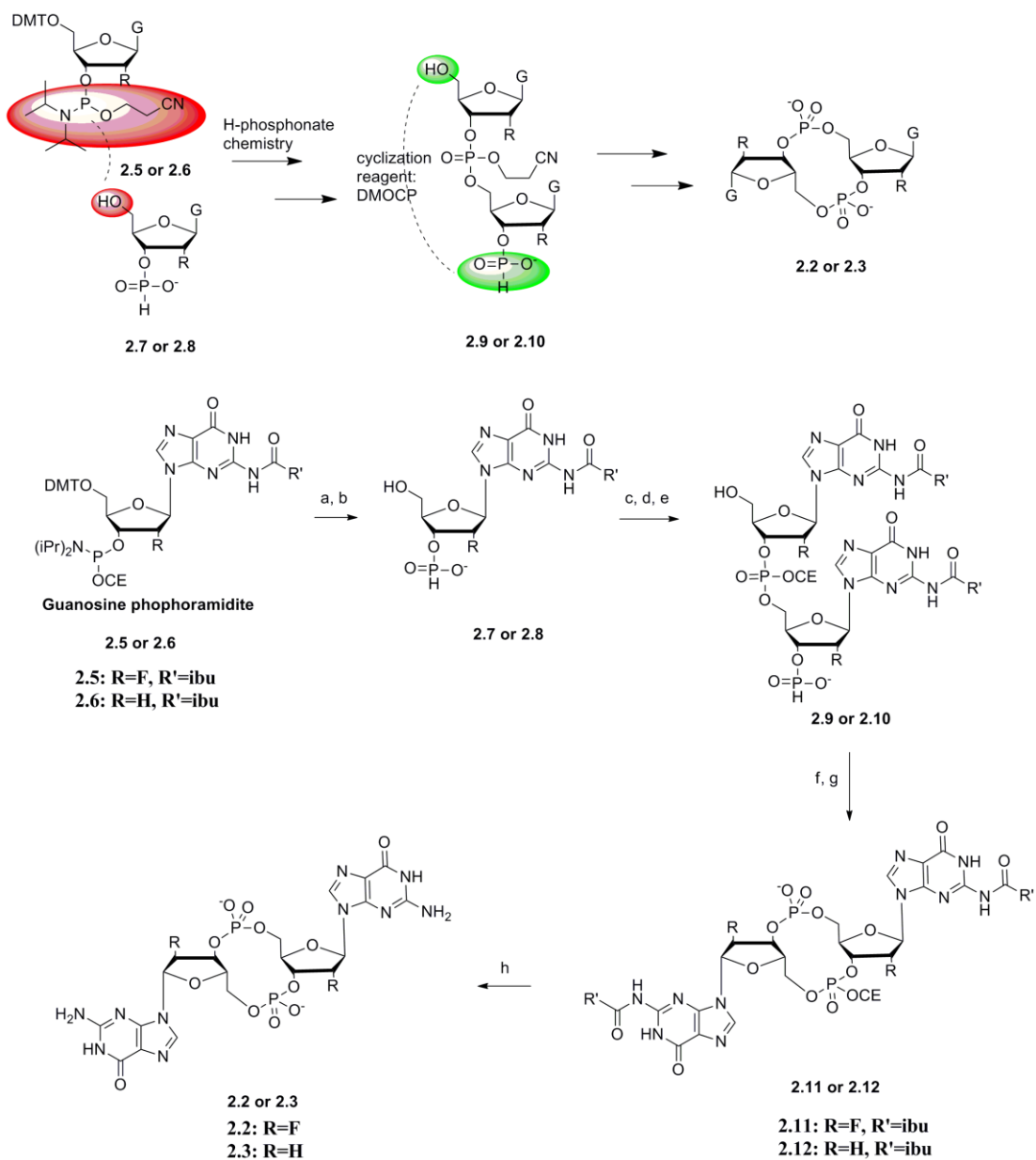


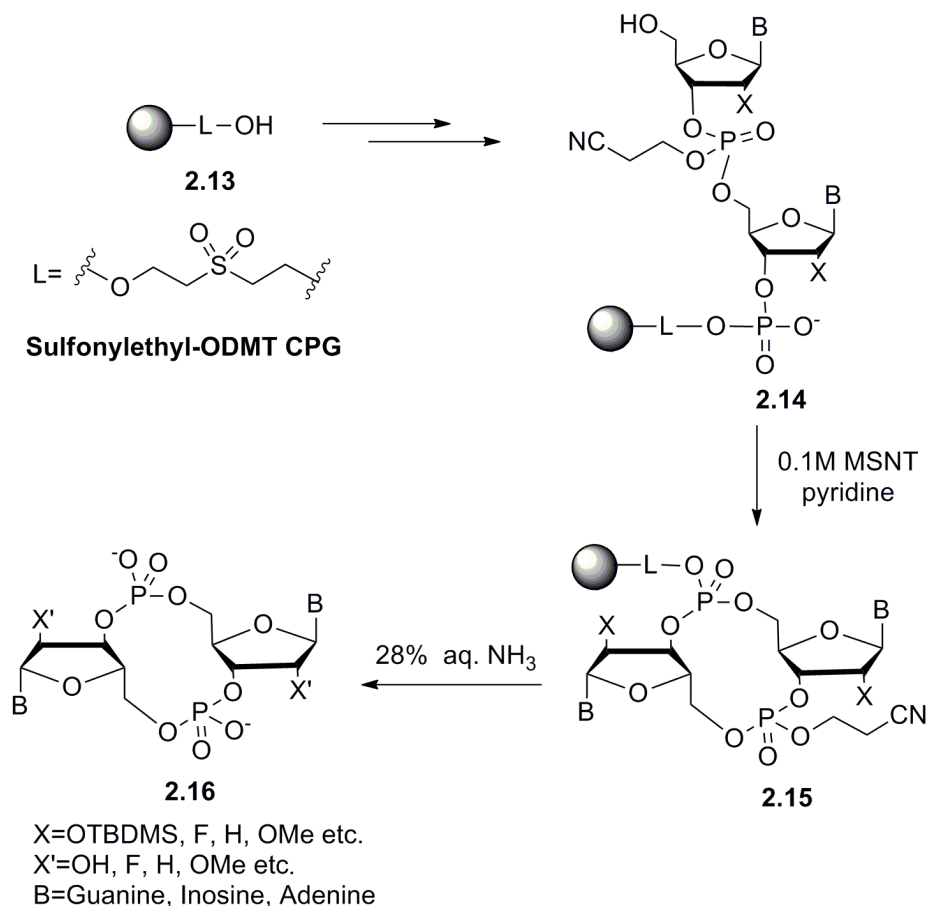
Figure 2.1 2'-modified analogs of c-di-GMP designed and synthesized.

2.1.2 Synthesis of c-di-GMP analogs



Scheme 2.1 Synthesis of compounds **2.2** and **2.3** via solution phase synthesis. Modified conditions of reported synthesis²² were used: (a) pyridinium trifluoroacetate, H₂O, then *t*-BuNH₂. (b) dichloroacetic acid, then quenched with pyridine. (c) compound **2.5** or **2.6**. (d) *t*-BuOOH. (e) dichloroacetic acid, then quenched with pyridine. (f) 5,5-dimethyl-2-oxo-2-chloro-1,3,2-dioxaphosphinane

(DMOCP). (g) I₂, H₂O, then HPLC purification. (h) 30% NH₄OH, then HPLC purification.



Scheme 2.2 Solid-phase synthesis strategy of c-di-GMP and/or analogs.

The facile solid-phase synthesis of c-di-GMP or analogs have been reported by Sintim and co-workers.²¹ (**Scheme 2.2**) The general synthesis strategy used sulfonylethyl-ODMT CPG coupling with two different phosphoramidites (*P*-methoxyphosphoramidite and cyanoethyl phosphate protected phosphoramidite).²¹ Cyclization was carried out by using 0.1 M 1-mesitylenesulfonyl-3-nitro-1, 2, 4-triazole (MSNT) in pyridine, followed by the selective deprotection on the phosphate group of the first coupled phosphoramidite. We chose to prepare analogs **2.2** and **2.3**

using a modified version of solution phase synthesis (**Scheme 2.1**) due to the need for larger quantities of these c-di-GMP analogs. Jones recently disclosed a simple synthesis of c-di-GMP in one flask without any purification of the intermediates.²² In our hands however, we have observed that purification of the protected cyclic dinucleotide (compound **2.11** or **2.12**, **Scheme 2.1**) before the global deprotection step made the purification of the final product significantly easier (see **Figure 2.2** for HPLC chromatograms).

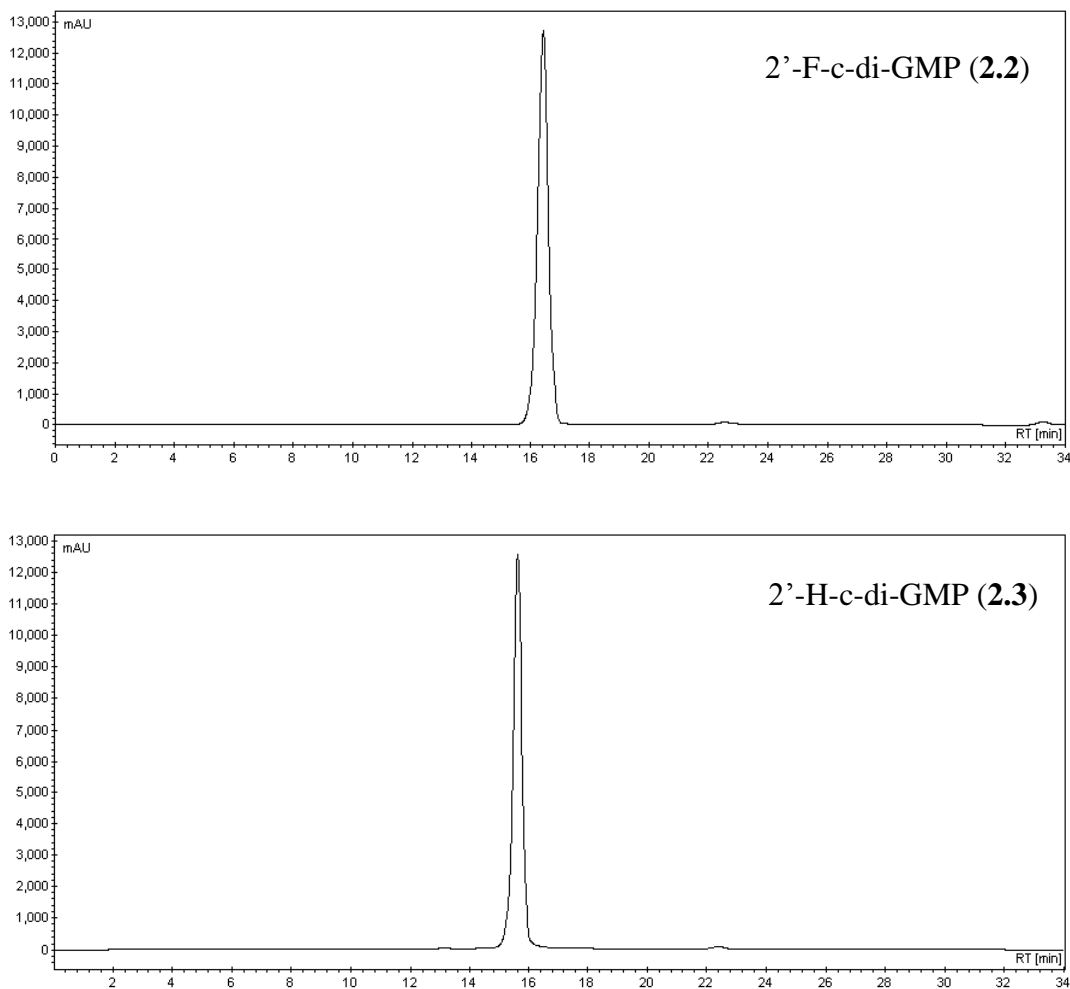


Figure 2.2 HPLC chromatography of c-di-GMP analogs (**2.2** and **2.3**). HPLC conditions: Nacalai Tesque Cosmosil[®] C18-PAQ column (4.6 x 250 mm), eluting

with 1 → 13 % B at 0 → 17 min (A: 100 mM triethylammonium acetate (TEAA) in water; B: acetonitrile, pH 7.0), rt with a UV detector.

The aggregative behavior of c-di-GMP has already been characterized using both CD and NMR.^{18,23-27} At low micromolar concentrations (below 100 μM), it is known that c-di-GMP exists as monomeric and dimeric forms. The monomeric and dimeric forms are in fast equilibrium with an association constant of $1.3 \pm 0.5 \times 10^{-3} \text{ M}$.²⁷ Grzesiek, Schirmer and co-workers have shown that at low concentrations (such as 10 μM), c-di-GMP is predominantly monomeric.²⁷ On the other hand, at higher concentrations (such as 400 μM), c-di-GMP forms G-quadruplexes (predominantly octameric) in the presence of monovalent cations, such as potassium.²⁷

1D ¹H NMR spectra revealed that compounds **2.2** and **2.3** exist as MD (MD stands for monomeric/dimeric forms in fast equilibrium, see reference 27) at 30 °C without added K⁺ (see **Figure 2.3c** and **2.4c**). For 2'-F-c-di-GMP (**Figure 2.3c**), the singlet peak at 7.98 ppm was assigned to the guanine H8 and a doublet at 6.11 ppm was assigned to the anomeric H1'. Upon adding 100 mM K⁺ to the 2'-F-c-di-GMP solution (**Figure 2.3b**), more peaks appeared near 7.95 ppm and 6.07 ppm. These new peaks correspond to the octameric form (labeled as O) of 2'-F-c-di-GMP, which form when potassium is present, vide infra. Upon heating the sample to 60 °C (which will break all aggregates, **Figure 2.3a**), the multiple peaks disappeared and new peaks appeared at 8.28 and 6.40 ppm. For the MD form of 2'-H-c-di-GMP (**Figure 2.3c**), a singlet peak at 8.05 ppm was assigned to the guanine H8 proton and a multiplet from

6.31 and 6.29 ppm were assigned to the anomeric H1' proton. Upon adding 100 mM K⁺ to the 2'-H-c-di-GMP solution (**Figure 2.4b**), more peaks appeared near 8.05 ppm and 6.30 ppm, due to the formation of different aggregates of 2'-H-c-di-GMP. We characterized the aggregates following literature precedents.²⁴ We used diffusion ordered spectroscopy (DOSY) experiments, followed by T1/T2 relaxation analysis of the diffusion constants to obtain the diffusion constants of the MD, tetrameric (T) and octameric (O) forms of c-di-GMP and its analog.¹⁸ The diffusion constant, D, can be calculated using the Stokes-Einstein equation, $D = k T / (6 \pi \eta R)$, where k is the Boltzmann constant, T is the temperature, η is the solvent viscosity and R is the radius of the molecular sphere.

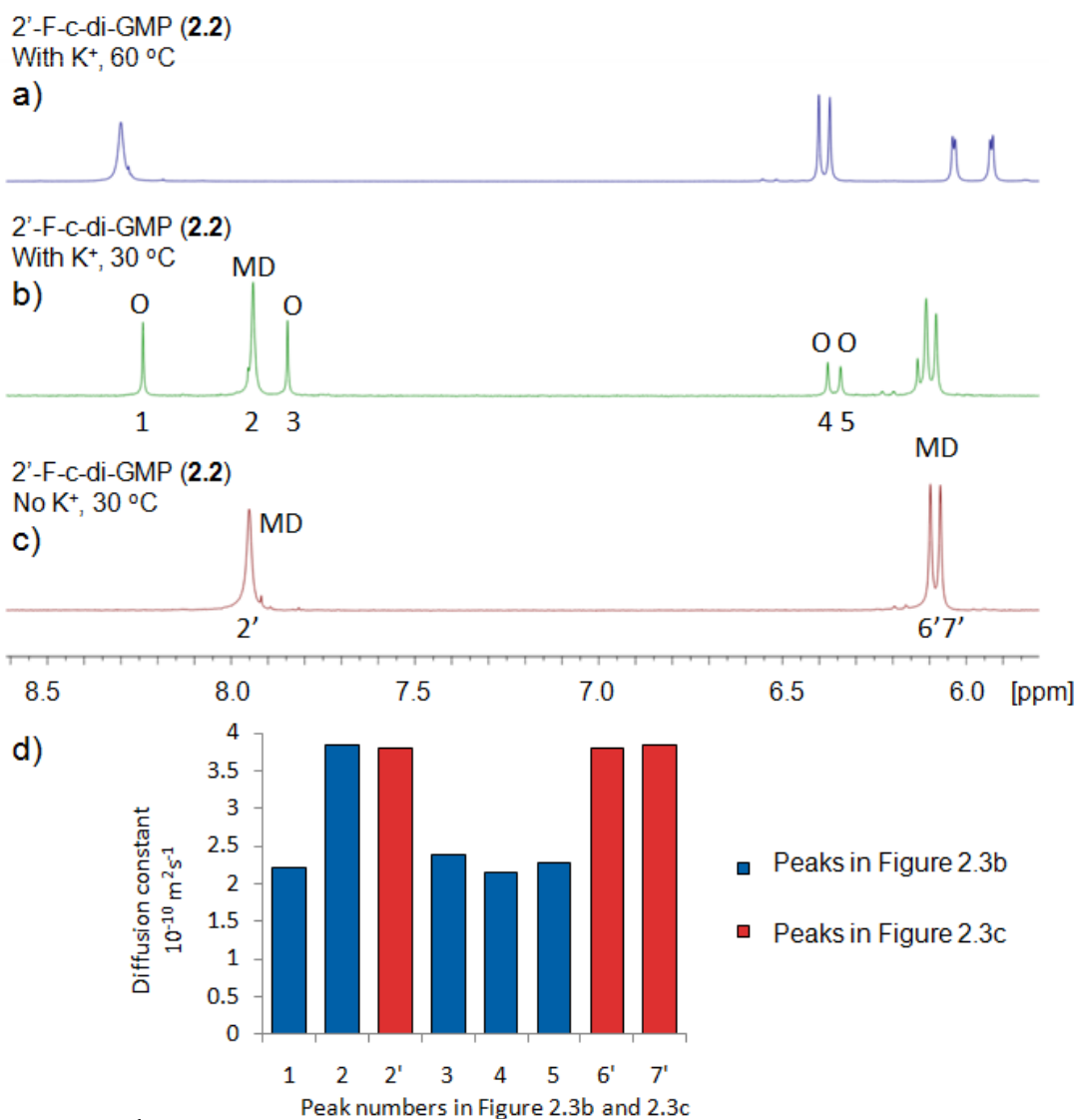


Figure 2.3 ¹H NMR stacked spectra of 3.0 mM analog **2.2** in D₂O. Conditions: (a) 3.0 mM 2'-F-c-di-GMP, 100 mM KCl 60 °C. (b) 3.0 mM 2'-F-c-di-GMP, 100 mM KCl, 30 °C. (c) 3.0 mM 2'-F-c-di-GMP, no metal cation, 30 °C. (d) 3.0 mM 2'-F-c-di-GMP, T1/T2 relaxation analysis (from DOSY experiments).

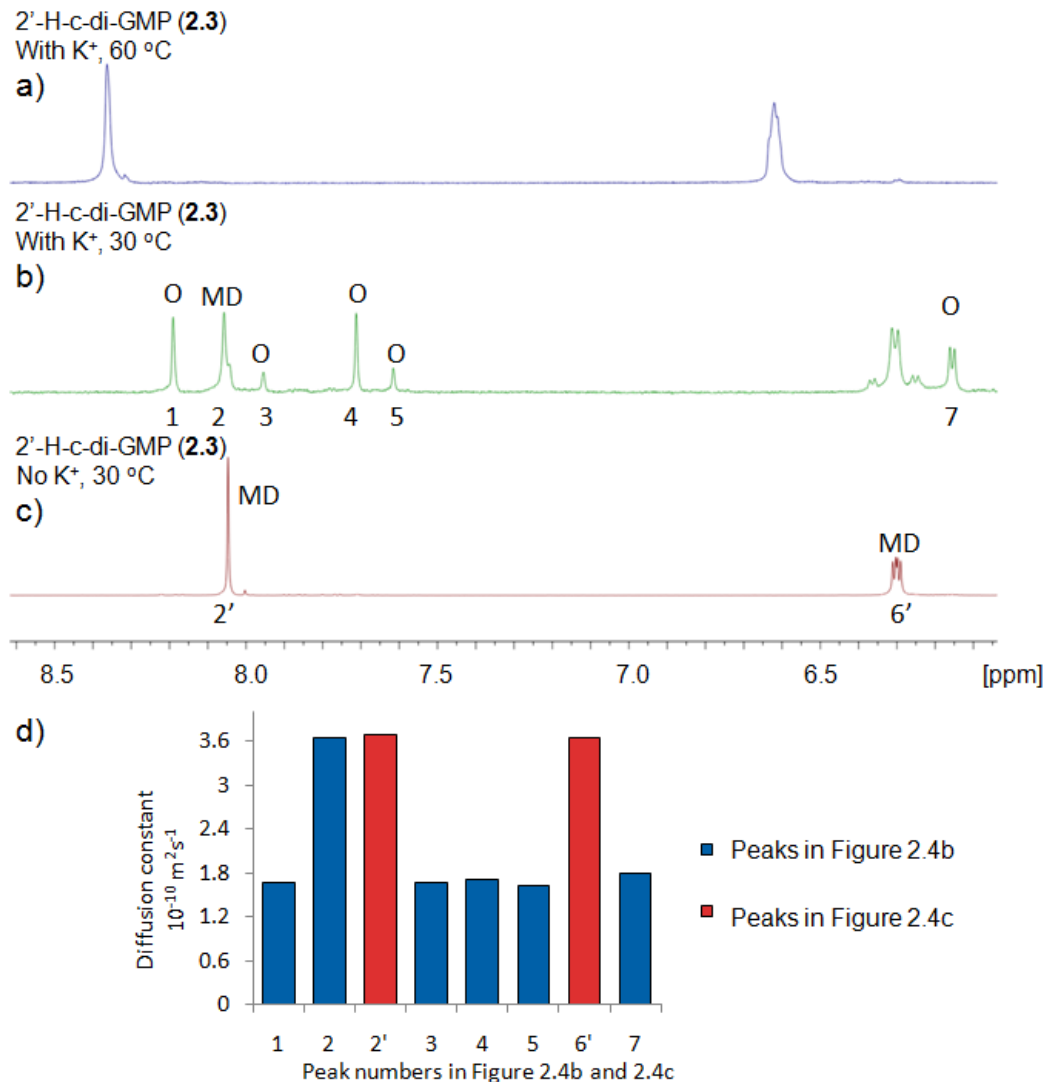


Figure 2.4 ¹H NMR stacked spectra of 3.0 mM analog **2.3** in D₂O. Conditions: (a) 3.0 mM 2'-H-c-di-GMP, 100 mM KCl 60 °C. (b) 3.0 mM 2'-H-c-di-GMP, 100 mM KCl, 30 °C. (c) 3.0 mM 2'-H-c-di-GMP, no metal cation, 30 °C. (d) 3.0 mM 2'-H-c-di-GMP, T1/T2 relaxation analysis (from DOSY experiments).

The diffusion constants of 2'-F-c-di-GMP and 2'-H-c-di-GMP in their MD form could be obtained by DOSY experiments using the samples that did not contain potassium. According to Grzesiek et al.²⁷, when total c-di-GMP concentration is 3

mM, MD is made up of approximately 80-90% monomeric form so the diffusion constant obtained for the MD peak could be approximated for the monomeric form. From the Stokes-Einstein equation, the diffusion constants for tetrameric (T) and octameric (O) forms of 2'-F-c-di-GMP and 2'-H-c-di-GMP were calculated following precedent,²⁴ using calculated radii for these complexes (see **Table 2.1**).

For both 2'-H and 2'-F-c-di-GMP in the presence of K⁺, the main species that existed in solution were the monomeric and octameric forms. Predicted diffusion constant of 2.03×10^{-10} m²/s, and experimental diffusion constant of 2.18×10^{-10} m²/s for the octameric (O) form of 2'-F-c-di-GMP G-quadruplexes were obtained. For 2'-H-c-di-GMP in the presence of K⁺, a predicted diffusion constant of 1.90×10^{-10} m²/s and an experimental value of 1.69×10^{-10} m²/s for the octameric form were obtained. These aggregation studies indicate that substitution of the 2'-position of c-di-GMP does not reduce the propensity to form octameric aggregates in the presence of potassium.

Table 2.1 Calculations of the radii of c-di-GMP and analogs (**2.2** and **2.3**) in their different aggregation states.

Aggregates	Calculate radii (Å)	Symmetry of the structures	Calculated diffusion constant (10^{-10} m/s^2)
2'-F-c-di-GMP			
Monomeric (<i>cis</i>)	6.37	C2	3.81 (average measured value) ^a
Monomeric (<i>tran</i>)	6.16	C2	--
Dimeric	8.01	--	3.03
Tetrameric	10.03	D4	2.42
Octameric	11.96	D4	2.03
2'-H-c-di-GMP			
Monomeric (<i>cis</i>)	6.19	C2	3.66 (average measured) ^a
Monomeric (<i>tran</i>)	6.16	C2	--
Dimeric	7.74	--	2.92
Tetrameric	9.78	D4	2.31
Octameric	11.92	D4	1.90

^aThe diffusion constants of monomeric form of 2'-F-c-di-GMP and 2'-H-c-di-GMP were measured from DOSY T_1/T_2 relaxation analysis with no metal cation added.

2.2 Effect of 2'-modification on binding to proteins

2.2.1 Theoretical analysis of c-di-GMP binding proteins

We analyzed 20 c-di-GMP binding proteins in the PDB databank for H-bonding interactions between the protein residues and the 2'-OH of c-di-GMP.²⁸ Six (three DGCs^{28a,e,g}, one PDE^{28k}) and two PilZ domain proteins^{28n,o}) of the 20 proteins analyzed (30%) utilized H-bonding interactions between protein residues and the 2'-OH moiety of c-di-GMP for recognition (see **Figure 2.5a-c**).

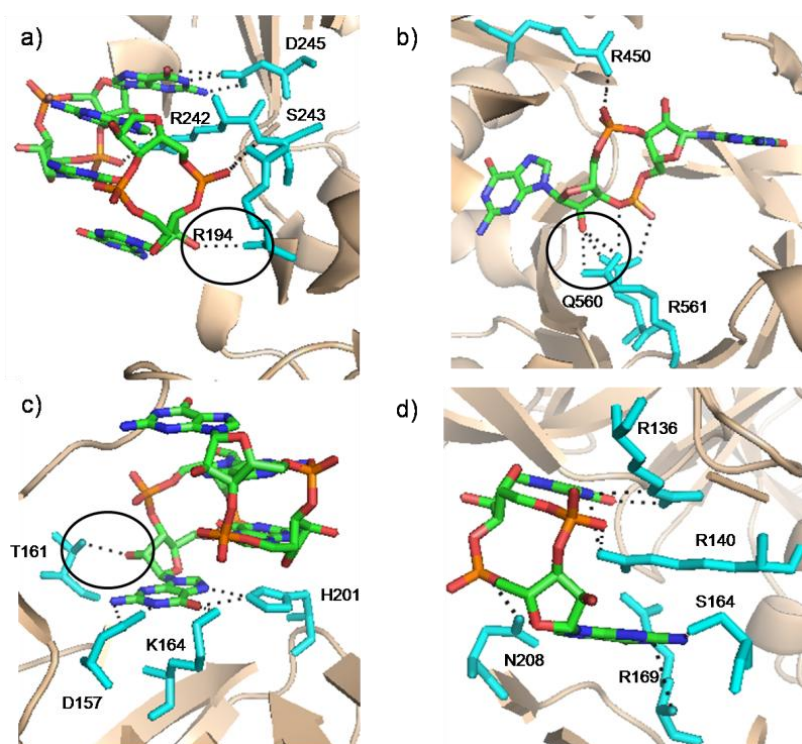


Figure 2.5 C-di-GMP is shown in sticks and colored by atom (oxygen in red, nitrogen in blue, carbon in green and phosphorus in orange); amino acid residues are shown in blue sticks. a) dimeric c-di-GMP bound to WspR (DGC domain; PDB code 3I5C). b) Monomeric c-di-GMP bound to LapD (EAL domain; PDB code 3PJT). c) Dimeric c-di-GMP bound to PP4397 (PilZ domain; PDB code 3KYF). d) Monomeric c-di-GMP bound to VCA0042 (PilZ domain; PDB code 2RDE).

2.2.2 IC₅₀s against c-di-GMP binding proteins and analogs

The effect of the 2'-OH substitution on biological activity was interrogated by testing the ability of each analog to compete for ³²P-c-di-GMP binding to the diguanylate cyclase WspR^{9,29}, the phosphodiesterase RocR^{30,31} and the PilZ domain-containing Alg44^{32,33}. As a positive control, unlabeled c-di-GMP was used as a competitor. The IC₅₀ of c-di-GMP for WspR, RocR and Alg44 was 48.9 μM, 21 nM and 7.7 μM, respectively (**Table 2.2**). 2'-H-c-di-GMP (**2.3**) was able to compete for binding to RocR with an IC₅₀ of 25 nM and to Alg44 with an IC₅₀ of 13.4 μM, but it was unable to compete for binding to WspR with an IC₅₀ greater than 100 μM (**Table 2.2**). 2'-F-c-di-GMP (**2**) was able to compete for binding to WspR, RocR and Alg44 with an IC₅₀ of 11 μM, 723 nM and 3.1 μM, respectively (**Table 2.2**). The binding profile of 2'-F-c-di-GMP is interesting because it appears to bind to the I-site of WspR tighter (4 times) than c-di-GMP, whereas for RocR, c-di-GMP binds tighter (~35 times) than 2'-F-c-di-GMP. The crystal structure of WspR in complex with c-di-GMP (see **Figure 2.5a**) reveals that residue R194 contacts c-di-GMP via H-bonding. If the 2'-F modification of c-di-GMP does not grossly affect the sugar puckering (see **Table 2.3**), then one could assume that the fluorine isostere allows for fluorine-hydrogen bonding interactions between 2'-F and arginine in the I-site.^{34,35} Most c-di-GMP binding proteins utilize arginine patches to recognize c-di-GMP. It is assumed that the arginine residues are critical for salt bridge interactions with the phosphate groups as well as both Hoogsteen hydrogen bonding interactions and cation-nucleobase interactions. Herein, we provide data that suggests that arginine-2'-OH interactions could also be important for c-di-GMP recognition at the I-site of about 30% DGCs

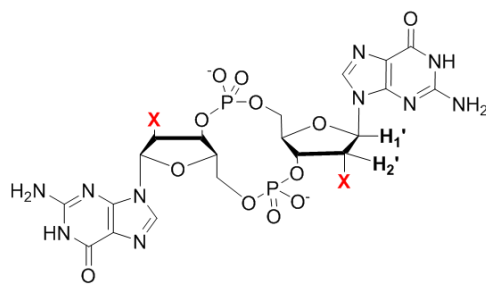
(three out of ten DGCs analyzed^{28a-h} displayed H-bonding interactions between protein residue and 2'-OH). Future structural studies using c-di-GMP analogs and various DGCs should help shed more light on the role 2'-OH on I-site binding.

Table 2.2 IC₅₀ value against protein (WspR, RocR and Alg44) by c-di-GMP and analogs (**2.1** to **2.4**).

	IC ₅₀ (μM)		
	WspR	RocR	Alg44
c-di-GMP	48.91	0.02	7.69
2'-F-c-di-GMP	11.01	0.72	3.12
2'-H-c-di-GMP	>100	0.02	13.36
2'-OMe-c-di-GMP	>100	3.14	>100

As already mentioned, 2'-F-c-di-GMP binds to RocR worse than c-di-GMP. Although the crystal structure of RocR (an EAL-domain protein) R286W mutant protein has been solved, the structure did not contain the c-di-GMP ligand.³⁶ We however note that some EAL-containing proteins, such as LapD, display extensive interactions between polar residues and c-di-GMP (see **Figure 2.5b**). The 2'-deoxy analog of c-di-GMP (2'-H-c-di-GMP), however, binds to RocR as well as c-di-GMP does (see **Table 2.2**). Therefore we do not believe that the reduction in polar interactions between RocR residues and the 2'-position of c-di-GMP accounts for the reduced binding of 2'-F-c-di-GMP to RocR. It must be noted that the modification of the 2'-position of nucleic acids not only affects the sugar puckering and/or H-bonding interactions at the 2'-position, but also affects the dihedral angle between H1 and H2,

and hence the orientation of the nucleobase (see **Table 2.3** for computed dihedral angles). The replacement of the 2'-OH with 2'-OMe can be considered conservative for the purposes of H-bonding interactions and sugar puckering (both groups can accept hydrogen bonds from arginines and both substitutions lead to 3'-endo, 2'-exo puckering modes).^{37,38} The 2'-OMe moiety is, however, more sterically encumbered, and so for proteins whereby there is little room to spare in the binding pocket, especially around the region surrounding the 2'-position of c-di-GMP, it is expected that 2'-OMe analog of c-di-GMP would bind poorly. 2'-OMe-c-di-GMP was the worst competitor with ³²P-c-di-GMP for binding to all tested proteins with an IC₅₀ greater than 100 μM for WspR and Alg44, and with an IC₅₀ of 3.14 μM for RocR (compare IC₅₀ of 20 nM for c-di-GMP competing with ³²P-c-di-GMP for RocR binding). This means that c-di-GMP binds to RocR at least two orders of magnitude tighter than 2'-OMe-c-di-GMP does. The sensitivity of WspR towards 2'-modification of c-di-GMP is surprising because the bound c-di-GMP in WspR is mostly solvent exposed (see **Figure 2.4a**). We have earlier observed that WspR is also sensitive to phosphate modification of c-di-GMP¹⁸ and so it appears that this particular DGC has evolved to be very selective for c-di-GMP.

Table 2.3 Sugar pucker ring mode of c-di-GMP and analogs (**2.1** to **2.3**)

1. X=OH, 2. X=F, 3. X=H

	Coupling constant $J_{H1', H2'}$ (Hz) from NMR	Sugar puckering mode, determined via NMR	Dihedral Angle, calculated ³⁹ H1'-C1'_C2'-H2'(H2'')
c-di-GMP	2.2	3'-endo, 2'-exo	104.0
2'-F-c-di-GMP	1.1	3'-endo, 2'-exo	88.4
2'-H-c-di-GMP	4.7 ($J_{H1', H2'}$)	Mix	92.3/-29.2
	7.5 ($J_{H1', X}$) (X=H)		

2.2.3 2'-F-c-di-GMP is a potent inhibitor of c-di-GMP synthase WspR

Since 2'-F-c-di-GMP competes with the ³²P-labeled c-di-GMP for binding to both WspR and RocR, we asked whether the compound affected the enzymatic activity of these enzymes and additional enzymes PA1107⁴⁰ (DGC) and PvrR⁴¹ (PDE). In the absence of competitor or with cGMP, WspR and PA1107 were active and converted GTP to c-di-GMP (see **Figure 2.6a** and **2.6b**). In the presence of c-di-GMP, the activity of both WspR and PA1107 were reduced. 2'-F-c-di-GMP, which binds better to WspR than c-di-GMP (see **Table 2.2**), caused a greater inhibition of the diguanylate cyclase activities of WspR and PA1107. These results suggest that 2'-F-

c-di-GMP occupies the I-site and acts to inhibit the activity of WspR and PA1107. RocR and PvrR phosphodiesterases were able to convert c-di-GMP to pGpG in the absence of competitor or with cGMP. However in the presence of c-di-GMP and 2'-F-c-di-GMP, the activity of RocR (but not PvrR) was inhibited (see **Figure 2.6c** and **2.6d**).

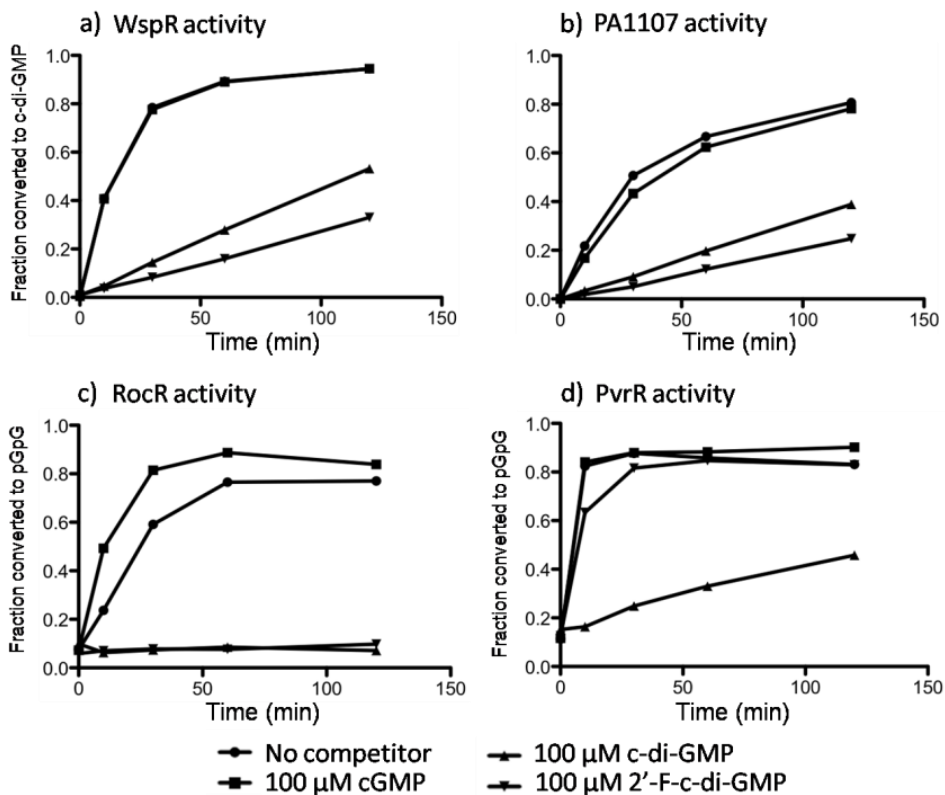


Figure 2.6 a) and b) Inhibition of c-di-GMP synthesis by WspR and PA1107 with guanine-containing nucleotides. c) and d) Inhibition of c-di-GMP hydrolysis by RocR and PvrR with guanine-containing nucleotides. Measurements were done in triplicate.

The ability of 2'-F-c-di-GMP to alter WspR activity was further interrogated by determining the effect of the inhibitor on V_{max} and K_m for each enzyme. For WspR, the effect of c-di-GMP and 2'-F-c-di-GMP on diguanylate cyclase activity was

determined by performing time course assays at the indicated GTP substrate concentrations. Increasing either c-di-GMP or 2'-F-c-di-GMP led to a decrease of both the V_{max} and the K_m , indicating that binding at the I-site leads to allosteric inhibition of the diguanylate cyclase activity (**Figure 2.7** and **Table 2.4**).

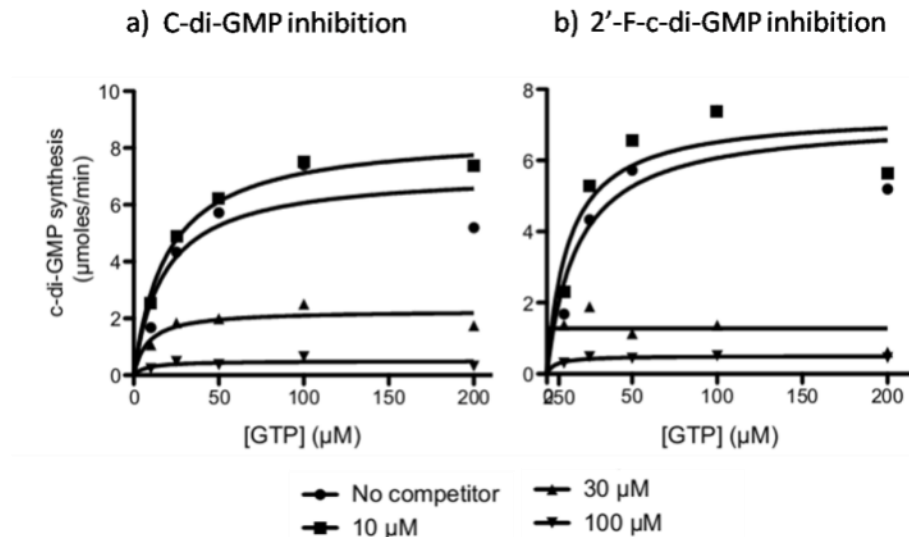


Figure 2.7 Inhibition of c-di-GMP synthesis by different concentrations of c-di-GMP or 2'-F-c-di-GMP. Measurements were done in triplicate.

Table 2.4 Effect of c-di-GMP and 2'-F-c-di-GMP on WspR enzyme kinetics.

Inhibitors	Concentration (μM)	V_{max} ($\mu\text{mole}/\text{min}$)	K_m^{app} (μM)
None	0	13.9 ± 1.2	29.8 ± 7.9
c-di-GMP	10	8.5 ± 0.4	19.7 ± 3.7
	30	2.3 ± 0.3	8.3 ± 6.1
	100	0.5 ± 0.1	7.2 ± 10.8
2'-F-c-di-GMP	10	11.3 ± 1.5	31.7 ± 13.3
	30	2.8 ± 0.3	17.7 ± 7.8
	100	0.5 ± 0.04	4.9 ± 2.7

2.3 Conclusion

In the last decade, there have been intensive efforts to control bacterial virulence and biofilm formation with small molecules.⁴²⁻⁵⁰ C-di-GMP has emerged as a master regulator of bacterial biofilm formation and small molecules that could perturb c-di-GMP signaling could have anti-biofilm properties. C-di-GMP signaling in bacteria is intricate and involves myriads of metabolism and effector proteins and RNAs. In order to perturb this signaling, with a view of disrupting bacterial biofilm formation, one could use a small molecule to either inhibit c-di-GMP synthesis or compete with c-di-GMP binding to effector molecules. This work reveals that different effector molecules (or receptors of c-di-GMP) are differentially sensitive to c-di-GMP modification and suggests that these proteins might be using different strategies to recognize c-di-GMP. As it would be challenging to find one small molecule that could simultaneously inhibit many classes of c-di-GMP effector proteins and RNAs, each with different binding pockets, it appears that the most effective strategy to inhibit c-di-GMP signaling is to either inhibit synthesis by DGC or to “quench” the signaling molecule itself via small molecule-induced aggregation.⁵¹ The discovery that 2'-F-c-di-GMP is a potent suppressor of c-di-GMP synthesis lays the foundation for the preparation of cell permeable analogs of 2'-F-c-di-GMP, which could be used to perturb c-di-GMP signaling.

References and notes

- 1 Ross, P.; Weinhouse, H.; Aloni, Y.; Michaeli, D.; Weinberger-Ohana, P.; Mayer, R.; Braun, S.; de Vroom, E.; van der Marel, G. A.; van Boom, H. H.; Benziman, M. *Nature* **1987**, *325*, 279.
- 2 Römbling, U.; Gomelsky, M.; Galperin, M. Y. *Mol. Microbiol.* **2005**, *57*, 629.
- 3 Sondermann, H.; Shikuma, N. J.; Yildiz, F. H. *Curr. Opin. Microbiol.* **2012**, *15*, 140.
- 4 Krasteva, P. V.; Giglio, K. M.; Sondermann, H. *Protein Sci.* **2012**, *21*, 929.
- 5 Ryan, R. P.; Tolker-Nielsen, T.; Dow, J. M. *Trends Microbiol.* **2012**, *20*, 235.
- 6 Römbling, U. *Environ. Microbiol.* **2012**, *14*, 1817.
- 7 Tamayo, R.; Pratt, J. T.; Camilli, A. *Annu. Rev. Microbiol.* **2007**, *61*, 131.
- 8 Smith, K. D.; Shanahan, C. A.; Moore, E. L.; Simon, A. C.; Strobel, S. A. *Proc. Natl. Acad. Sci. U. S. A.* **2011**, *108*, 7757.
- 9 Chan, C.; Paul, R.; Samoray, D.; Amiot, N. C.; Giese, B.; Jenal, U.; Schirmer, T. *Proc. Natl. Acad. Sci. U. S. A.* **2004**, *101*, 17084.
- 10 Schmidt, A. J.; Ryjenkov, D. A.; Gomelsky, M. *J. Bacteriol.* **2005**, *187*, 4774.
- 11 Ryjenkov, D. A.; Tarutina, M.; Moskvina, O. V.; Gomelsky, M. *J. Bacteriol.* **2005**, *187*, 1792.
- 12 Jonas, K.; Melefors, O.; Römbling, U. *Future Microbiol.* **2009**, *4*, 341.
- 13 Bobrov, A. G.; Kirillina, O.; Ryjenkov, D. A.; Waters, C. M.; Price, P. A.; Fetherston, J. D.; Mack, D.; Goldman, W. E.; Gomelsky, M.; Perry, R. D. *Mol. Microbiol.* **2011**, *79*, 533.
- 14 Mills, E.; Pultz, I. S.; Kulasekara, H. D.; Miller, S. I. *Cell Microbiol.* **2011**, *13*, 1122.
- 15 Christen, B.; Christen, M.; Paul, R.; Schmid, F.; Folcher, M.; Jenoe, P.; Meuwly, M.; Jenal, U. *J. Biol. Chem.* **2006**, *281*, 32015.
- 16 Shanahan, C. A.; Gaffney, B. L.; Jones, R. A.; Strobel, S. A. *J. Am. Chem. Soc.* **2011**, *133*, 15578.
- 17 Furukawa, K.; Gu, H.; Sudarsan, N.; Hayakawa, Y.; Hyodo, M.; Breaker, R. R. *ACS Chem. Biol.* **2012**, *7*, 1436.
- 18 Wang, J.; Zhou, J.; Donaldson, G. P.; Nakayama, S.; Yan, L.; Lam, Y. F.; Lee, V. T.; Sintim, H. O. *J. Am. Chem. Soc.* **2011**, *133*, 9320.
- 19 Luo, Y.; Zhou, J.; Watt, S. K.; Lee, V. T.; Dayie, T. K.; Sintim, H. O. *Mol. Biosyst.* **2012**, *8*, 772.
- 20 Ching, S. M.; Tan, W. J.; Chua, K. L.; Lam, Y. *Bioorg. Med. Chem.* **2010**, *18*, 6657.
- 21 Kiburu, I.; Shurer, A.; Yan, L.; Sintim, H. O. *Mol. Biosyst.* **2008**, *4*, 518.
- 22 Gaffney, B. L.; Veliath, E.; Zhao, J.; Jones, R. A. *Org. Lett.* **2010**, *12*, 3269.
- 23 Zhang, Z.; Gaffney, B. L.; Jones, R. A. *J. Am. Chem. Soc.* **2004**, *126*, 16700-16701.
- 24 Zhang, Z.; Kim, S.; Gaffney, B. L.; Jones, R. A. *J. Am. Chem. Soc.* **2006**, *128*, 7015.
- 25 Nakayama, S.; Kelsey, I.; Wang, J.; Sintim, H. O. *Chem. Commun. (Camb)* **2011**, *47*, 4766.

- 26 Nakayama, S.; Kelsey, I.; Wang, J.; Roelofs, K.; Stefane, B.; Luo, Y.; Lee, V. T.; Sintim, H. O. *J. Am. Chem. Soc.* **2011**, *133*, 4856.
- 27 Gentner, M.; Allan, M. G.; Zaehring, F.; Schirmer, T.; Grzesiek, S. *J. Am. Chem. Soc.* **2012**, *134*, 1019.
- 28
- a) ref 9. (PDB code 1W25)
- b) Wassmann, P.; Massa, C.; Zaehring, F.; Schirmer, T. Unpublished result. (PDB code 2WB4)
- c) Wassmann, P.; Chan, C.; Paul, R.; Beck, A.; Heerklotz, H.; Jenal, U.; Schirmer, T. *Structure* **2007**, *15*, 915. (PDB code 2V0N)
- d) De, N.; Pirruccello, M.; Krasteva, P. V.; Bae, N.; Raghavan, R. V.; Sondermann, H. *PLoS Biol.* **2008**, *6*, e67. (PDB code 3BRE)
- e) ref 29. (PDB code 3I5A, 3I5B and 3I5C)
- f) Vorobiev, S.; Neely, H.; Seetharaman, J.; Wang, H.; Foote, E. L.; Ciccocanti, C.; Sahdev, S.; Xiao, R.; Acton, T. B.; Montelione, G. T.; Tong, L.; Hunt, J. F. Unpublished result. (PDB code 3IGN)
- g) Yang, C. Y.; Chin, K. H.; Chuah, M. L.; Liang, Z. X.; Wang, A. H.; Chou, S. H. *Acta Crystallogr., Sect. D* **2011**, *67*, 997. (PDB code 3QYY)
- h) Whitney, J. C.; Colvin, K. M.; Marmont, L. S.; Robinson, H.; Parsek, M. R.; Howell, P. L. *J. Biol. Chem.* **2012**, *287*, 23582. (PDB code 4DN0)
- i) Minasov, G.; Padavattan, S.; Shuvalova, L.; Brunzelle, J. S.; Miller, D. J.; Baslé, A.; Massa, C.; Collart, F. R.; Schirmer, T.; Anderson, W. F. *J. Biol. Chem.* **2009**, *284*, 13174. (PDB code 2W27)
- j) Navarro, M. V.; De, N.; Bae, N.; Wang, Q.; Sondermann, H. *Structure* **2009**, *17*, 1104. (PDB code 3HV8 and 3HV9)
- k) Navarro, M. V.; Newell, P. D.; Krasteva, P. V.; Chatterjee, D.; Madden, D. R.; O'Toole, G. A.; Sondermann, H. *PLoS Biol.* **2011**, *9*, e1000588. (PDB code 3PJT and 3PJU)
- l) Chang, C.; Xu, X.; Cui, H.; Savchenko, A.; Yakunin, A.; Edwards, A.; Joachimiak, A. *J. Mol. Biol.* **2010**, *402*, 524. (PDB code: 3N3T)
- m) Benach, J.; Swaminathan, S. S.; Tamayo, R.; Handelman, S. K.; Folta-Stogniew, E.; Ramos, J. E.; Forouhar, F.; Neely, H.; Seetharaman, J.; Camilli, A.; Hunt, J. F. *EMBO J.* **2007**, *26*, 5153. (PDB code 2RDE)
- n) Habazettl, J.; Allan, M. G.; Jenal, U.; Grzesiek, S. *J. Biol. Chem.* **2011**, *286*, 14304. (PDB code 2L74)
- o) Ko, J.; Ryu, K. S.; Kim, H.; Shin, J. S.; Lee, J. O.; Cheong, C.; Choi, B. S. *J. Mol. Biol.* **2010**, *398*, 97. (PDB code 3KYF and 3KYG)
- 29 De, N.; Navarro, M. V.; Raghavan, R. V.; Sondermann, H. *J. Mol. Biol.* **2009**, *393*, 619.
- 30 Rao, F.; Yang, Y.; Qi, Y.; Liang, Z. X. *J. Bacteriol.* **2008**, *190*, 3622.
- 31 Kulasekara, B. R.; Kulasekara, H. D.; Wolfgang, M. C.; Stevens, L.; Frank, D. W.; Lory, S. *J. Bacteriol.* **2006**, *188*, 4037.
- 32 Merighi, M.; Lee, V. T.; Hyodo, M.; Hayakawa, Y.; Lory, S. *Mol. Microbiol.* **2007**, *65*, 876.
- 33 Remminghorst, U.; Rehm, B. H. *FEBS Lett.* **2006**, *580*, 3883.

- 34 Khakshoor, O.; Wheeler, S. E.; Houk, K. N.; Kool, E. T. *J. Am. Chem. Soc.* **2012**, *134*, 3154.
- 35 Kool, E. T.; Sintim, H. O. *Chem. Commun. (Camb)* **2006**, 3665.
- 36 Chen, M. W.; Kotaka, M.; Vonrhein, C.; Bricogne, G.; Rao, F.; Chuah, M. L.; Svergun, D.; Schneider, G.; Liang, Z. X.; Lescar, J. *J. Bacteriol.* **2012**, *194*, 4837.
- 37 Lubini, P.; Zürcher, W.; Egli, M. *Chem. Biol.* **1994**, *1*, 39.
- 38 Cummins, L. L.; Owens, S. R.; Risen, L. M.; Lesnik, E. A.; Freier, S. M.; McGee, D.; Guinosso, C. J.; Cook, P. D. *Nucleic Acids Res.* **1995**, *23*, 2019.
- 39 Frisch, M. J.; et al. *Gaussian 09, Revision A02 ed.*, Gaussian Inc., Wallingford, CT, **2009**.
- 40 Merritt, J. H.; Ha, D. G.; Cowles, K. N.; Lu, W.; Morales, D. K.; Rabinowitz, J.; Gitai, Z.; O'Toole, G. A. *mBio* **2010**, *1*, e00183.
- 41 Kulasakara, H.; Lee, V.; Brencic, A.; Liberati, N.; Urbach, J.; Miyata, S.; Lee, D. G.; Neely, A. N.; Hyodo, M.; Hayakawa, Y.; Ausubel, F. M.; Lory, S. *Proc. Natl. Acad. Sci. U. S. A.* **2006**, *103*, 2839.
- 42 Sintim, H. O.; Smith, J. A.; Wang, J.; Nakayama, S.; Yan, L. *Future Med. Chem.* **2010**, *2*, 1005.
- 43 Rogers, S. A.; Huigens, R. W.; Melander, C. *J. Am. Chem. Soc.* **2009**, *131*, 9868.
- 44 Huigens, R. W.; Richards, J. J.; Parise, G.; Ballard, T. E.; Zeng, W.; Deora, R.; Melander, C. *J. Am. Chem. Soc.* **2007**, *129*, 6966.
- 45 Frei, R.; Breitbach, A. S.; Blackwell, H. E. *Angew. Chem. Int. Ed. Engl.* **2012**, *51*, 5226.
- 46 Furukawa, S.; Akiyoshi, Y.; O'Toole, G. A.; Ogihara, H.; Morinaga, Y. *Int. J. Food Microbiol.* **2010**, *138*, 176.
- 47 Gamby, S.; Roy, V.; Guo, M.; Smith, J. A.; Wang, J.; Stewart, J. E.; Wang, X.; Bentley, W. E.; Sintim, H. O. *ACS Chem. Biol.* **2012**, *7*, 1023.
- 48 Guo, M.; Gamby, S.; Nakayama, S.; Smith, J.; Sintim, H. O. *Sensors* **2012**, *12*, 3762.
- 49 Singh, V.; Evans, G. B.; Lenz, D. H.; Mason, J. M.; Clinch, K.; Mee, S.; Painter, G. F.; Tyler, P. C.; Furneaux, R. H.; Lee, J. E.; Howell, P. L.; Schramm, V. L. *J. Biol. Chem.* **2005**, *280*, 18265.
- 50 Singh, V.; Shi, W.; Almo, S. C.; Evans, G. B.; Furneaux, R. H.; Tyler, P. C.; Painter, G. F.; Lenz, D. H.; Mee, S.; Zheng, R.; Schramm, V. L. *Biochemistry* **2006**, *45*, 12929.
- 51 Kelsey, I.; Nakayama, S.; Sintim, H. O. *Bioorg. Med. Chem. Lett.* **2012**, *22*, 881.
- 52 Roelofs, K. G.; Wang, J.; Sintim, H. O.; Lee, V. T. *Proc. Natl. Acad. Sci. U. S. A.* **2011**, *108*, 15528.

Chapter 3. Binding studies between c-di-GMP analogs and c-di-GMP riboswitch

(This chapter was published in Zhou et al. Molecules 2012, 17, 13376)

3.1 Synthesis and polymorphism of endo-S-c-di-GMP analogs

3.1.1 Introduction

As described previously, c-di-GMP is known to bind to DGCs¹⁻³, PDEs^{4,5}, PilZ domain proteins⁶⁻⁸, transcriptional regulators^{9,10} and RNA riboswitches^{11,12}. Small molecules that could compete with c-di-GMP for binding to receptors have the potential to inhibit biofilm formation and virulence factors production in bacteria. There are several precedents whereby the modifications of natural nucleotides have produced analogs with interesting biological profiles and some of these analogs could even have clinical utility.¹³⁻²¹ Previously, we showed that a conservative change to one of the phosphodiester “bridging” oxygens in c-di-GMP gave an analog called endo-S-c-di-GMP (**3.2**), see **Figure 3.1**, which has a much lower propensity to form aggregates compared to c-di-GMP.²² Importantly, endo-S-c-di-GMP could compete with the natural c-di-GMP for binding to RocR, a PDE, but had little affinity for WspR (a DGC) or Alg44 (a PilZ-containing protein). This suggests that modifications to the phosphate moiety of c-di-GMP, at the bridging oxygen position at the phosphodiester moiety could give analogs of c-di-GMP, which could be used to selectively target c-di-GMP receptors.

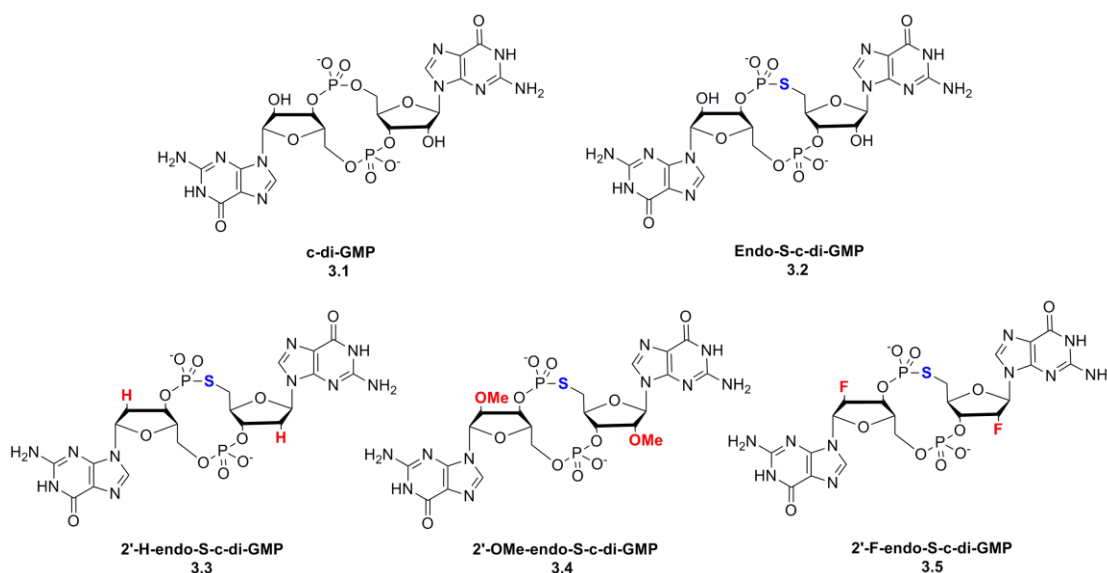


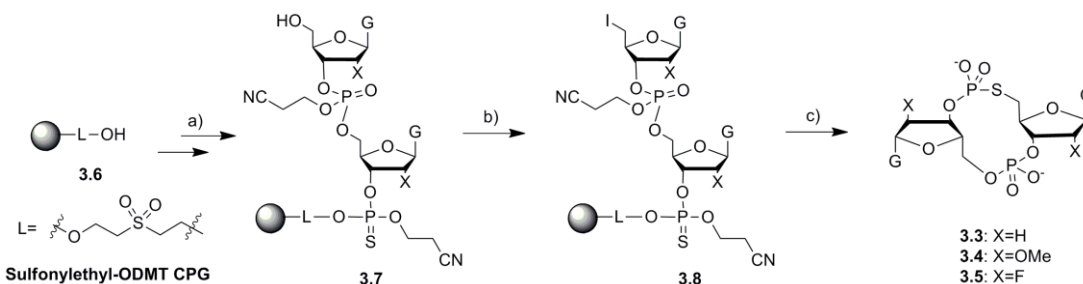
Figure 3.1 Family of dual-modified c-di-GMP analogs (endo-S-c-di-GMP analogs) synthesized.

Recent reports suggest that the 2'-modification of c-di-GMP differentially affected binding of these analogs to c-di-GMP riboswitches.^{12,23-26} We wondered if the simultaneous modification of both the phosphate, at the bridging oxygen position of the phosphodiester moiety, and the 2'-position would lead to another series of c-di-GMP analogs with differential binding profiles. Herein, we describe the synthesis, biophysical characterization and binding to Vc2 RNA of this new class of c-di-GMP analogs (called endo-S-c-di-GMP analogs), see **Figure 3.1** for structures.

3.1.2 Synthesis of endo-S-c-di-GMP analogs

Endo-S-c-di-GMP analogs (3.3 to 3.5) were facilely synthesized on a solid support,²⁷ following the strategy outlined in Scheme 3.1. Briefly, a guanosine phosphoramidite was coupled to a phosphate CPG and the first nucleotide was sulfurized using commercially available Beaucage reagent. The second coupling was done, also with

the same guanosine phosphoramidite, but this time iodine was used for the oxidation step to give an interlinking phosphate. The DMT group was then deprotected, using trichloroacetic acid and the 5'-hydroxyl group was converted into an iodide. The dinucleotide was then cleaved from the solid support with NH_4OH (30% in water). This step also cleaved the cyanoethyl protecting group on the phosphate as well as the acetyl group on the exocyclic amine of the guanine. Upon cleavage from the solid support, a cyclization ensued via a $\text{S}_\text{N}2$ displacement of the 5'-iodide with the 3'-phosphorothioate group. The 2'-OTBS group was then deprotected, using $\text{NEt}_3 \cdot 3\text{HF}$.



Scheme 3.1 Synthesis of endo-S-c-di-GMP analogs (**3.3** to **3.5**). *Reagents and conditions:* a) programmed DNA synthesizer; b) methyltriphenoxyphosphonium iodide, 2,6-lutidine, anhydrous DMF, rt, 1h; c) 30% NH_4OH , 40 °C, 12h.

3.1.3 Polymorphism of endo-S-c-di-GMP analogs

The equilibrium of different polymorphic states of c-di-GMP, dictated by the physiological condition of the bacterial cells, is highly relevant to the bacterial virulence and mobility. Given the flexibility of the c-di-GMP macrocycle, different sugar pucker modes of the nucleosides, the rotation of the glycosidic bonds and the intercalation of the two guanosine moieties, it is expected that c-di-GMP and its analogs may exhibit polymorphs with subtle energy difference. The adoption of the

conformation for each c-di-GMP molecule in physiological condition depends on various factors, including the ion intensity, c-di-GMP concentration and the receptor protein or RNA that it interacts with. The crystal structures of c-di-GMP/protein or c-di-GMP/RNA complexes show that c-di-GMP can bind to different receptors using in different conformational modes. For example, c-di-GMP binds to most I-sites of DGCs as a self intercalated dimer¹ whereas for PDEs and some PilZ proteins, c-di-GMP binds to the active site as a monomer in either the open form (whereby the two guanines are relatively far away to each other)⁴ or the closed form (whereby the two guanines are relatively closed to each other).⁷ Recently Chou et al. further observed that different proteins could bind to different conformers (with different glycosidic bond angles and/or the sugar pucker modes) of the open form of c-di-GMP.²⁸ Thus it is possible to selectively target c-di-GMP receptors with c-di-GMP-like molecules that mainly exist in a particular conformation, which nicely fits into the binding site of an effector protein or RNA.

C-di-GMP (**3.1**) at millimolar concentrations and in the presence of potassium cations also forms several polymorphs of aggregates, including dimers, tetramers and octamers (which contain G-tetrads).^{22,29,30} Interestingly, by replacing one of the bridging oxygens of the phosphodiester units in c-di-GMP with a sulfur atom (a conservative modification) to give an analog that we name endo-S-c-di-GMP (**3.2**), the propensity to form G-quadruplex drastically diminishes.²² We have proposed that one could therefore make a gross prediction for the relative propensity of c-di-GMP analogs to form G-quadruplexes by calculating the relative energies of one of the

open conformers (where the two guanines are 13.5 Å apart, using distances obtained from crystal structures of self-intercalated c-di-GMP complexes) to the closed conformer (where the two guanines are 6.8 Å apart).²² To simplify the computational study, the structures computed in this paper all adopt C2 symmetry, which resemble either the closed conformer (*anti* C3'-endo) or one of the three open conformers (*anti* C2'-endo) demonstrated in Chou's work.²⁸ Following our precedent²², and using Gaussian 09 software³¹ we obtained relative energy differences between the “closed” and “open” conformers of c-di-GMP and each analog (**3.2** to **3.5**), see Table 1. The closed conformers of both c-di-GMP (**3.1**), endo-S-c-di-GMP (**3.2**) and 2'-F-endo-S-c-di-GMP (**3.5**) seem to be more stable than the open conformers, whereas for 2'-H-endo-S-c-di-GMP (**3.3**) the energies of both conformers are similar. On the other hand, the open conformer of 2'-OMe-endo-S-c-di-GMP (**3.4**) appears to be more stable than the closed conformer. We note however that these calculations are simplistic and might not model hydration and salt effects very well, so the obtained values have to be interpreted with caution. Nonetheless, the computed data reveals that subtle differences at the phosphate and 2'-position of c-di-GMP could drastically affect the conformation of the molecule. Based on our computational study, we expected that the conformational preference for 2'-F-endo-S-c-di-GMP (**3.5**) would be similar to endo-S-c-di-GMP (**3.2**) whereas 2'-H-endo-S-c-di-GMP (**3.3**) and 2'-OMe-c-di-GMP (**3.4**) would behave differently from endo-S-c-di-GMP (**3.2**) and might have a lower propensity to form G-quadruplexes, because the closed conformer, which is required for G-quadruplex formation is predicted to be the minor conformer in these analogs.

When c-di-GMP forms G-quadruplexes, each monomer unit exists in the closed conformer.³⁰ We wondered if the trend seen in our computational study (**Table 3.1**) would correlate with the aggregative properties of the various endo-S-c-di-GMP analogs. We used NMR to characterize the aggregates in the absence or presence of potassium. Previously we used DOSY experiment followed by T₁/T₂ relaxation analysis to obtain the diffusion constants of c-di-GMP (**3.1**) and endo-S-c-di-GMP (**3.2**).²² Because an inverse relationship exists between the size of a particle and diffusion rate, the T₁/T₂ relaxation analysis can be used to deduce the size of an aggregate, if data for the monomer can be obtained.

Table 3.1 Computed energy difference between “open” and “closed” forms of c-di-GMP (**3.1**) and analogs (**3.2** to **3.5**).

	$\Delta E^{sol}(\text{open-closed})^a$	ratio (open : closed) ^b
c-di-GMP	1.9	1:25
endo-S-c-di-GMP	1.3	1:9
2'-H-endo-S-c-di-GMP	-0.3	2:1
2'-OMe-endo-S-c-di-GMP	-2.2	39:1
2'-F-endo-S-c-di-GMP	0.5	1:3

^aThe electronic energy was computed with Gaussian 09 software with HF/6-31G(d) basis set. Solvent effect (H₂O) was calculated using Onsager's model in a self-consistent reaction field.^bThe ratio was determined from the equilibrium constant *K*, obtained from the equation $\Delta E = -RT \ln K$ (*T* = 298 K).

NMR data revealed that 2'-H-endo-S-c-di-GMP (**3.3**) and 2'-OMe-endo-S-c-di-GMP (**3.4**) did not form higher aggregates, even upon the addition of K^+ (see **Figures 3.2b** and **3.3b**), which show that no new peaks appeared when potassium was added to a solution containing these two endo-S-c-di-GMP analogs. However, 2'-F-endo-S-c-di-GMP (**3.5**) formed higher aggregates (octamers) in the presence of potassium cations, see **Figure 3.4**. For 2'-F-endo-S-c-di-GMP, the two singlet at 8.05 and 7.92 ppm are assigned to the two guanine H8 and two sets of doublet at 6.28 and 6.18 ppm are assigned to the anomeric H1' (see **Figure 3.4c**). We notice that the line width of the 2'-F-endo-S-c-di-GMP peaks at 8.05 and 7.92 ppm are quite broad at 30 °C but become narrow when potassium is added. Grzesiek and co-workers have shown that monomeric c-di-GMP is in equilibrium with dimeric form and it is plausible that the line broadening in the absence of potassium is the effect of the dynamic process arising from the monomer-dimer exchange.³² An alternative explanation could be that the line broadening is due to conformational heterogeneity (i.e. introduction of a fluorine atom at the 2' position changes the C2'-endo or C3'-endo equilibrium in the sugar ring, and the addition of K^+ ion changes this equilibrium rate). Upon adding 100 mM K^+ to a solution containing 2'-F-endo-S-c-di-GMP (**3.5**), more peaks appeared near 8.00 ppm and 6.10 ppm, (see **Figure 3.4b**), which we interpret as evidence of aggregate formation.²² Our interpretation is augmented by the fact that heating the solution to 60 °C resulted in the disappearance of the additional peaks, meaning that the new species that gave rise to the additional peaks contained non-covalent interactions. Additionally, DOSY experiments also confirmed that potassium promoted higher aggregation of 2'-F-endo-S-c-di-GMP; the new peaks (8.30 and 7.72

ppm, see peaks **1** and **4** on **Figure 3.4b**) that appeared in the 2'F-endo-S-c-di-GMP ¹H NMR, when potassium was added, have diffusion constants of $2.80 \times 10^{-10} \text{ m}^2\text{s}^{-1}$ and $2.72 \times 10^{-10} \text{ m}^2\text{s}^{-1}$, whereas the peak at 8.00 ppm and 6.10 ppm (see peaks **2** and **3** on **Figure 3.4b**) have diffusion constants $4.67 \times 10^{-10} \text{ m}^2\text{s}^{-1}$ and $4.75 \times 10^{-10} \text{ m}^2\text{s}^{-1}$. If peaks **2** and **3** mainly correspond to monomeric c-di-GMP with calculated radius of 6.82 Å, then the peaks at **1** and **4**, which have experimental diffusion constants of $2.80 \times 10^{-10} \text{ m}^2\text{s}^{-1}$ and $2.72 \times 10^{-10} \text{ m}^2\text{s}^{-1}$ would correspond to a species of radius 11.60 Å. This radius corresponds to the calculated radius (11.92 Å) of octameric 2'F-endo-S-c-di-GMP and hence provides additional evidence that the addition of potassium to 2'F-endo-S-c-di-GMP causes aggregation mainly to octameric forms.

We have previously shown that endo-S-c-di-GMP (**3.2**) does not readily form G-quadruplexes and commented that c-di-GMP G-quadruplex formation is sensitive to modifications (even conservative ones). Here we observe that a double modification (phosphate to phosphorothioates and 2'-OH to 2'-F) can restore the propensity to form G-quadruplexes. Conversely, we found that for the other two double modifications analyzed in this study (2'-H and 2'-OMe from 2'-OH), there is no restoration of the ability to form G-quadruplexes. This suggests that there is selectivity of the 2' modification in the ability to form G-quadruplexes which is able to override the deleterious endo-S modification in the case of the 2'-F-endo-S analog.

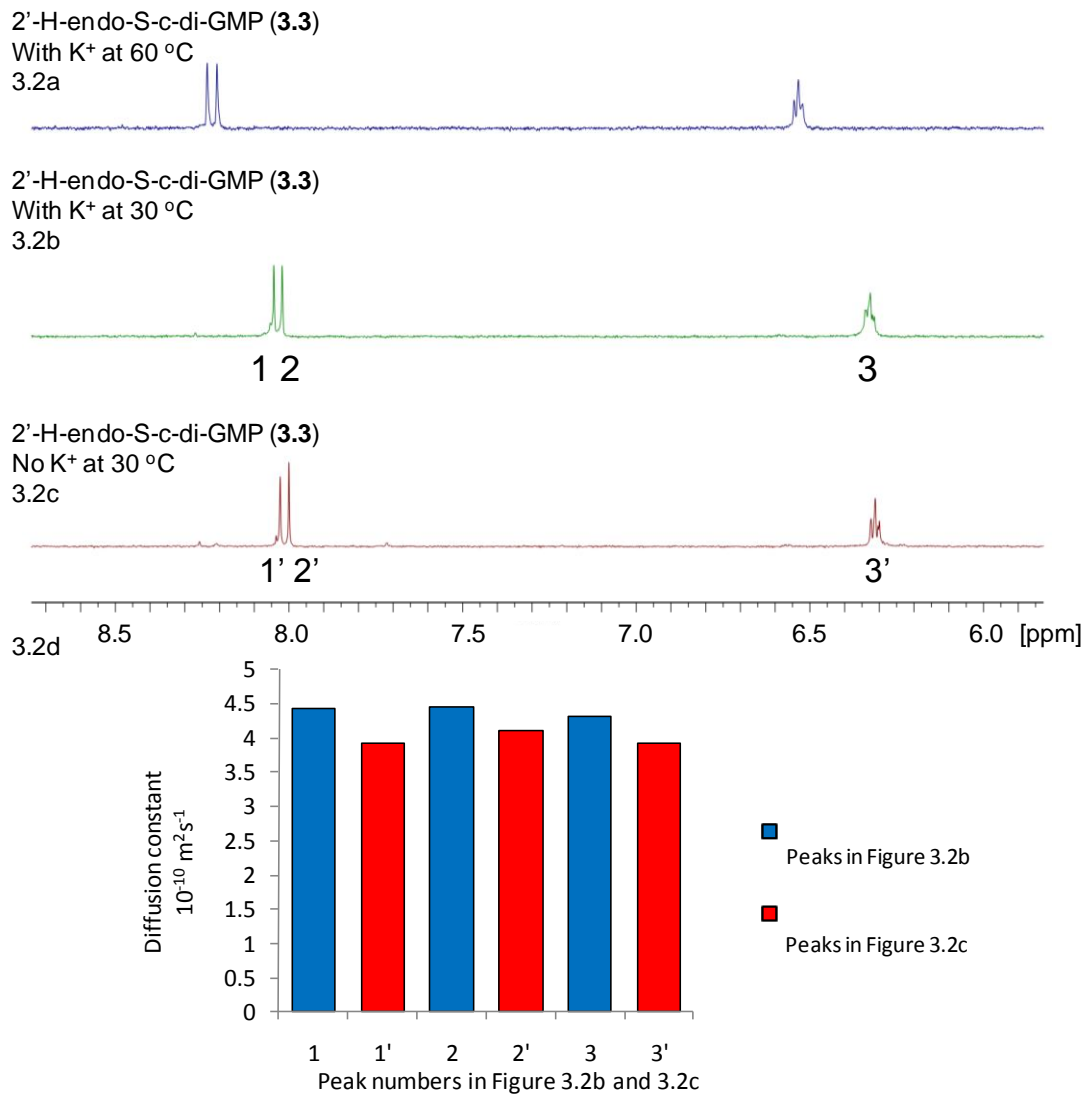


Figure 3.2 ¹H NMR stacked spectra of 3.0 mM analog **3.3** in D₂O. (a) 3.0 mM 2'-H-endo-S-c-di-GMP, 100 mM KCl, 60 °C. (b) 3.0 mM 2'-H-endo-S-c-di-GMP, 100 mM KCl, 30 °C. (c) 3.0 mM 2'-H-endo-S-c-di-GMP, no metal cation, 30 °C. (d) 3.0 mM 2'-H-endo-S-c-di-GMP, T₁/T₂ relaxation analysis (from DOSY experiments).

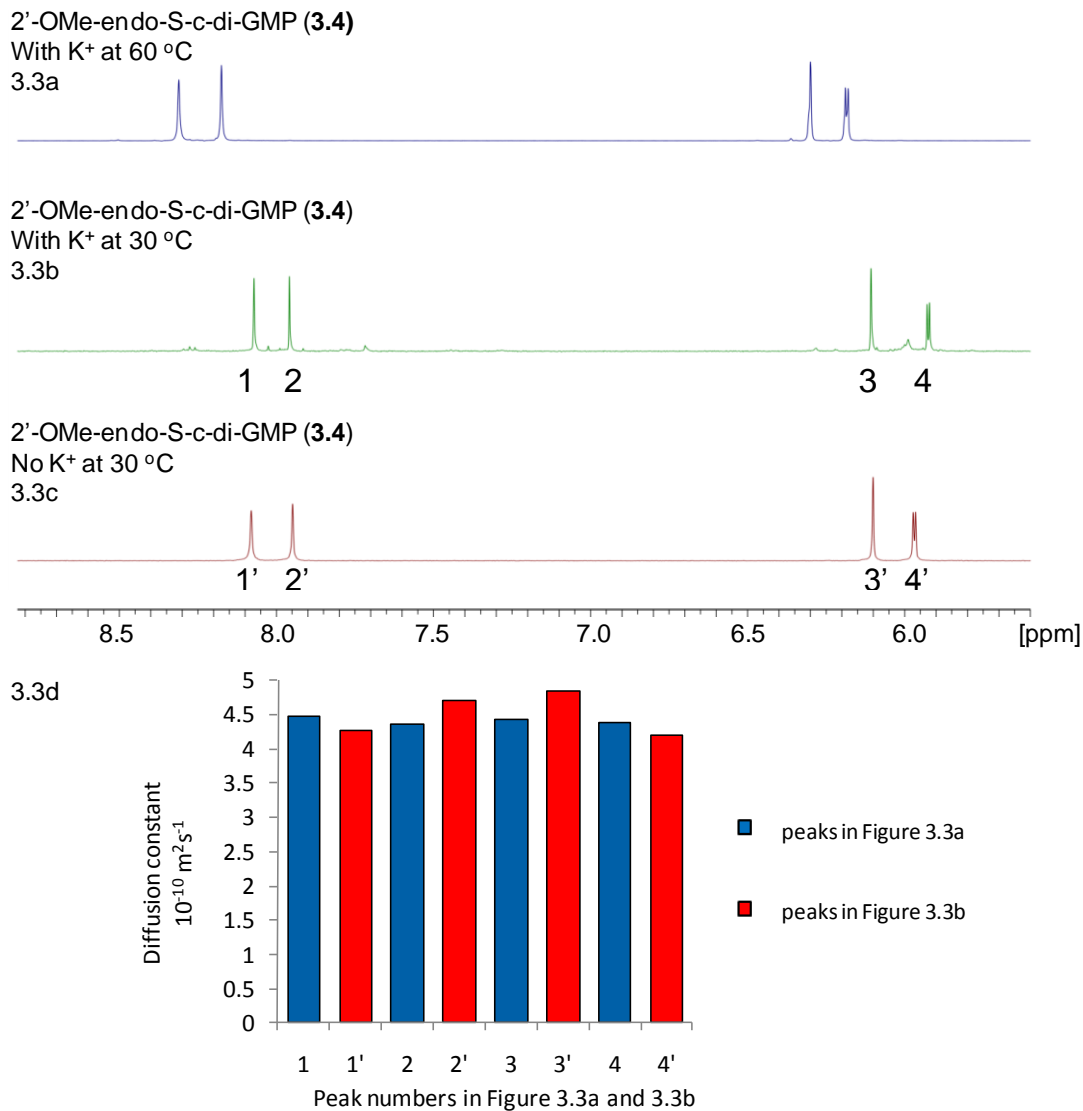


Figure 3.3 ¹H NMR stacked spectra of 3.0 mM analog **3.4** in D₂O. (a) 3.0 mM 2'-OMe-endo-S-c-di-GMP, 100 mM KCl, 60 °C. (b) 3.0 mM 2'-OMe-endo-S-c-di-GMP, 100 mM KCl, 30 °C. (c) 3.0 mM 2'-OMe-endo-S-c-di-GMP, no metal cation, 30 °C. (d) 3.0 mM 2'-OMe-endo-S-c-di-GMP, T1/T2 relaxation analysis (from DOSY experiments).

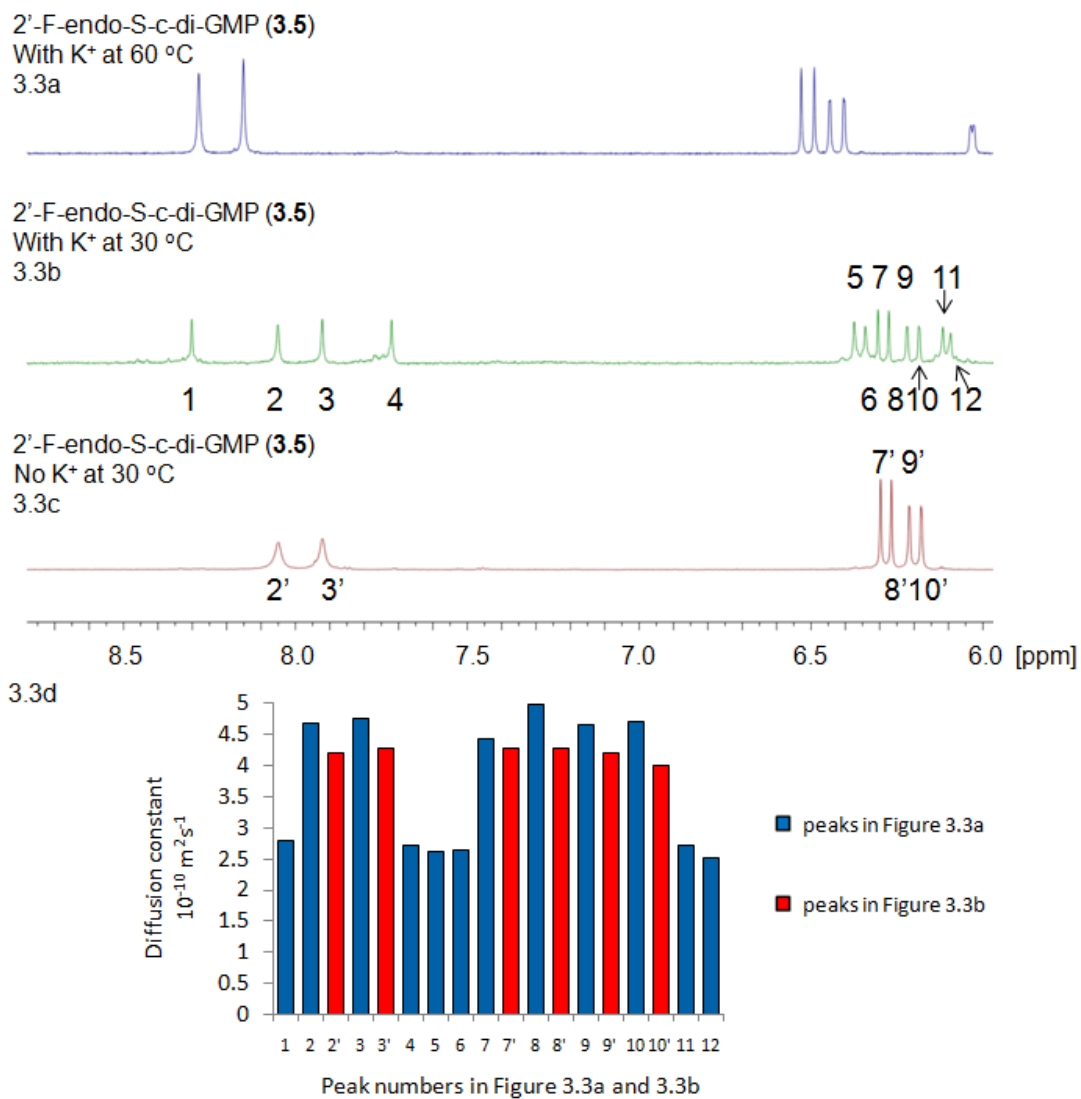


Figure 3.4 ¹H NMR stacked spectra of 3.0 mM analog **3.5** in D₂O. (a) 3.0 mM 2'-F-endo-S-c-di-GMP, 100 mM KCl, 60 °C. (b) 3.0 mM 2'-F-endo-S-c-di-GMP, 100 mM KCl, 30 °C. (c) 3.0 mM 2'-F-endo-S-c-di-GMP, no metal cation, 30 °C. (d) 3.0 mM 2'-F-endo-S-c-di-GMP, T1/T2 relaxation analysis (from DOSY experiments).

3.2 Binding Studies between endo-S-c-di-GMP analogs and Class I riboswitch

One of the motivations for making c-di-GMP analogs is to obtain small molecules that could have the potential to disrupt c-di-GMP signaling in bacteria. C-di-GMP has been shown to bind to several receptors types (both proteins and RNA).^{22-26,33,34} The crystal structures of c-di-GMP bound to both class I and II riboswitches have been solved.³⁵⁻³⁷ For class I riboswitch, c-di-GMP is bound in the closed form (see **Figure 3.5**). In a detailed study by Strobel and co-workers, it was demonstrated that substitution of the 2'-position of c-di-GMP was detrimental for binding to class I riboswitch, Vc2 RNA.²³ We have also revealed that the modification of the phosphate moiety of c-di-GMP decreased affinity for class I riboswitch Vc2 RNA,²⁶ whereas binding to RocR (a phosphodiesterase) was not affected.²² Therefore it might be possible to design c-di-GMP analogs that could selectively bind to one class of c-di-GMP receptor (for example proteins) and not others (for example RNA riboswitches).

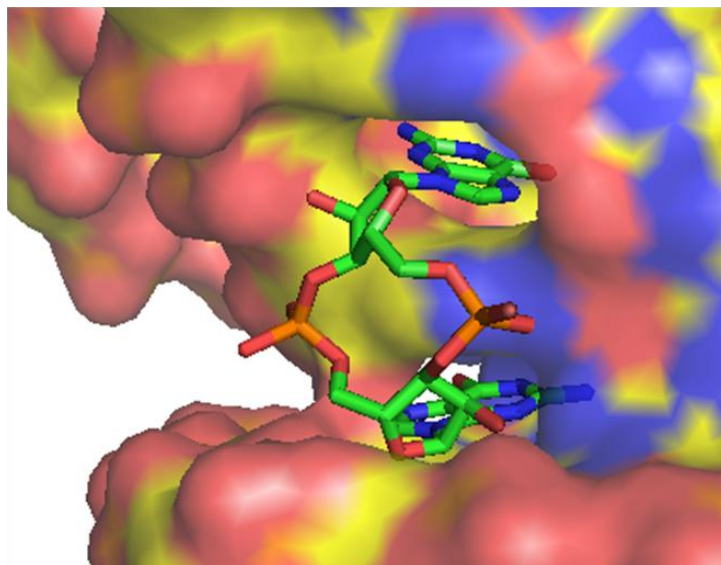


Figure 3.5 Co-crystal structure of c-di-GMP bound to Vc2 RNA (PDB code: 3IRW). C-di-GMP is shown in sticks and colored by atom (oxygen in red, nitrogen in blue, carbon in green and phosphorus in orange). Vc2 RNA is shown as surface and colored by atom (oxygen in red, nitrogen in blue and carbon in yellow).

We investigated if the simultaneous modification of the phosphate and 2'-position of c-di-GMP would additively abrogate binding to the class I riboswitch. Several binding assays to investigate the binding of c-di-GMP and analogs to RNA receptors have been described, including competition with radio-labeled c-di-GMP²³, equilibrium microdialysis²⁶ and fluorescent c-di-GMP sensor, based on Vc2 RNA riboswitch (class I)³⁸. To gain a qualitative picture of the relative binding order of analogs, we opted to use the safer but qualitative fluorescent binding assay for c-di-GMP or analog. The fluorescent c-di-GMP sensor would bind to c-di-GMP or analog in the riboswitch binding site and the binding event is transduced to another domain, which rearranges to bind to DFHBI, a molecule that is weakly fluorescent in water but becomes highly fluorescent upon binding to RNA (called Spinach RNA, see

Figure 3.6). Using this class I riboswitch sensor, it was determined that the relative binding of c-di-GMP and analogs to class I riboswitch is as follows: c-di-GMP (3.1) > endo-S-c-di-GMP (3.2) > 2'-F-endo-S-c-di-GMP (3.5) > 2'-H- and 2'-OMe-endo-S-c-di-GMP (3.3 and 3.4), see **Figure 3.7**.

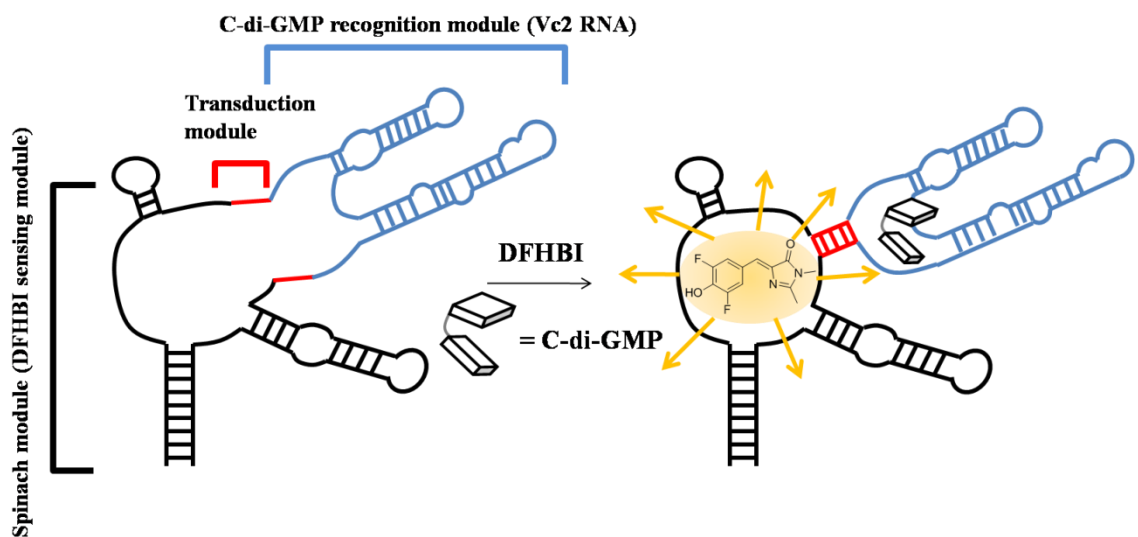


Figure 3.6 C-di-GMP fluorescent riboswitch. Sequence of RNA is, 5'-GAC GCG ACU GAA UGA AAU GGU GAA GGA CGG GUC CAG GC C GCA CAG GGC AAA CCA UUC GAA AGA GUG GGA CGC AAA GCC UCC GGC CUA AAC UUC GGU AGG UAG CGG GGU UAC CGA GC CUU GUU GAG UAG AGU GUG AGC UCC GUA ACU AGU CGC GUC -3'

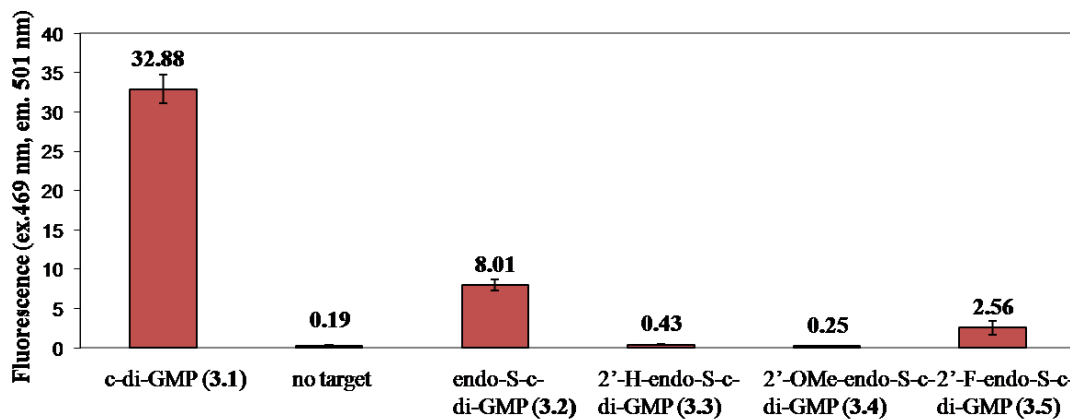


Figure 3.7 Fluorescent c-di-GMP sensor screening for c-di-GMP and analogs (3.2 to 3.5). Conditions: [RNA, SP_2] = 1 μ M, [c-di-GMP and/or analogs] = 10 μ M. Buffer: 100 mM HEPES (pH 6.8) containing 100 mM NaCl, 100 mM KCl and 6 mM MgCl₂. Measurements were done in triplicate.

3.3 Conclusion

We conclude that the modifications of the phosphate and 2'-position of c-di-GMP are additively detrimental to class I riboswitch binding. Curiously we note that this trend is also observed in the propensity to form G-quadruplexes (see **Figures 3.2, 3.3 and 3.4**) and also the computed open:closed conformer ratio (**Table 3.1**). The computed energy differences between the various closed:open forms of c-di-GMP analogs (≤ 2.2 kcal/mol) is however too small, compared to the binding affinity of c-di-GMP and the riboswitch (> 30 kcal/mol) so it is unlikely that the conformer distribution solely accounts for the differences seen in analog binding to class I riboswitch.

References and notes

- 1 Chan, C.; Paul, R.; Samoray, D.; Amiot, N. C.; Giese, B.; Jenal, U.; Schirmer, T. *Proc. Natl. Acad. Sci. U. S. A.* **2004**, *101*, 17084.
- 2 Yang, C. Y.; Chin, K. H.; Chuah, M. L.; Liang, Z. X.; Wang, A. H.; Chou, S. H. *Acta. Crystallogr. D Biol. Crystallogr.* **2011**, *67*, 997.
- 3 Zhou, J.; Sayre, D. A.; Wang, J.; Pahadi, N.; Sintim, H. O. *Molecules* **2012**, *17*, 13376.
- 4 Minasov, G.; Padavattan, S.; Shuvalova, L.; Brunzelle, J. S.; Miller, D. J.; Baslé A.; Massa, C.; Collart, F. R.; Schirmer, T.; Anderson, W. F. *J. Biol. Chem.* **2009**, *284*, 13174.
- 5 Tchigvintsev, A.; Xu, X.; Singer, A.; Chang, C.; Brown, G.; Proudfoot, M.; Cui, H.; Flick, R.; Anderson, W. F.; Joachimiak, A.; Galperin, M. Y.; Savchenko, A.; Yakunin, A. F. *J. Mol. Biol.* **2010**, *402*, 524.
- 6 Ko, J.; Ryu, K. S.; Kim, H.; Shin, J. S.; Lee, J. O.; Cheong, C.; Choi, B. S. *J. Mol. Biol.* **2010**, *398*, 97.
- 7 Benach, J.; Swaminathan, S. S.; Tamayo, R.; Handelman, S. K.; Folta-Stogniew, E.; Ramos, J. E.; Forouhar, F.; Neely, H.; Seetharaman, J.; Camilli, A.; Hunt, J. F. *EMBO J.* **2007**, *26*, 5153.
- 8 Habazettl, J.; Allan, M. G.; Jenal, U.; Grzesiek, S. *J. Biol. Chem.* **2011**, *286*, 14304.
- 9 Hickman, J. W.; Harwood, C. S. *Mol. Microbiol.* **2008**, *69*, 376.
- 10 Baraquet, C.; Murakami, K.; Parsek, M. R.; Harwood, C. S. *Nucleic Acids Res.* **2012**, *40*, 7207.
- 11 Sudarsan, N.; Lee, E. R.; Weinberg, Z.; Moy, R. H.; Kim, J. N.; Link, K. H.; Breaker, R. R. *Science* **2008**, *321*, 411.
- 12 Smith, K. D.; Shanahan, C. A.; Moore, E. L.; Simon, A. C.; Strobel, S. A. *Proc Natl Acad Sci U. S. A.* **2011**, *108*, 7757.
- 13 Cheek, M. A.; Dobrikov, M. I.; Wenefors, C. K.; Xu, Z.; Hashmi, S. N.; Shen, X.; Shaw, B. R. *Nucleic Acids Symp. Ser. (Oxf)* **2008**, *52*, 81.
- 14 Wenefors, C. K.; Dobrikov, M. I.; Xu, Z.; Li, P.; Shaw, B. R. *Bioorg. Chem.* **2008**, *36*, 169.
- 15 Hamm, M. L.; Cholera, R.; Hoey, C. L.; Gill, T. J. *Org. Lett.* **2004**, *6*, 3817.
- 16 Hamm, M. L.; Gill, T. J.; Nicolson, S. C.; Summers, M. R. *J. Am. Chem. Soc.* **2007**, *129*, 7724.
- 17 Wauchope, O. R.; Johnson, C.; Krishnamoorthy, P.; Andrei, G.; Snoeck, R.; Balzarini, J.; Seley-Radtke, K. L. *Bioorg. Med. Chem.* **2012**, *20*, 3009.
- 18 Novikov, M. S.; Ivanova, O. N.; Ivanov, A. V.; Ozerov, A. A.; Valuev-Elliston, V. T.; Temburnikar, K.; Gurskaya, G. V.; Kochetkov, S. N.; Pannecouque, C.; Balzarini, J.; Seley-Radtke, K. L. *Bioorg. Med. Chem.* **2011**, *19*, 5794.
- 19 Cassera, M. B.; Zhang, Y.; Hazleton, K. Z.; Schramm, V. L. *Curr. Top. Med. Chem.* **2011**, *11*, 2103.
- 20 Chemama, M.; Fonvielle, M.; Villet, R.; Arthur, M.; Valéry, J. M.; Etheve-Quellejeu, M. *J. Am. Chem. Soc.* **2007**, *129*, 12642.
- 21 Shukla, S.; Sumaria, C. S.; Pradeepkumar, P. I. *ChemMedChem* **2010**, *5*, 328.

- 22 Wang, J.; Zhou, J.; Donaldson, G. P.; Nakayama, S.; Yan, L.; Lam, Y.-f.; Lee, V. T.; Sintim, H. O. *J. Am. Chem. Soc.* **2011**, *133*, 9320.
- 23 Shanahan, C. A.; Gaffney, B. L.; Jones, R. A.; Strobel, S. A. *J. Am. Chem. Soc.* **2011**, *133*, 15578.
- 24 Smith, K. D.; Strobel, S. A. *Biochem. Soc. Trans.* **2011**, *39*, 647.
- 25 Furukawa, K.; Gu, H.; Sudarsan, N.; Hayakawa, Y.; Hyodo, M.; Breaker, R. R. *ACS Chem. Biol.* **2012**, *7*, 1436.
- 26 Luo, Y.; Zhou, J.; Watt, S. K.; Lee, V. T.; Dayie, T. K.; Sintim, H. O. *Mol. Biosyst.* **2012**, *8*, 772.
- 27 Smietana, M.; Kool, E. T. *Angew. Chem. Int. Ed. Engl.* **2002**, *41*, 3704.
- 28 Chin, K. H.; Kuo, W. T.; Yu, Y. J.; Liao, Y. T.; Yang, M. T.; Chou, S. H. *Acta Crystallogr. D Biol. Crystallogr.* **2012**, *68*, 1380.
- 29 Zhang, Z.; Gaffney, B. L.; Jones, R. A. *J. Am. Chem. Soc.* **2004**, *126*, 16700.
- 30 Zhang, Z.; Kim, S.; Gaffney, B. L.; Jones, R. A. *J. Am. Chem. Soc.* **2006**, *128*, 7015.
- 31 Frisch, M. J.; et al. *Gaussian 09, Revision A02 ed., Gaussian Inc., Wallingford, CT, 2009*.
- 32 Gentner, M.; Allan, M. G.; Zaehring, F.; Schirmer, T.; Grzesiek, S. *J. Am. Chem. Soc.* **2012**, *134*, 1019.
- 33 Ching, S. M.; Tan, W. J.; Chua, K. L.; Lam, Y. *Bioorg. Med. Chem.* **2010**, *18*, 6657.
- 34 Sharma, I. M.; Dhanaraman, T.; Mathew, R.; Chatterji, D. *Biochemistry* **2012**, *51*, 5443.
- 35 Kulshina, N.; Baird, N. J.; Ferré-D'Amaré A. R. *Nat. Struct. Mol. Biol.* **2009**, *16*, 1212.
- 36 Smith, K. D.; Lipchock, S. V.; Ames, T. D.; Wang, J.; Breaker, R. R.; Strobel, S. A. *Nat. Struct. Mol. Biol.* **2009**, *16*, 1218.
- 37 Smith, K. D.; Lipchock, S. V.; Livingston, A. L.; Shanahan, C. A.; Strobel, S. A. *Biochemistry* **2010**, *49*, 7351.
- 38 Nakayama, S.; Luo, Y.; Zhou, J.; Dayie, T. K.; Sintim, H. O. *Chem. Commun. (Camb)* **2012**, *48*, 9059.

Chapter 4. Unexpected Complex Formation between Coralyne and Cyclic Diadenosine Monophosphate Providing a Simple Fluorescent Turn-on Assay to Detect This Bacterial Second Messenger

(This chapter was published in Zhou et al. Anal. Chem. 2014, 86, 2412)

4.1 A simple and selective detection of c-di-AMP by coralyne

4.1.1 Introduction

Cyclic dinucleotides have come to the forefront of microbial research due to the impressive arrays of processes in bacteria that they regulate.¹⁻³ For example, c-di-GMP (the first cyclic dinucleotide to be discovered by Benziman almost three decades ago) has been shown to regulate motility, sessility and biofilm formation, virulence, cell cycle progression, heavy metal resistance, phage resistance, antibiotic resistance, quorum sensing amongst others in myriads of bacteria, including bacteria of clinical and military relevance.⁴⁻⁶ Due to the varied processes in bacteria that c-di-GMP regulates, there has been an explosion of investigations aimed at unraveling processes, which are regulated by this nucleotide.⁷ Recently, another cyclic dinucleotide, c-di-AMP,^{8,9} has also stoked the interests of microbiologists as it has emerged that c-di-AMP is as important a second messenger in bacteria as c-di-GMP. C-di-AMP, originally discovered as a signaling molecule that controls DNA integrity in *B subtilis* has now been shown to regulate bacterial cell size and/or cell wall formation^{8,10} and hence receptors involved in c-di-AMP signaling could become

important antibacterial targets.¹¹ In *S. aureus*, *Listeria monocytogenes* (*L. monocytogenes*) or *B. subtilis*, it has been shown that increased intracellular c-di-AMP endowed these pathogens with the ability to resist β -lactam antibiotics whereas decreased intracellular c-di-AMP concentrations made the bacteria susceptible to antibiotics that target bacterial cell wall synthesis.¹²⁻¹⁶ In some bacteria, c-di-AMP also modulates ion transport across bacterial membranes and is hypothesized to modulate bacterial physiology as the concentration of metals in the environment changes.¹⁷ Apart from the aforementioned processes, c-di-AMP is also involved in resistance to acid¹⁸ and heat stress¹⁹ in some bacteria. In addition to controlling bacterial physiology, c-di-AMP also affects eukaryotic host cells and elicits type I interferon response.²⁰⁻²² Unlike c-di-GMP, for which many of the protein and RNA receptors have been biochemically and biophysically characterized, the metabolism proteins and “adaptor/effector” proteins for c-di-AMP remain largely uncharacterized and the coming years will undoubtedly witness an explosion of biochemical and structural characterizations of c-di-AMP-related proteins and RNA. In this regard, tools that would aid the characterization of c-di-AMP receptors would help delineate the details of c-di-AMP signaling in bacteria. Herein, we provide a surprisingly simple fluorescent detection of c-di-AMP, using readily available coralyne (**Figure 4.1**). We then demonstrate that this new assay can be used to monitor the synthesis c-di-AMP by diadenyl cyclase (DAC), DisA⁸ as well as the degradation of c-di-AMP by the phosphodiesterases YybT¹⁸ and SVPD (snake venom phosphodiesterase). In addition to providing a practical detection of c-di-AMP, this work also suggests that coralyne associates with cyclic adenine nucleotides in a mode that is markedly

different from the well-characterized complex formation between coralyne and linear polyadenine oligonucleotides.²³ The interactions between aromatic heterocycles and DNA/RNA have been intensively studied for several decades due to the link between cancer and these planar intercalators.²⁴ Many of these heterocyclic molecules are known to intercalate into Watson-Crick duplexes, whereas a few have also been reported to intercalate into non-Watson-Crick duplexes²⁵⁻²⁷ and higher order structures, such as triplexes²⁸⁻³³ and G-quadruplexes³⁴⁻³⁹. In the past few years, efforts to design small molecules that could stabilize adenine-rich oligonucleotides have intensified due to potential biotechnological and medical applications of these molecules.⁴⁰⁻⁴⁸ For example, it has been demonstrated that adenine-rich oligonucleotides can form hydrogels in the presence of metals and that these hydrogels are responsive to pH changes.⁴⁹ Polyadenylation is also known to play a role in the progression of cancer and it has been known for more than a decade that tumor cells overexpress poly rA polymerases,⁴³ suggesting that perhaps targeting poly rA could be a viable anti-cancer strategy.⁵⁰⁻⁵³ Poly A duplex formation in the presence of π -system is well known, however, formation of higher order structure with poly A in the presence of heterocyclic intercalators has not been well explored.^{54,55}

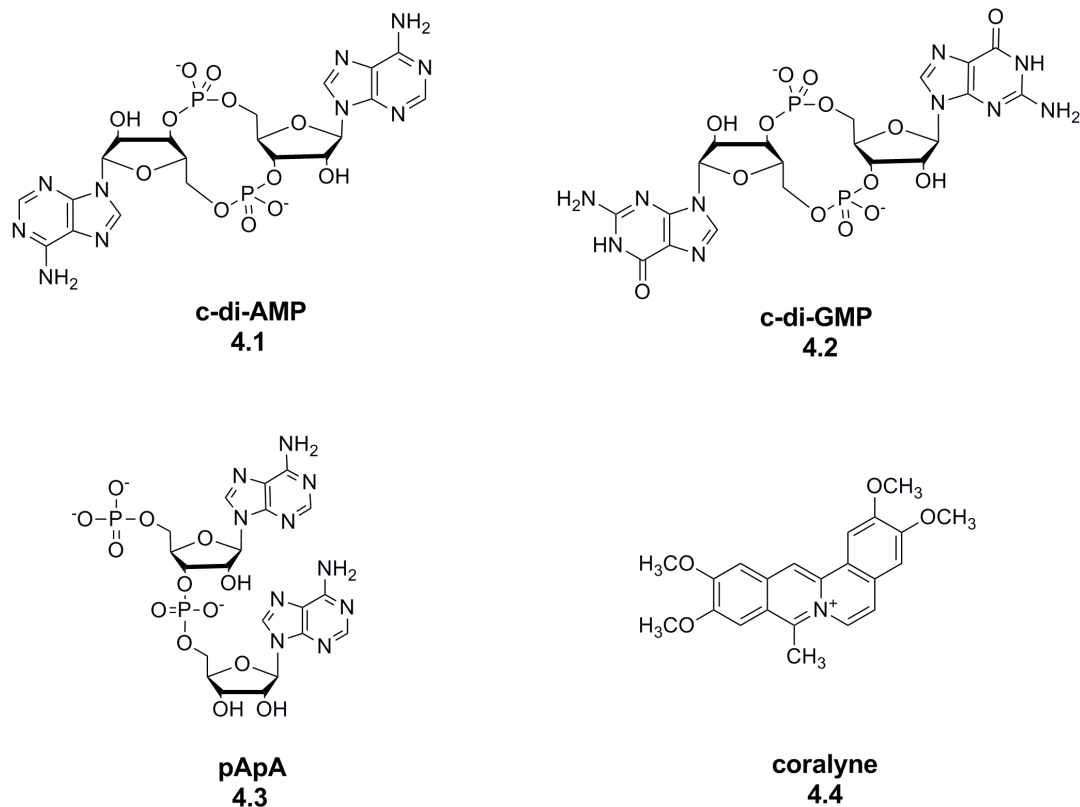


Figure 4.1 Structures of c-di-AMP, c-di-GMP, pApA and coralyne.

4.1.2 The quenching study of coralyne by halide ion

Isoquinoline alkaloids, such as coralyne, are known to bind to adenine-rich oligonucleotides and stabilize adenine-adenine duplexes.^{25,29,30,56-59} In an important paper by Hud and co-workers, it was demonstrated that oligonucleotides containing long tracts of adenine, such as (dA)₁₆ but not (dA)₄, could bind to coralyne and form fibres.⁵⁶ Subsequent works by others have revealed that the fluorescence of coralyne is quenched when bound to poly dA⁶⁰ or rA²⁵. In line with Hud's observation that short polyadenines do not bind coralyne,⁵⁶ when coralyne was incubated with pApA (the degradation product of c-di-AMP by phosphodiesterases) or cAMP in a buffer containing KCl, there was no significant change in both the UV and fluorescence

profiles of coralyne (see **Figure 4.2**). On the other hand, when c-di-AMP (which contains the same number of adenine as pApA) was incubated with coralyne in the presence of KCl, both the UV and fluorescence intensities of coralyne increased (see **Figure 4.2**). It is known that when coralyne binds to polyadenine, its fluorescence and UV absorbance is decreased⁴¹ but here c-di-AMP enhanced the fluorescence and absorbance of coralyne, and this suggests that the binding mode between c-di-AMP and coralyne might be different from the proposed duplex intercalation model.⁴¹

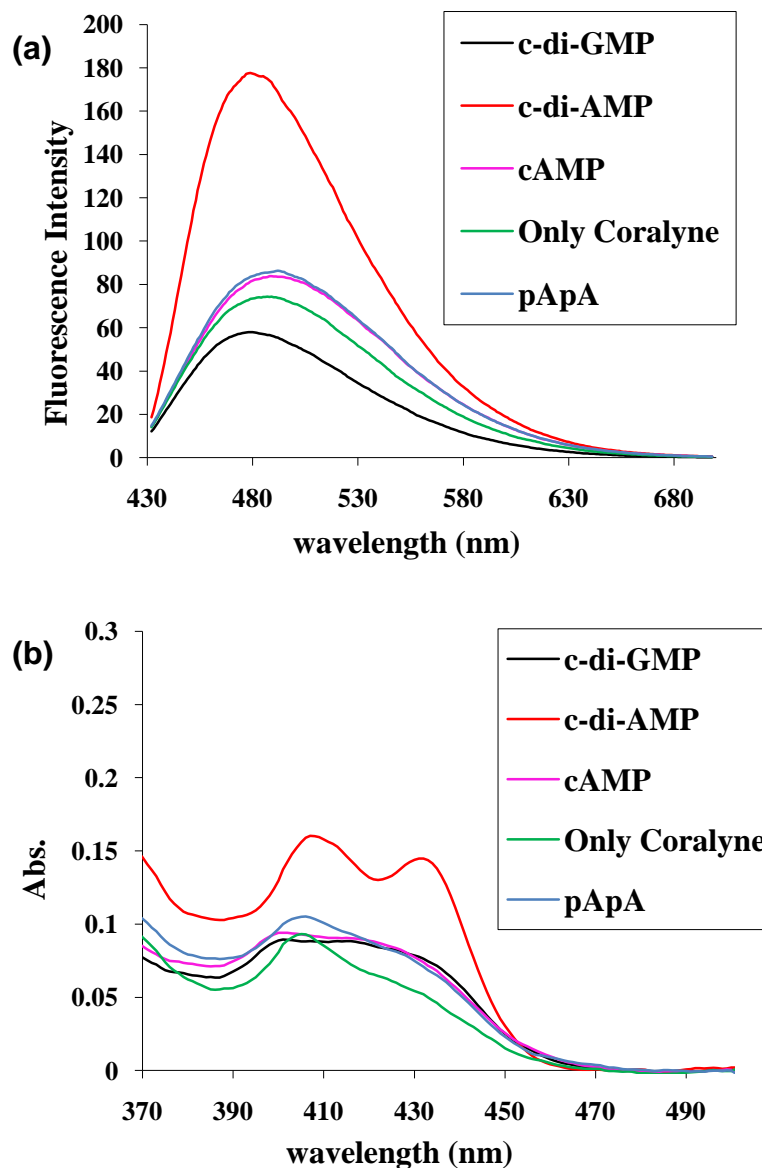


Figure 4.2 Fluorescence (a) and UV (b) profiles of coralyne in the presence of various nucleotides. Condition: [coralyne] = 10 μ M, [nucleotides] = 40 μ M, Buffer: 50 mM Tris- H_3PO_4 (pH 7.5) containing 250 mM KCl. Temperature = 10 $^\circ\text{C}$. ex. 420 nm, em. 475 nm.

Although the fluorescence of coralyne was enhanced by c-di-AMP (~ 3 fold fluorescence increase), in the presence of 250 mM KCl, the high fluorescence of free

coralyne impeded our initial efforts to use coralyne to detect c-di-AMP concentrations lower than 20 μM (see **Figure 4.3**). We therefore sought ways to reduce the fluorescence of the unbound coralyne. We hypothesized that the fluorescence enhancement of coralyne, in the presence of c-di-AMP, was the result of coralyne intercalating between the two adenine bases of c-di-AMP. If this was the case, then it was expected that the bound coralyne would be protected from fluorescence quenchers whereas the unbound coralyne could be readily quenched by anions. Therefore it would be possible to increase the signal-to-noise ratio of c-di-AMP detection using anion-quenching phenomenon.

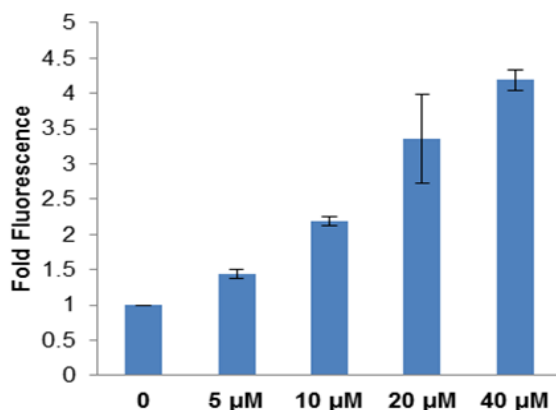


Figure 4.3 The fold fluorescence of coralyne in the presence of c-di-AMP. In the absence of a halogen quencher the unbound coralyne is also fluorescent and therefore changes in fluorescence intensity in the presence of different concentrations of c-di-AMP are not large. For example, the fluorescence fold changes for 10 μM c-di-AMP and 20 μM c-di-AMP or 20 μM and 40 μM are almost similar. The addition of bromide or iodide improves the discrimination between different c-di-AMP concentrations (see **Figure 4.10**). Condition: [coralyne] = 10 μM , Buffer Tris- H_3PO_4 (pH 7.5), [c-di-AMP] = 0, 5, 10, 20 or 40 μM . Temperature = 10 $^\circ\text{C}$. ex. 420 nm, em. 475 nm.

The quenching of coralyne by KBr in absence of c-d-AMP is dominantly static with K_s of 101.2 M^{-1} (from intercept of modified SV plot, $110.2 \text{ M}^{-1} - 9.03 \text{ M}^{-1} \approx 101.2 \text{ M}^{-1}$) compared with dynamic constant of 9.03 M^{-1} (lifetime data, $0.00903 \text{ mM}^{-1} = 9.03 \text{ M}^{-1}$), see **Table 4.1** and **Figure 4.4**. After complexing with c-d-AMP the quenching is significantly reduced; from intensity measurements that include static and dynamic quenching $K_{sv}=0.918 \text{ M}^{-1}$ ($0.00918 \text{ mM}^{-1} = 0.918 \text{ M}^{-1}$) and from lifetime data by 0.521 M^{-1} ($0.00512 \text{ mM}^{-1} = 0.512 \text{ M}^{-1}$), see **Table 4.1** and **Figure 4.5**. For construction of the Stern-Volmer plot, we used average lifetime from two-component fit. There is a slightly better fit with three-exponential, which reveals a long lifetime component of about 30 ns which is in agreement with previous reports on coralyne dimers.⁶¹

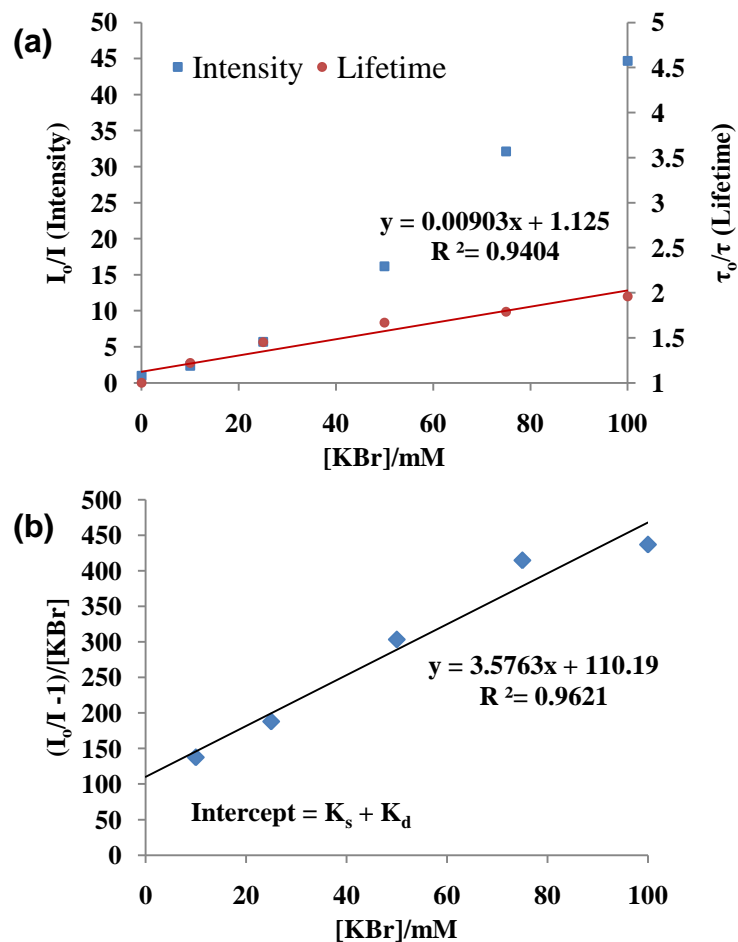


Figure 4.4 (a) KBr quenching of coralyne in 50 mM Tris- H_3PO_4 Buffer (pH 7.5) at 25 °C. The squares show the values of relative intensity and circles of lifetimes. (b) Modified Stern-Volmer plot for quenching of Coralyne with KBr.

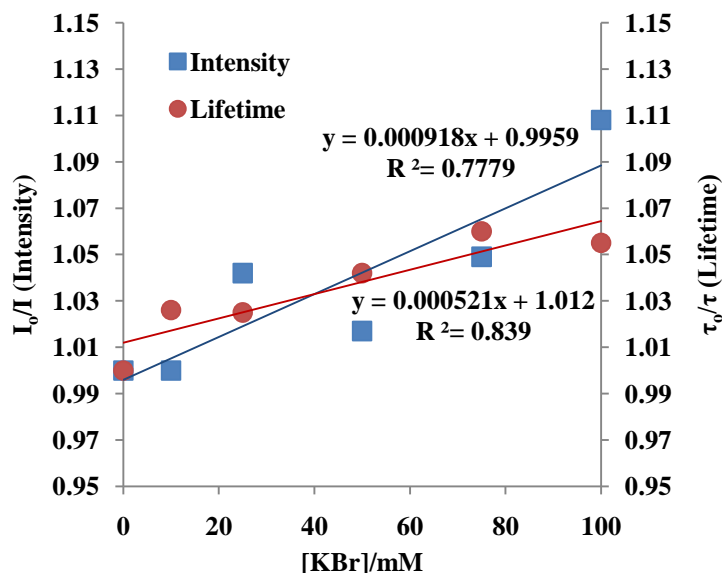


Figure 4.5 KBr quenching of coralyne in presence of 40 μM of c-d-AMP at 25 $^\circ\text{C}$. Buffer: 50 mM Tris- H_3PO_4 (pH 7.5). Squares are intensity and circles are lifetime data.

The quenching of coralyne by KI in absence of c-d-AMP is also dominantly static with K_s of $35,860 \text{ M}^{-1}$ (intensity data, $35.86 \text{ mM}^{-1} = 35,860 \text{ M}^{-1}$) compared with dynamic constant of 912.0 M^{-1} (lifetime data, $0.912 \text{ mM}^{-1} = 912.0 \text{ M}^{-1}$), see **Figure 4.6**. After complexing with c-d-AMP the quenching by KI is significantly reduced (see **Figure 4.6**); from intensity measurements that include static and dynamic quenching $K_{\text{svc}} = 25.6 \text{ M}^{-1}$ ($0.0256 \text{ mM}^{-1} = 25.6 \text{ M}^{-1}$) and from lifetime data $K_{\text{sv}} = 6.4 \text{ M}^{-1}$ ($0.0064 \text{ mM}^{-1} = 6.4 \text{ M}^{-1}$). Overall, KI is significantly stronger quencher than KBr for coralyne and similar quenching effect can be obtained with ~ 100 times lower concentration compared to KBr. However, KI also partially quenches coralyne even when c-di-AMP is present so for our c-di-AMP detection, we decided to use KBr as the quencher.

Table 4.1 Fluorescence quenching of coralyne with KBr. ex. 445 nm, em 480/30 nm.

Quencher (KBr) [mM]	In absence of c-di-AMP					In presence of 40 μ M of c-di-AMP					I
	τ_1 ($\nu\sigma$)	f_i	$\tau_{\alpha\omega\gamma}$ ($\nu\sigma$)	χ^2	τ_o / τ (I_0/I)	τ_1 ($\nu\sigma$)	f_i	$\tau_{\alpha\omega\gamma}$ ($\nu\sigma$)	χ^2	τ_o / τ (I_0/I)	
0	14.22	1	14.2	1.92							
I=242	9.82	0.317			1	n/a	n/a	n/a	n/a	n/a	n/a
I=228	<32>	0.683	24.97	1.16							
10	11.56	1	11.56	1.45	1.23	12.13	1	12.13	30		
I=96	9.66	0.562			(2.38)	2.33	0.137				
	<32>	0.438	19.45	1.07		19	0.863	16.73	1.86	1	428
						1.29	0.072				
						5.92	0.131				
						28.73	0.797	23.76	1.04		
25	9.86	1	9.86	1.3	1.44	12.39	1	12.04	31		
I=48	8.96	0.744			(4.75)	2.5	0.136				
	<32>	0.256	14.86	1.04		19.43	0.864	17.11	1.4	0.98	411
						1.46	0.075			(1.04)	
						6.79	0.144				
						30.52	0.781	24.52	1.21		
50	8.62	1	8.62	1.24	1.65	12.04	1	12.04	25		
I=14.3	7.57	0.697			(15.94)	2.31	0.139				
	<32>	0.303	14.97	1.11		18.58	0.861	16.32	1.54	1.02	420
						1.48	0.073			(1.02)	
						7.04	0.148				
						31.3	0.779	25.52	1.21		
75	7.11	1	7.11	1.37	2	11.9	1	11.9	26		
I=12.3	4.11	0.228			(18.54)	2.49	0.141				386

	8.22	0.772	7.29	1.12		18.63	0.859	16.35	1.6	1.02	
						1.4	0.064			(1.11)	
						6.82	0.154				
						33.67	0.782	27.46	1.14		
100	6.67	1	6.67	1.35	2.13	11.89	1	11.89	27		
I=6.6	2.18	0.131			(34.55)	2.5	0.142				
	7.19	0.869	6.53	1.03		18.7	0.858	16.4	1.51	1.02	
						1.37	0.067			(1.11)	387
						6.33	0.149				
						30.39	0.784	24.86	1.06		
250	4.38	1	4.38	3.77	3.25	11.36	1	1	28		
I=3.9	6.19	0.506			(58.46)	2.37	0.152				
	2.02	0.494	4.13	1.03		16.96	0.848	14.75	1.69	1.13	
						1.07	0.088			(1.35)	317
						5.14	0.153				
						23.05	0.759	18.37	1.09		

Condition: [coralyne] = 10 μ M, [c-di-AMP] = 40 μ M, Buffer: 50 mM Tris-H₃PO₄ (pH 7.5) at 25 °C. Lifetimes are single exponential.

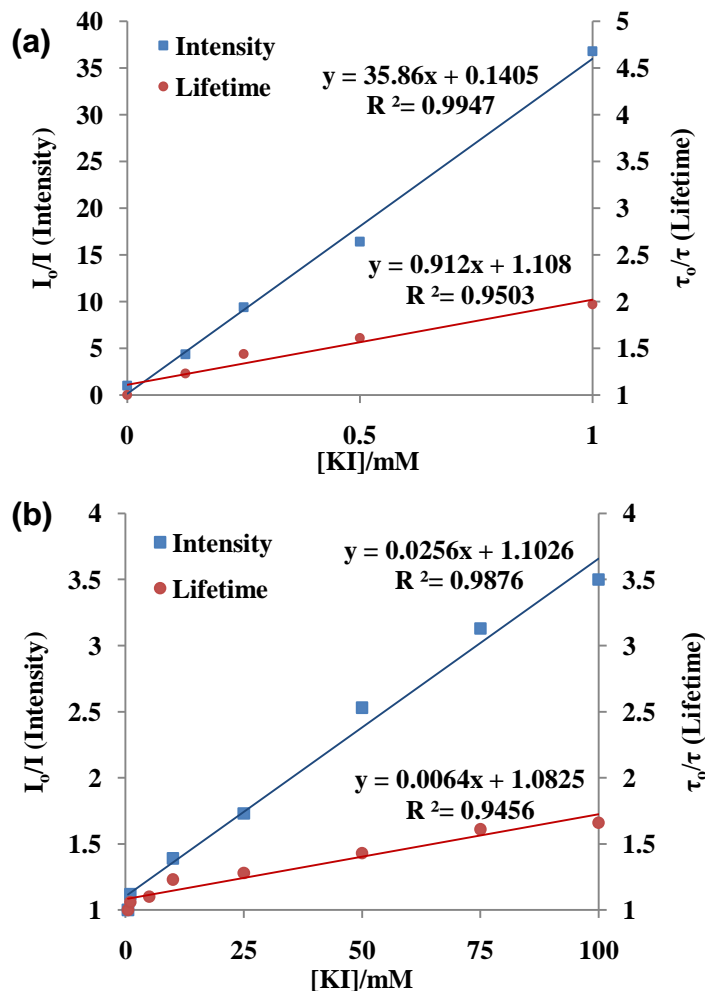


Figure 4.6 KI quenching of Coralyne fluorescence in absence (a) and presence of $40 \mu M$ c-d-AMP (b) at $25^\circ C$. Buffer: $50 mM$ Tris- H_3PO_4 (pH 7.5)

4.1.3 The complex formation between coralyne and c-di-AMP

At higher temperature ($60^\circ C$), c-di-AMP did not “protect” coralyne from fluorescence quenching by bromide or iodide and the value of I_0/I was ~ 1 (see **Figures 4.7** and **4.8**). This observation suggests that coralyne forms a supramolecular inclusion complex with c-di-AMP but at higher temperatures, the complex is not stable and

hence coralyne would no longer be protected from halide quenching at high temperatures.

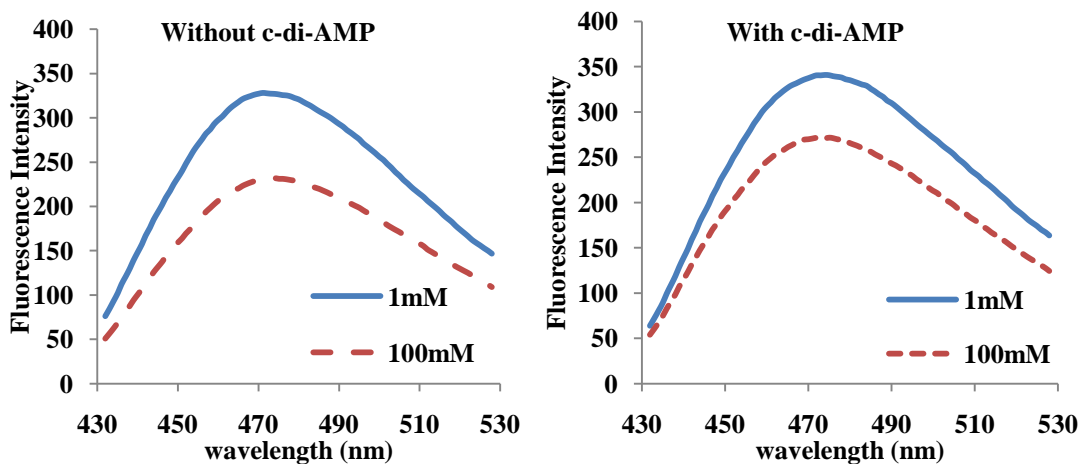


Figure 4.7 KI quenching in the absence of c-di-AMP or in the presence of c-di-AMP at 60 °C. Condition: [coralyne] = 10 μ M, [c-di-AMP] = 0 or 40 μ M, Buffer: 50 mM Tris-H₃PO₄ (pH 7.5) containing KI = 1 or 100 mM. ex. 420 nm, em. 475 nm.

In contrast to the data at 10 °C (**Figure 4.8**), where c-di-AMP “protected” coralyne from quenching, at 60 °C, KI can quench the fluorescence of coralyne even in the presence of c-di-AMP. This is consistent with a model whereby coralyne forms a complex with c-di-AMP to become “protected” from quenching but at higher temperature, the complex would collapse and hence the protection from quenching will be minimal.

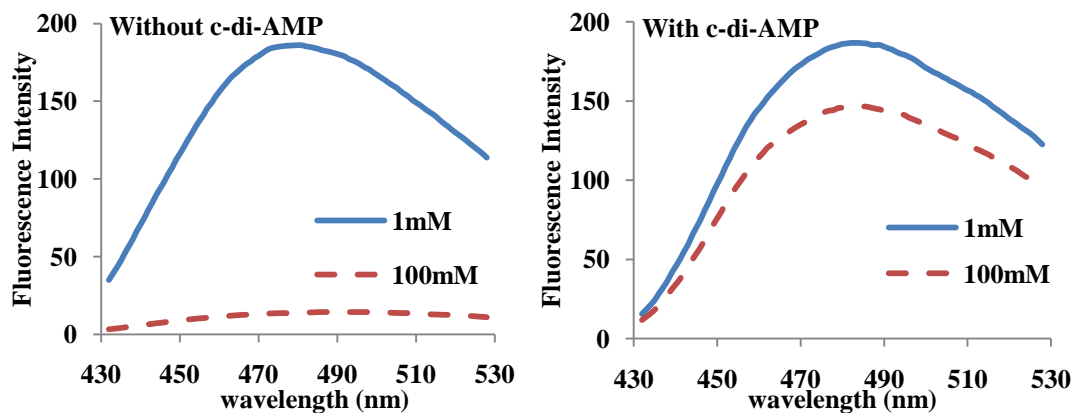


Figure 4.8 KI quenching in the absence of c-di-AMP or in the presence of c-di-AMP at 10 °C. Condition: [coralyne] = 10 μ M, [c-di-AMP] = 0 or 40 μ M, Buffer: 50 mM Tris-H₃PO₄ (pH 7.5) containing KI = 1 or 100 mM. ex. 420 nm, em. 475 nm.

C-di-AMP could be detected with coralyne at both acidic and basic pH (see **Figure 4.9**), although the fold fluorescence increase at basic pH 9.2 (22.4), was slightly better than at pH 7.5 or 4.5 (13 and 14.5 respectively). Having established that the inclusion of a bromide quencher and conducting the c-di-AMP detection assay at pH 9.2 was optimal for sensitive detection, we proceeded to investigate if c-di-AMP concentrations lower than 40 μ M could be detected with our new system. Pleasing lower concentrations of c-di-AMP (down to 5 μ M) could be detected using our system, see **Figure 4.10**. This simple fluorescent detection system could therefore be suitable for determining the enzymatic proficiencies of c-di-AMP synthases or phosphodiesterases, *vide infra*.

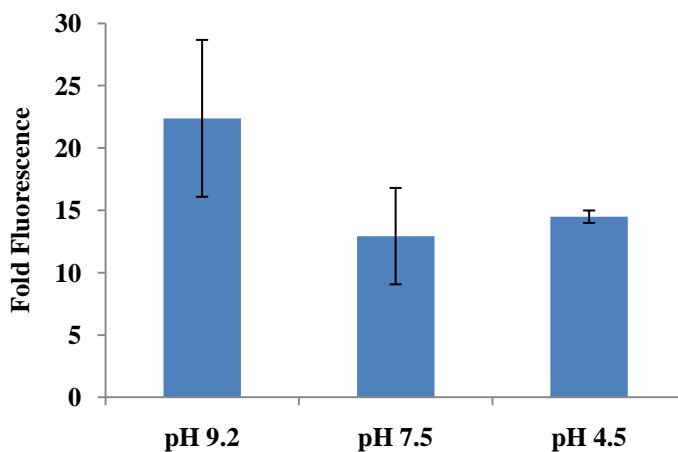


Figure 4.9 Fold fluorescence profiles of coralyne in the presence of c-di-AMP at different pHs. Condition: [coralyne] = 10 μM , [c-di-AMP] = 40 μM , Buffer: 50 mM Tris- H_3PO_4 (pH 4.5, 7.5 or 9.2), containing 250 mM KBr. Temperature = 10 $^\circ\text{C}$. ex. 420 nm, em. 475 nm.

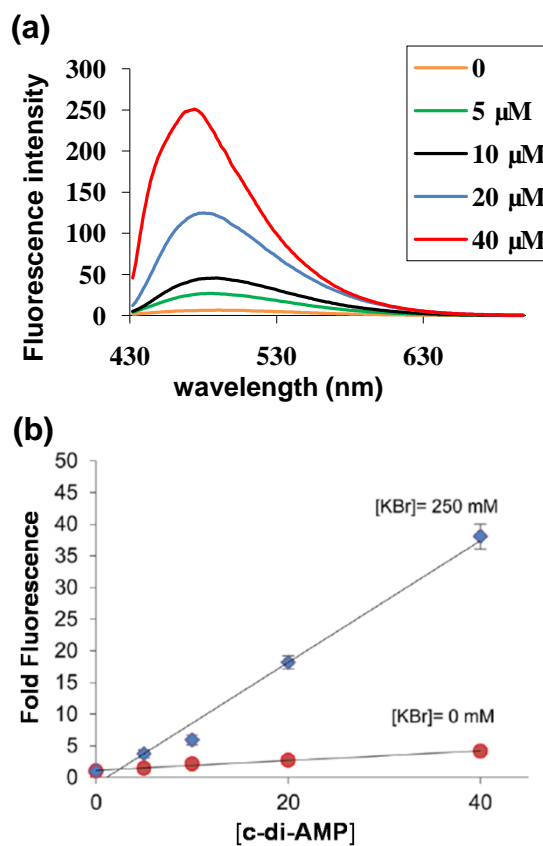


Figure 4.10 The fluorescence of coralyne is proportional to the concentration of c-di-AMP. Condition: [coralyne] = 10 μM , [c-di-AMP] = 0, 5 μM , 10 μM , 20 μM and 40

μM , Buffer: 50 mM Tris- H_3PO_4 (pH 9.2) containing 250 mM KBr, showing c-di-AMP concentration dependence on fluorescence enhancement. Temperature = 10 °C. ex. 420 nm, em. 475 nm. Measurements were done in triplicate.

Circular dichroism (CD) is an excellent tool to study structural perturbations that result from the association of a chiral molecule with another molecule. The CD spectrum of c-di-AMP in the absence of coralyne is different from in the presence of coralyne (**Figure 4.11**). Upon the addition of coralyne to c-di-AMP, both the negative and positive CD bands of c-di-AMP increase, indicating that both the helicity and π - π stacking interactions in c-di-AMP changes upon the addition of coralyne. An increase in the CD band is indicative of increased π - π stacking (presumably due to coralyne-adenine π - π stacking). For pApA, however, there is no difference between the presence and absence of coralyne (see **Figures 4.11** and **4.12**). This CD data augments the UV and fluorescence data, which suggested that coralyne associates with c-di-AMP but not with pApA (refer to **Figure 4.2**). Whereas the inability of pApA to form a complex with coralyne, at the tested micromolar concentrations, was in line with earlier studies by Hud et al.⁵⁶ the complex formation between the cyclic dinucleotide, c-di-AMP, and coralyne was unexpected. To gain some insights into the stoichiometry of the c-di-AMP/coralyne complex, we performed a Job plot analysis (**Figures 4.13** and **4.14**). This analysis revealed that c-di-AMP forms a higher order complex with coralyne (not the expected 2:1 complex that would have been predicted from the polyadenine-coralyne model).

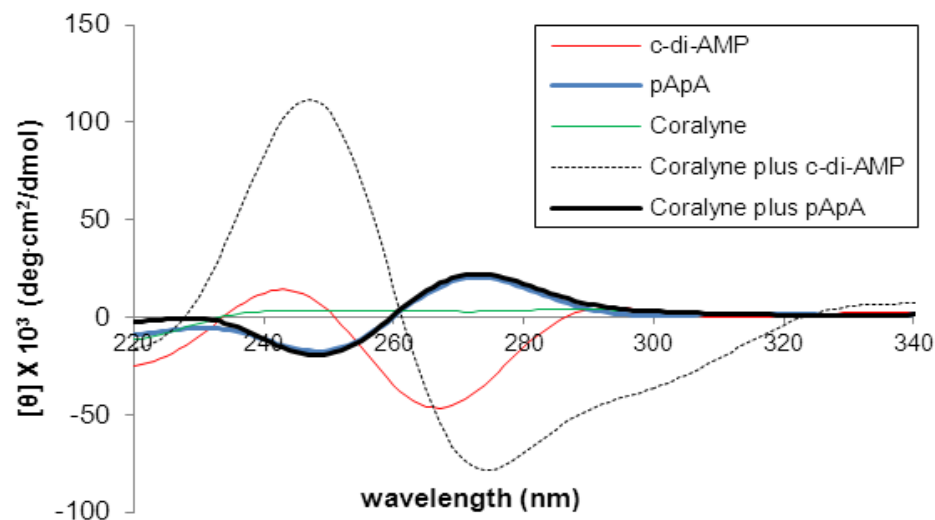


Figure 4.11 CD of coralyne-c-di-AMP or pApA complex. Condition: [coralyne] = 10 μ M, [c-di-AMP] = 40 μ M, Buffer: 50 mM Tris- H_3PO_4 (pH 7.5) containing 250 mM KBr. Coralyne plus c-di-AMP or pApA indicates coralyne incubated with c-di-AMP or pApA with incubation conditions listed in experimental section.

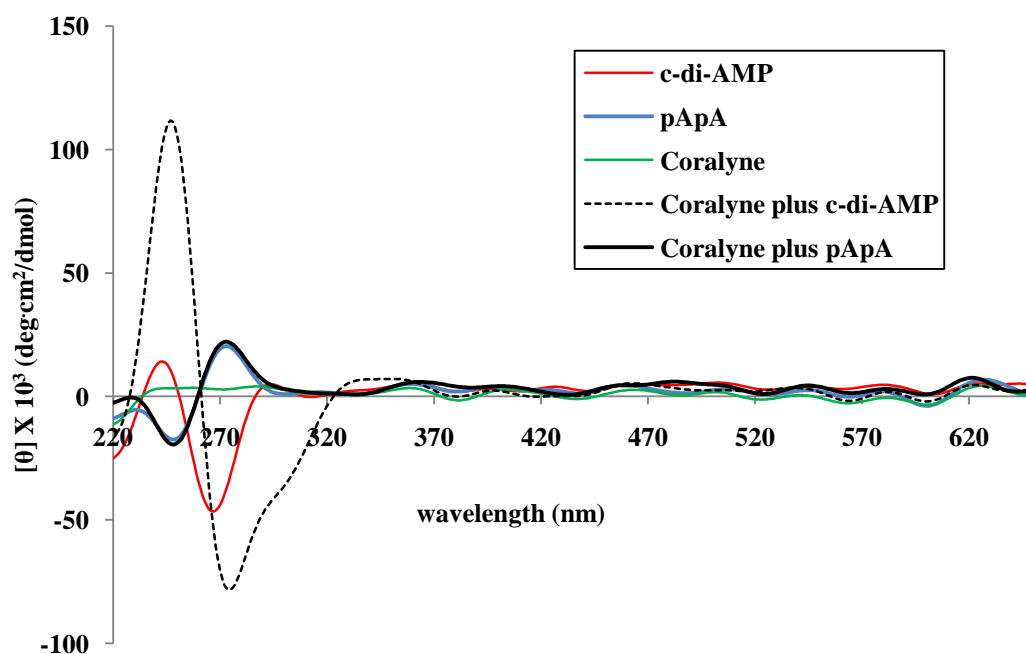


Figure 4.12 CD of coralyne-c-di-AMP or pApA complex (220-700 nm). Condition: [coralyne] = 10 μ M, [c-di-AMP] = 40 μ M, Buffer: 50 mM Tris- H_3PO_4 (pH 7.5) containing 250 mM KBr. Temperature = 10 $^\circ\text{C}$.

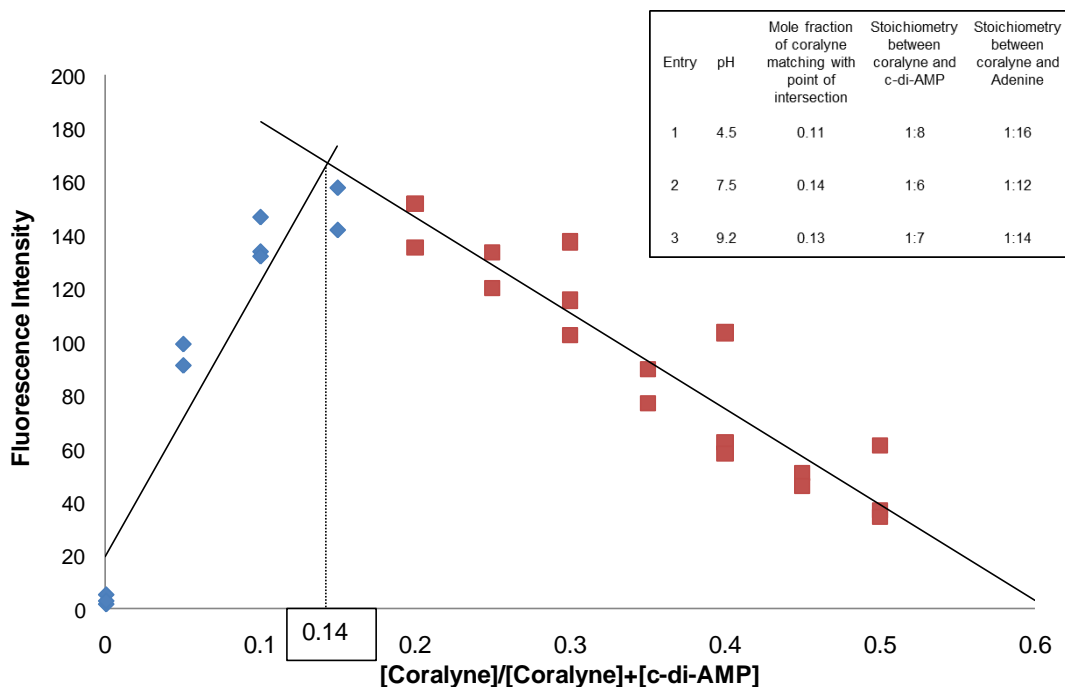
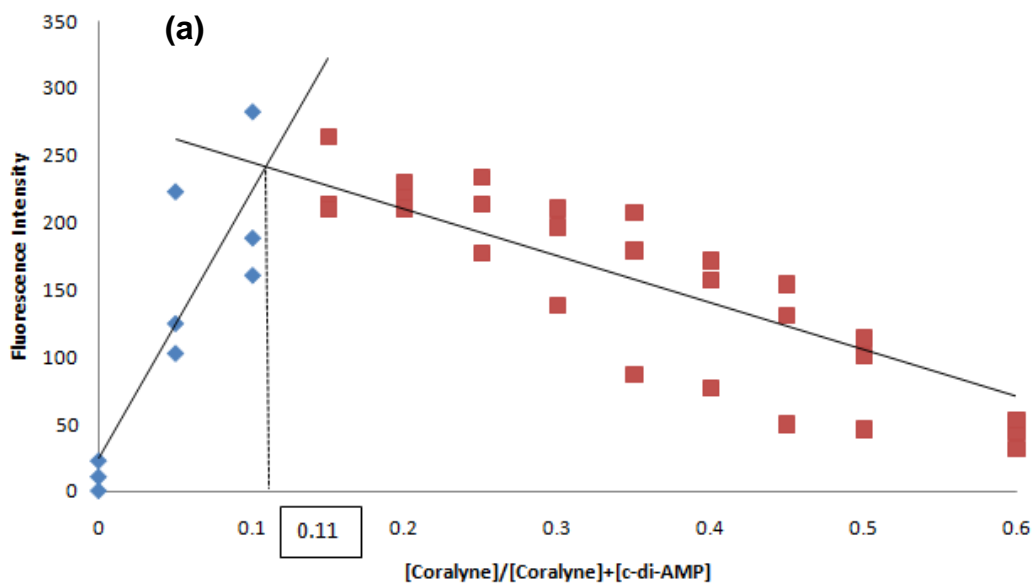


Figure 4.13 Job plot of coralyne and c-di-AMP interaction. $[coralyne] + [c-di-AMP]$ was fixed at 50 μM . The experiment was done in triplicate and plotted together on the graphs. Buffer: 50 mM Tris- H_3PO_4 (pH 7.5) containing 250 mM KBr. Temperature = 10 $^\circ\text{C}$. ex. 420 nm, em. 475 nm.



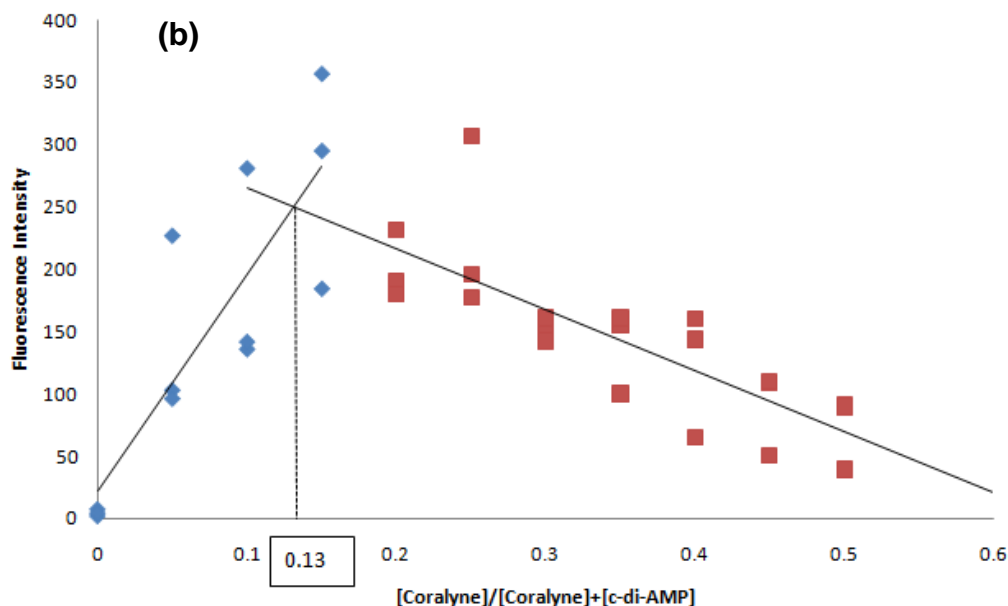


Figure 4.14 Job plot. [coralyne] + [c-di-AMP] was fixed at 50 μ M. The experiment was done in triplicate and plotted together on the graphs. Buffer: 50 mM Tris- H_3PO_4 (pH 4.5, **Figure 4.14a** or pH 9.2, **Figure 4.14b**) containing 250 mM KBr. Temperature = 10 $^{\circ}$ C. ex. 420 nm, em. 475 nm.

To corroborate the Job plot data, which indicated that c-di-AMP forms higher order supramolecular aggregate in the presence of coralyne, we proceeded to conduct NMR titration experiment. The addition of only 0.1 equivalence of coralyne to c-di-AMP, in the presence of potassium cations (100 mM) resulted in the complete disappearance of the c-di-AMP 1H NMR peaks around 8.24, 7.98 and 6.01 ppm (see **Figure 4.15**). The complete disappearance of the proton NMR peaks is indicative of polymer formation. The complete disappearance of the c-di-AMP peaks in the proton NMR (**Figure 4.15**) when only 0.1 equivalence of coralyne was added cannot be explained by a 2:1 complex between c-di-AMP and coralyne; a 2:1 complex between c-di-AMP and coralyne would have expected molecular weight of 1676.34, which should be visible by NMR. Secondly the Job plot revealed a c-di-AMP:coralyne

stoichiometry that is or greater than 6:1. Adenine is known to form hydrogen bonds with itself or other nucleobases to form various higher order structures, including quartets⁶², pentads⁶³, hexads^{64,65}, heptad⁶⁶. Adenine tetrads, which usually contain four hydrogen bonds per tetrad, are not as stable as G-tetrads (which contain eight hydrogen bonds per tetrad). Could coralyne promote A-tetrad formation by c-di-AMP? It has been shown that the formation adenine tetrads could be facilitated if the A-tetrad could π -stack with a proximal G-quadruplex.⁶⁷ Analogously, it is plausible that aromatic ligands could be used to promote the formation of adenine higher order structures.

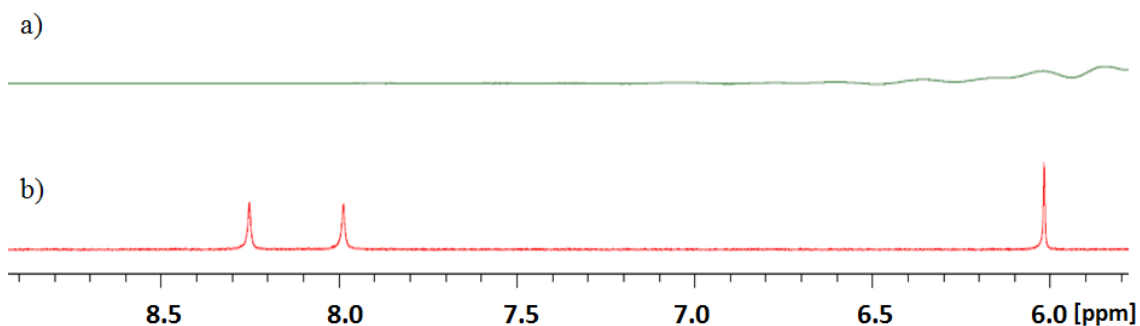


Figure 4.15 ¹H NMR spectra of c-di-AMP with (a) or without (b) coralyne. Addition of coralyne (0.1 equiv.) to c-di-AMP caused complete disappearance of the c-di-AMP peaks in the ¹H NMR spectrum (spectrum a). Condition: [coralyne] = 0 or 40 μ M, [c-di-AMP] = 400 μ M in D₂O containing 100 mM KBr. Temperature = 20 °C

4.1.4 The biological application of coralyne assay

Because c-di-AMP plays an important role in bacterial cell wall formation and susceptibility to antibiotics, which target cell wall formation, it is of interest to identify c-di-AMP synthases and phosphodiesterases in pathogenic bacteria, with the

ultimate goal that the inhibition of the synthases or phosphodiesterases could potentiate the activities of antibiotics, such as the β -lactams. We therefore investigated if coralyne could be used to assay the activities of c-di-AMP metabolism enzymes. It has been demonstrated that the PDE enzyme, YybT, is a c-di-AMP phosphodiesterase¹⁸ whereas DisA is a c-di-AMP synthase.⁸ We incubated YybT with c-di-AMP (40 μ M) and stopped the reaction at 1 min and 30 min. We then used our newly developed c-di-AMP detection assay to investigate the c-di-AMP cleavage reaction, **Figure 4.16b**. As a control, c-di-AMP (40 μ M) was also treated with snake venom phosphodiesterase and the cleavage reaction analyzed with our coralyne assay. Pleasingly, our assay revealed that under the reaction conditions, YybT (10 μ M) cleaved the majority of the c-di-AMP (40 μ M) within 1 min, see **Figure 4.16b**. Coralyne can also be used to monitor the synthesis of c-di-AMP from ATP by synthases, such as DisA, see **Figure 4.16a**.

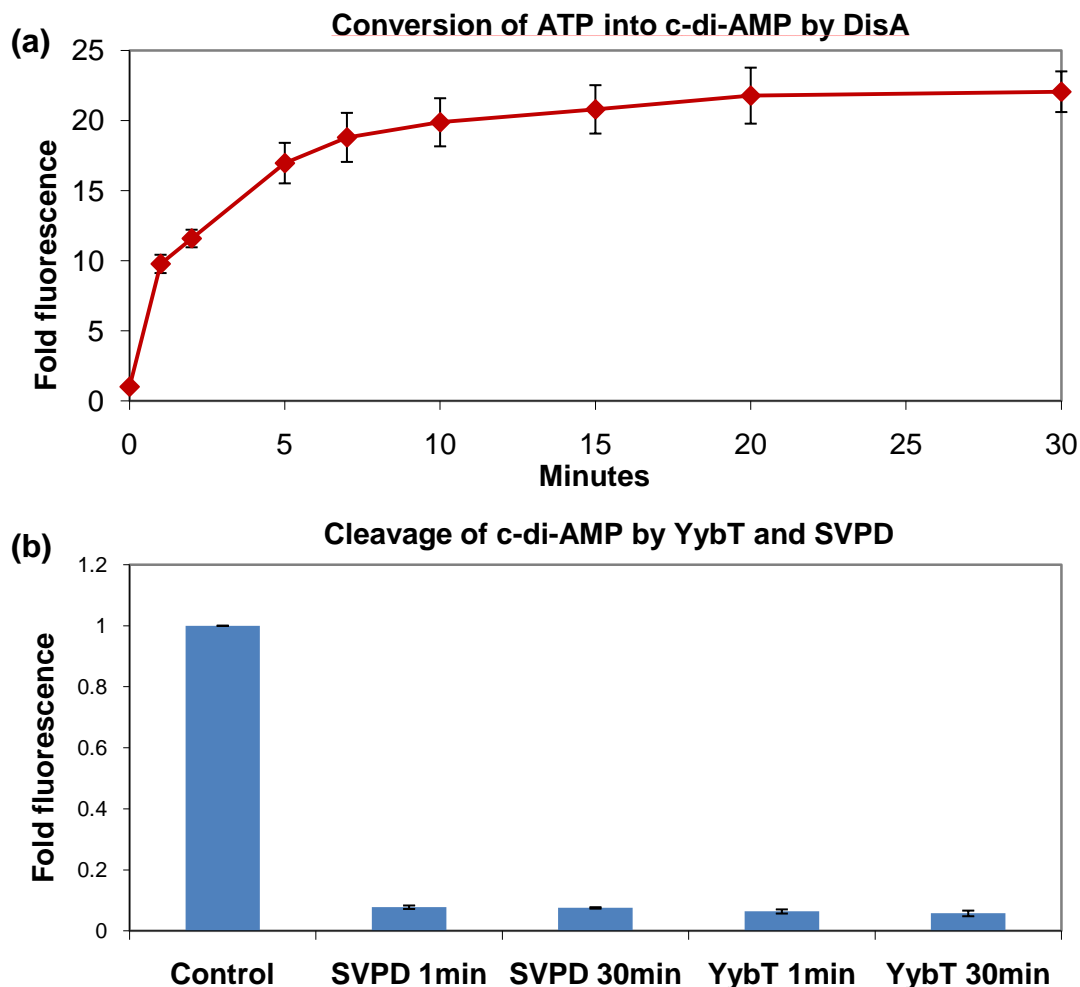


Figure 4.16 (a) Conversion of ATP into c-di-AMP by DisA. DisA (10 μM) was added to ATP (100 μM) in 200 mM Tris-HCl, pH 7.5, 100 mM NaCl and 10 mM MgCl_2 at 30 $^\circ\text{C}$. Reactions were stopped at 1 min, 2 min, 5 min, 7 min, 10 min, 15 min, 20 min and 30 min and incubated with conditions stated in the experimental part. The fluorescence was subsequently measured; (b) Cleavage of c-di-AMP by YybT and SVPD. YybT (10 μM) in 100 mM Tris-HCl, pH 8.3, 20 mM KCl, 500 μM MnCl_2 , 1 mM DTT or SVPD (1 mg/mL) in 50 mM Tris-HCl, pH 8.8 and 15 mM MgCl_2 were used to cleave c-di-AMP (100 μM) at 37 $^\circ\text{C}$. Reactions were stopped at 1 min and 30 min and incubated with conditions stated in the experimental part. Fluorescence measurements were taken after 1 min and 30 min.

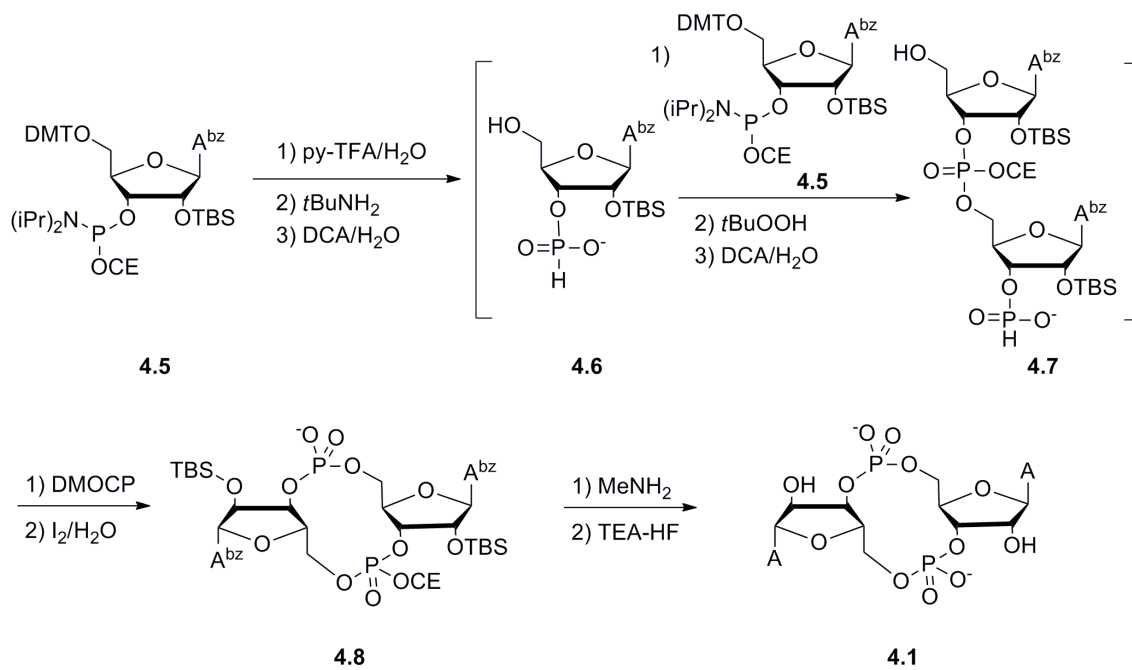
4.1.5 Conclusion

In our continuing efforts to investigate the interactions of heterocycles with bacterial dinucleotide second messengers we uncovered an unexpected interaction of coralyne with c-di-AMP but not the linear analog pApA, which also contains two rA. Although we have been unable to define the exact nature of the complex between coralyne and c-di-AMP, due to possible polymer formation, the optical properties of this supramolecular complex has facilitated the detection of c-di-AMP, which could be useful for c-di-AMP research. Nucleotide signaling has emerged as important in bacteria and regulates diverse bacterial phenotypes. Currently there are efforts to identify and characterize both synthase and phosphodiesterases of c-di-AMP and it is believed that c-di-AMP metabolism enzymes could become new drugable targets that could potentiate the effects of cell wall modifying antibiotics. Herein, we demonstrate an alternative non-radioactive assay to study the enzymatic proficiencies of c-di-AMP metabolism proteins (DAC and PDE). This simple fluorescent assay could also be adapted for a high-throughput screen for c-di-AMP phosphodiesterase inhibitors, which are expected to potentiate the killing effects of peptidoglycan inhibition drugs. This work also demonstrates that although at low micromolar concentrations, small nucleotides are not known to readily associate with heterocyclic intercalators (unlike polynucleotides), circularization of dinucleotides appear to enhance aggregate formation. Plausibly, the high entropic cost associated with bringing many small nucleotides together for complex formation, is reduced upon circularization because of reduction in degree of freedom. Circularization of oligonucleotides could be an

under-utilized strategy, which might improve oligonucleotide association kinetics or stability.

4.2 Synthesis of c-di-AMP

We chose to prepare c-di-AMP using a modified version of solution phase synthesis (Scheme 4.1) similarly to the synthesis of c-di-GMP.⁶⁸ Two portion of adenosine phosphoramidites (2 g) were used for the steps and reaction mixture was concentrated and then re-dissolved in water (5 mL), purified by HPLC (Merck Purosphser® STAR RP-18 column) with HPLC condition: 5-20% B, 0-16 min (A: 0.1 M TEAA in water; B: acetonitrile, pH 7.0), concentrated at a reduced pressure, and washed with acetone (2 mL × 5) to remove the excess of TEAA buffer.



Scheme 4.1 Synthesis scheme of c-di-AMP.

References and Notes

- 1 Kalia, D.; Merey, G.; Nakayama, S.; Zheng, Y.; Zhou, J.; Luo, Y.; Guo, M.; Roembke, B. T.; Sintim, H. O. *Chem. Soc. Rev.* **2013**, *42*, 305.
- 2 Gomelsky, M. *Mol. Microbiol.* **2011**, *79*, 562.
- 3 Zhou, J.; Sayre, D. A.; Zheng, Y.; Szmacinski, H.; Sintim, H. O. *Anal. Chem.* **2014**, *86*, 2412.
- 4 Römmling, U.; Gomelsky, M.; Galperin, M. Y. *Mol. Microbiol.* **2005**, *57*, 629.
- 5 Sondermann, H.; Shikuma, N. J.; Yildiz, F. H. *Curr. Opin. Microbiol.* **2012**, *15*, 140.
- 6 Ryan, R. P.; Fouhy, Y.; Lucey, J. F.; Dow, J. M. *J. Bacteriol.* **2006**, *188*, 8327.
- 7 Schirmer, T.; Jenal, U. *Nat. Rev. Microbiol.* **2009**, *7*, 724.
- 8 Witte, G.; Hartung, S.; Büttner, K.; Hopfner, K. P. *Mol. Cell.* **2008**, *30*, 167.
- 9 Romling, U. *Sci. Signal.* **2008**, *1*, pe39.
- 10 Bejerano-Sagie, M.; Oppenheimer-Shaanan, Y.; Berlatzky, I.; Rouvinski, A.; Meyerovich, M.; Ben-Yehuda, S. *Cell* **2006**, *125*, 679.
- 11 Corrigan, R. M.; Gründling, A. *Nat. Rev. Microbiol.* **2013**, *11*, 513.
- 12 Luo, Y.; Helmann, J. D. *Mol. Microbiol.* **2012**, *83*, 623.
- 13 Pozzi, C.; Waters, E. M.; Rudkin, J. K.; Schaeffer, C. R.; Lohan, A. J.; Tong, P.; Loftus, B. J.; Pier, G. B.; Fey, P. D.; Massey, R. C.; O'Gara, J. P. *PLoS Pathog.* **2012**, *8*, e1002626.
- 14 Griffiths, J. M.; O'Neill, A. J. *Antimicrob. Agents Chemother.* **2012**, *56*, 579.
- 15 Banerjee, R.; Gretes, M.; Harlem, C.; Basuino, L.; Chambers, H. F. *Antimicrob. Agents Chemother.* **2010**, *54*, 4900.
- 16 Witte, C. E.; Whiteley, A. T.; Burke, T. P.; Sauer, J. D.; Portnoy, D. A.; Woodward, J. J. *mBio* **2013**, *4*, e00282.
- 17 Corrigan, R. M.; Campeotto, I.; Jeganathan, T.; Roelofs, K. G.; Lee, V. T.; Gründling, A. *Proc. Natl. Acad. Sci. U. S. A.* **2013**, *110*, 9084.
- 18 Rao, F.; See, R. Y.; Zhang, D.; Toh, D. C.; Ji, Q.; Liang, Z. X. *J. Biol. Chem.* **2010**, *285*, 473.
- 19 Smith, W. M.; Pham, T. H.; Lei, L.; Dou, J.; Soomro, A. H.; Beatson, S. A.; Dykes, G. A.; Turner, M. S. *Appl. Environ. Microbiol.* **2012**, *78*, 7753.
- 20 Woodward, J. J.; Iavarone, A. T.; Portnoy, D. A. *Science* **2010**, *328*, 1703.
- 21 Barker, J. R.; Koestler, B. J.; Carpenter, V. K.; Burdette, D. L.; Waters, C. M.; Vance, R. E.; Valdivia, R. H. *mBio* **2013**, *4*, e00018.
- 22 Jin, L.; Hill, K. K.; Filak, H.; Mogan, J.; Knowles, H.; Zhang, B.; Perraud, A. L.; Cambier, J. C.; Lenz, L. L. *J. Immunol.* **2011**, *187*, 2595.
- 23 Joung, I. S.; Persil Cetinkol, O.; Hud, N. V.; Cheatham, T. E. *Nucleic Acids Res.* **2009**, *37*, 7715.
- 24 Song, G.; Ren, J. *Chem. Commun. (Camb)* **2010**, *46*, 7283.
- 25 Islam, M. M.; Chowdhury, S. R.; Kumar, G. S. *J. Phys. Chem. B* **2009**, *113*, 1210.
- 26 Wang, A. H.; Ughetto, G.; Quigley, G. J.; Rich, A. *Biochemistry* **1987**, *26*, 1152.

- 27 Kopka, M. L.; Yoon, C.; Goodsell, D.; Pjura, P.; Dickerson, R. E. *Proc. Natl. Acad. Sci. U. S. A.* **1985**, *82*, 1376.
- 28 Moraru-Allen, A. A.; Cassidy, S.; Asensio Alvarez, J. L.; Fox, K. R.; Brown, T.; Lane, A. N. *Nucleic Acids Res.* **1997**, *25*, 1890.
- 29 Polak, M.; Hud, N. V. *Nucleic Acids Res.* **2002**, *30*, 983.
- 30 Jain, S. S.; Polak, M.; Hud, N. V. *Nucleic Acids Res.* **2003**, *31*, 4608.
- 31 Biver, T.; Boggioni, A.; Garc á, B.; Leal, J. M.; Ruiz, R.; Secco, F.; Venturini, M. *Nucleic Acids Res.* **2010**, *38*, 1697.
- 32 Sandström, K.; W ä r m l ä n d e r, S.; Bergman, J.; Engqvist, R.; Leijon, M.; Gr ä s l u n d, A. *J. Mol. Recognit.* **2004**, *17*, 277.
- 33 Lee, J. S.; Latimer, L. J.; Hampel, K. J. *Biochemistry* **1993**, *32*, 5591.
- 34 Bhadra, K.; Kumar, G. S. *Biochim. Biophys. Acta.* **2011**, *1810*, 485.
- 35 Bertrand, H.; Granzhan, A.; Monchaud, D.; Saettel, N.; Guillot, R.; Clifford, S.; Gu é d i n, A.; Mergny, J. L.; Teulade-Fichou, M. P. *Chemistry* **2011**, *17*, 4529.
- 36 Monchaud, D.; Teulade-Fichou, M. P. *Org. Biomol. Chem.* **2008**, *6*, 627.
- 37 Alzeer, J.; Vummidi, B. R.; Roth, P. J.; Luedtke, N. W. *Angew. Chem. Int. Ed. Engl.* **2009**, *48*, 9362.
- 38 Luedtke, N. *Chimia* **2009**, *63*, 134.
- 39 Monchaud, D.; Granzhan, A.; Saettel, N.; Gu é d i n, A.; Mergny, J. L.; Teulade-Fichou, M. P. *J. Nucleic Acids* **2010**, *2010*.
- 40 Xing, F.; Song, G.; Ren, J.; Chaires, J. B.; Qu, X. *FEBS Lett.* **2005**, *579*, 5035.
- 41 Cetinkol, O. P.; Hud, N. V. *Nucleic Acids Res.* **2009**, *37*, 611.
- 42 Kumar, G. *J. Biosci.* **2012**, *37*, 539.
- 43 Topalian, S. L.; Kaneko, S.; Gonzales, M. I.; Bond, G. L.; Ward, Y.; Manley, J. L. *Mol. Cell Biol.* **2001**, *21*, 5614.
- 44 Topalian, S. L.; Gonzales, M. I.; Ward, Y.; Wang, X.; Wang, R. F. *Cancer Res.* **2002**, *62*, 5505.
- 45 Chaires, J.; Waring, M. *DNA Binders* **2005**, *253*, 33.
- 46 Wilson, W. D.; Gough, A. N.; Doyle, J. J.; Davidson, M. W. *J. Med. Chem.* **1976**, *19*, 1261.
- 47 Dower, K.; Kuperwasser, N.; Merrikh, H.; Rosbash, M. *RNA* **2004**, *10*, 1888.
- 48 Wickens, M.; Anderson, P.; Jackson, R. J. *Curr. Opin. Genet. Dev.* **1997**, *7*, 220.
- 49 Sukul, P.; Malik, S. *Soft Matter* **2011**, *7*, 4234.
- 50 Martins, S. B.; Rino, J.; Carvalho, T.; Carvalho, C.; Yoshida, M.; Klose, J. M.; de Almeida, S. F.; Carmo-Fonseca, M. *Nat. Struct. Mol. Biol.* **2011**, *18*, 1115.
- 51 Rask-Andersen, M.; Alm é n, M. S.; Schi ö t h, H. B. *Nat. Rev. Drug Discov.* **2011**, *10*, 579.
- 52 Das, A.; Suresh Kumar, G. *Mol. Biosyst.* **2012**, *8*, 1958.
- 53 Balatsos, N. A.; Havredaki, M.; Tsiapalis, C. M. *Int. J. Biol. Markers* **2000**, *15*, 171.
- 54 Xu, X.; Wang, J.; Yang, F.; Jiao, K.; Yang, X. *Small* **2009**, *5*, 2669.
- 55 Wang, Y.; Wang, J.; Yang, F.; Yang, X. *Anal. Chem.* **2012**, *84*, 924.

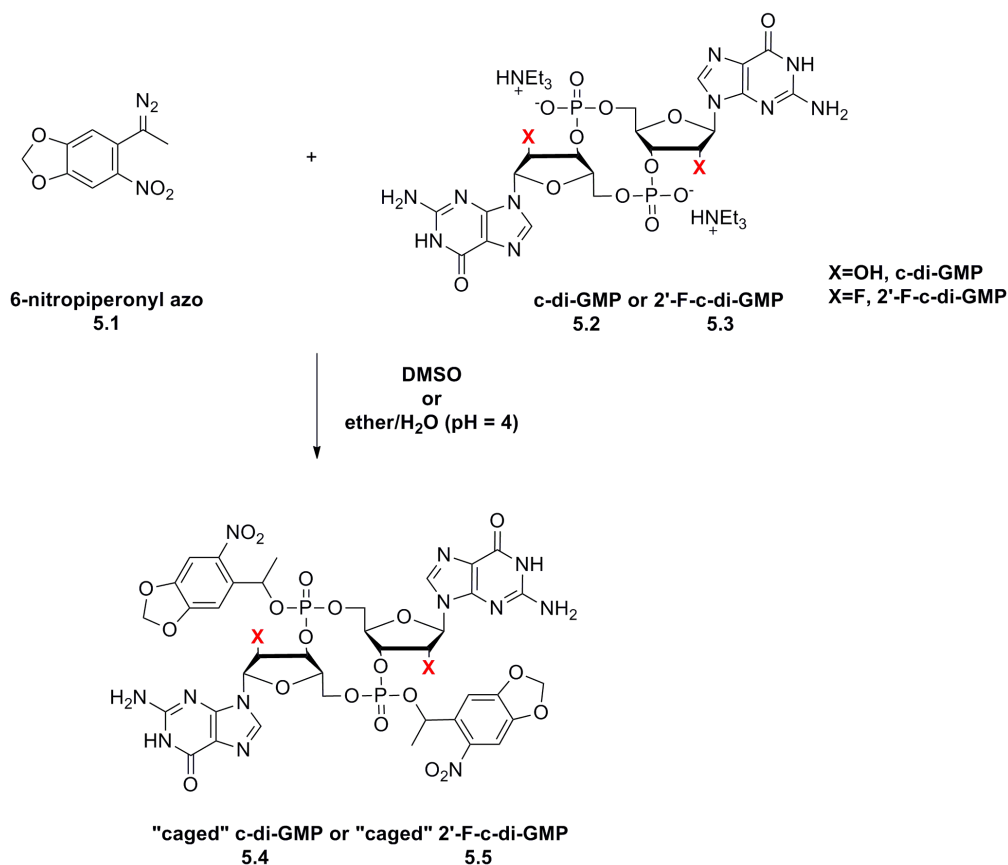
- 56 Persil, O.; Santai, C. T.; Jain, S. S.; Hud, N. V. *J. Am. Chem. Soc.* **2004**, *126*, 8644.
- 57 Buckley, R.; Enekwa, C. D.; Williams, L. D.; Hud, N. V. *ChemBioChem* **2011**, *12*, 2155.
- 58 Giri, P.; Kumar, G. S. *Mol. Biosyst.* **2008**, *4*, 341.
- 59 Islam, M.; Kumar, G. S. *Biochim. Biophys. Acta* **2009**, *1790*, 829.
- 60 Sinha, R.; Saha, I.; Kumar, G. *Chem. Biodiversity* **2011**, *8*, 1512.
- 61 Megyesi, M.; Biczák, L.; Görner, H. *Photochem. Photobiol. Sci.* **2009**, *8*, 556.
- 62 Patel, P. K.; Koti, A. S.; Hosur, R. V. *Nucleic Acids Res.* **1999**, *27*, 3836.
- 63 Zhang, N.; Gorin, A.; Majumdar, A.; Kettani, A.; Chernichenko, N.; Skripkin, E.; Patel, D. J. *J. Mol. Biol.* **2001**, *311*, 1063.
- 64 Liu, H.; Matsugami, A.; Katahira, M.; Uesugi, S. *J. Mol. Biol.* **2002**, *322*, 955.
- 65 Kettani, A.; Gorin, A.; Majumdar, A.; Hermann, T.; Skripkin, E.; Zhao, H.; Jones, R.; Patel, D. J. *J. Mol. Biol.* **2000**, *297*, 627.
- 66 Matsugami, A.; Ouhashi, K.; Kanagawa, M.; Liu, H.; Kanagawa, S.; Uesugi, S.; Katahira, M. *J. Mol. Biol.* **2001**, *313*, 255.
- 67 Pan, B.; Xiong, Y.; Shi, K.; Deng, J.; Sundaralingam, M. *Structure* **2003**, *11*, 815.
- 68 Gaffney, B. L.; Veliath, E.; Zhao, J.; Jones, R. A. *Org. Lett.* **2010**, *12*, 3269.

Chapter 5. Conclusion and Future Directions

With such overwhelming pieces of evidence to support the fact that increased intracellular concentrations of c-di-GMP lead to biofilm formation, one can safely assume that the disruption of c-di-GMP signaling would provide an effective means to disrupt biofilm and/or virulence factor formation in several bacteria of clinical relevance. C-di-GMP however achieves the regulation of bacterial phenotype via binding to several effector molecules including transcription factors, enzymes and riboswitches. Some of these c-di-GMP receptors have opposing effects. For example, whereas inhibiting a DGC would likely lead to biofilm reduction, inhibiting a PDE would increase biofilm formation. Thus the selective inhibition of c-di-GMP receptor proteins becomes critical for effective biofilm control. Crystal structure analyses of c-di-GMP effector molecules, in complex with the ligand, reveal that various classes of c-di-GMP receptors recognize this dinucleotide using different sets of recognition elements. Therefore, it is plausible that different analogs of c-di-GMP could be used to selectively modulate a specific class of c-di-GMP binding receptors, and hence modulate the bacterial phenotype. In Chapter 2, I reported that we prepared various 2'-modified analogs of c-di-GMP and studied both polymorphisms of these analogs using DOSY NMR and the binding to several effector proteins, such as PilZ-containing proteins, DGC containing I-sites, and PDE. 2'-modification of c-di-GMP did not adversely affect the propensity to form higher aggregates, such as octameric forms, in the presence of potassium salts. Interestingly, we found that the selective binding to different classes of c-di-GMP binding proteins could be achieved with the 2'-modified analogs and that 2'-F analog of c-di-GMP could bind to the I-site of

DGCs better (four times) than the native dinucleotide, c-di-GMP, whereas c-di-GMP binds to PDEs better (10 times) than 2'-F-c-di-GMP. Since unmodified c-di-GMP can hardly penetrate the intact plasma membrane, it is imperative that any future efforts aimed at using c-di-GMP analogs for in vivo perturbation of nucleotide signaling uses cell permeable analogs of c-di-GMP.

Several strategies to make cell-permeable analogs of c-di-GMP could be envisioned and one, currently being pursued by a new member of the Sintim group, is to install a caging group, 6-nitropiperonyl diazo¹ on c-di-GMP (Scheme 5.1). The chemistry is based on the enhanced reactivity of diazomethyl group toward phosphates, compared to the other functional groups on the molecule.² Caged c-di-GMP could be uncaged with light.³ Photocaged c-di-GMP would be valuable for studies related to how global increase in intracellular c-di-GMP would affect bacterial physiology. Many of the c-di-GMP metabolism proteins, have additional domains that are involved in other protein-protein interactions so studies that use over-expression of these proteins to study the effects of increased c-di-GMP concentrations are plagued with secondary effects that are different to disentangle. Photocaged c-di-GMP analogs are however not viable drug candidates, especially ones that need near-UV light or even visible light for uncaging because of toxicity or tissue penetration problems respectively. An alternative strategy to make cell permeable analogs of c-di-GMP or related dinucleotides might include moieties on the phosphate group, which could be deprotected in vivo via enzymatic means. This strategy has been used extensively for other phosphate prodrugs, such as antiviral agents.^{4,5}



Scheme 5.1 Proposed “caging” strategy on c-di-GMP or 2'-F-c-di-GMP.

Beyond dinucleotide analogs, other small molecules could also be developed as inhibitors of dinucleotide signaling. The identification of a new lead compound for optimization is non-trivial and typically involves massive screening exercises, using large compound libraries with diverse collections. To facilitate the identification of c-di-GMP signaling inhibitors, previous members of the Sintim group developed innovative fluorescence-based assays that lend themselves to high-throughput screening, such as the thiazole orange assay for detecting c-di-GMP. During my PhD training, I also developed a surprisingly simple fluorescent assay for detecting c-di-AMP, using commercially available coralyne. With this assay fully developed, the

stage is now set to discover new inhibitors of bacterial nucleotide signaling pathways. New members of the Sintim group are now utilizing the TO and coralyne assays to discover non-nucleotide-based inhibitors of various c-di-GMP metabolism proteins. These inhibitors could become next-generation antibacterial agents.

References and Notes

- 1 Gardner, L.; Zou, Y.; Mara, A.; T.; , C. A.; Deiters, A. *Mol. BioSyst.* **2011**, *7*, 2554.
- 2 Bernal-Méndez, E.; Tora, C.; Sothier, I.; Kotera, M.; Troesch, A.; Laayoun, A. *Nucleosides Nucleotides Nucleic Acids* **2003**, *22*, 1647.
- 3 Shah, S.; Jain, P. K.; Kala, A.; Karunakaran, D.; Friedman, S. H. *Nucleic Acids Res.* **2009**, *37*, 4508.
- 4 Riggsbee, C. W.; Deiters, A. *Trends Biotechnol.* **2010**, *28*, 468.
- 5 Priestman, M.; Sun, L.; Lawrence, D. *ACS Chem. Biol.* **2011**, *6*, 377.

Chapter 6. Experimental Section

6.1 General procedure

6.1.1 General reaction conditions

Reactions were carried out in oven-dried glassware, stirred with teflon-coated magnetic stir bars and sealed with rubber septa under a positive pressure of anhydrous argon. High temperatures were obtained using silicone oil baths and monitored by a thermometer or under dry heating block with temperature controlled electronically. Organic solutions were all concentrated using a Büchi rotary evaporator. High boiling solvents (H₂O or DMF) were removed under high vacuum for 0.5–1.5 hours.

6.1.2 Preparation of dry solvents

Dry acetonitrile and pyridine were obtained from distillation over CaH₂ and dried overnight with drying kit containing molecular sieves (4Å) purchased from Chemgenes prior to use. Dry DMF was directly purchased from Sigma-Aldrich without further purification.

6.1.3 Reagents

Phosphoramidites and Beaucage Reagent were purchased from Chemgenes and/or Glen Research. 2'-OMe-c-di-GMP was purchased from Axxora. Columns used in HPLC as well as C18-coated silica-gel packing material were obtained from Nacalai[®]. Solvent used in HPLC were purchased from VWR and/or Fisher Scientific. Other reagents including intercalator coralyne were all purchased from Sigma-Aldrich unless indicated otherwise.

6.1.4 Instruments

HPLC was performed with a Varian 210 system equipped with a UV detector. Samples were all filtered by a 0.2 μm syringe filter (PTFE) prior to the injection.

NMR spectra were measured on Bruker AV-400, Bruker DRX-400, Bruker DRX-500 or Bruker AVIII-600. Data for ^1H -NMR spectra are reported as follows: chemical shift (ppm, relative to residual solvent peaks or indicated external standards; s = singlet, d = doublet, t = triplet, q = quartet, m = multiplet), coupling constant (Hz), and integration. Coupling constants were rounded to 0.5 Hz. 2D COSY experiments were carried out with Bruker AVANCE II at 600 MHz, 30 $^\circ\text{C}$. Pulse sequence used in ‘‘COSYGPMFPH’’ from Bruker TOPSPIN 2.1, double quantum filtered COSY. The size of matrix is 4096 by 320, with 52 scans on each serial file. The FID resolutions are 1.1 Hz and 13.9 Hz for F2 and F1 domains, respectively. Linear Prediction was used for F1 domain to 2K points. 2D DOSY experiments were carried out with Bruker AVANCE II at 600 MHz, 30 $^\circ\text{C}$. The concentration of the samples was 3 mM in D_2O (with or without K^+). After the addition of KCl, the samples were heated and then kept at 95 $^\circ\text{C}$ for 5 min, cooled down to room temperature, and stored at 4 $^\circ\text{C}$ for overnight before use. Shigemi NMR tubes (D_2O) were used for all experiments. DOSY was measured with the stimulated echo pulse sequence (Bruker pulse program `stebpgp1s19`) using bipolar gradient pulses and `watrgate 3-9-19` to suppress the solvent. Key acquisition parameters for the DOSY experiment include the big delta (Δ) at 0.09 s, the number of scans at 32, relaxation delay at 2.5 s, and the gradient strength was varied 32 times lineary from 5 to 95%. The gradient pulse length (small

delta δ) within the range of 1.4–1.8 ms was optimized under the experiment condition until the region of 6.0–9.0 ppm showed good decays for the major peaks. The data were processed with TopSpin 2.1 software with T_1/T_2 relaxation analysis. Exponential function was applied for the raw data and the curve-fitting of the decays was based on the area of the peaks. Shigemi NMR tubes (D_2O) were used for all experiments, in which 0.30 mL sample solution was applied.

Mass spectra (MS) were recorded by JEOL AccuTOF-CS (ESI positive and negative modes). High resolution mass spectra (HRMS) for ESI spectrometer were calibrated with an aqueous solution of PEG600.

UV absorbance spectra were obtained on a JASCO V-630 spectrophotometer with 1 cm path length cuvette. The concentration of a stock solution of c-di-GMP and analogs were determined by the measuring of absorbance at 253 nm using $28,600 \text{ M}^{-1}\text{cm}^{-1}$ as a molar extinction coefficient. The concentrations of c-di-AMP and analogs were determined by the measuring of absorbance at 259 nm using $27,000 \text{ M}^{-1}\text{cm}^{-1}$ as a molar extinction coefficient.

Fluorescence measurements were carried out on a Cary Eclipse fluorescence spectrophotometer, with λ_{ex} 420 nm (slit 5 nm) and λ_{em} 475 nm (slit 5 nm) chosen for coralyne.

Circular dichroism (CD) experiments were performed on a JASCO J-81 spectropolarimeter with 1 cm path length cuvette.

Fluorescence lifetime was measured using a time-domain system integrated with a fluorescence lifetime imaging microscope (FLIM) system Alba V (ISS, Urbana, IL). The system is equipped with a SPC-830 TCSPC module and pulsed laser system (Becker and Hickl GmbH). Laser BHL-445 nm and observation through band-pass filter 485/30 nm was used. Data analysis was performed using Vista Vision software v. 218 from ISS.

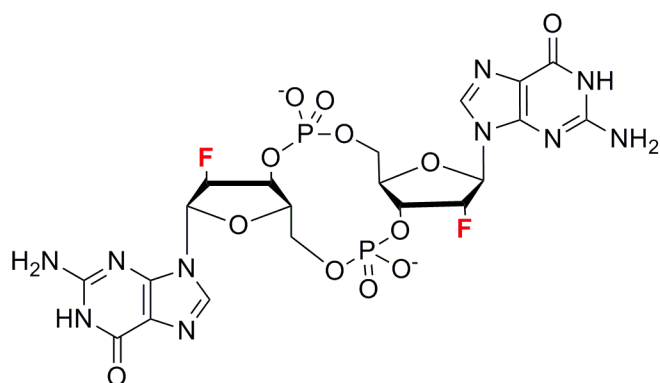
DNA/RNA synthesizer (ABI Applied Biosynthesis 392) was used for making dinucleotides. Sulfonyl-ODMT CPG (10 $\mu\text{mol/g}$) was prepared following literature.¹

6.2 Synthetic protocols for compounds in Chapter 2-4

6.2.1 Synthesis of 2'-modified c-di-GMP analogs in Chapter 2

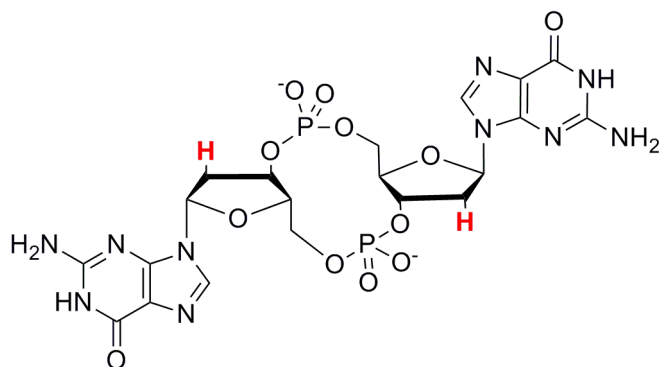
Synthesis of 2'-modified c-di-GMP is summarized in **Scheme 2.1**. Literature procedure² was used but with a slight modification. Two portion of guanosine phosphoramidites (2 g) were used for the steps up until intermediate **2.11** or **2.12** before the first purification was done. After mono-cyanoethyl protected **2.11** or **2.12** was obtained, the solvent was removed from the reaction mixture by high vacuum to yield a sticky yellow solid. This crude material was transferred to a centrifuge tube and was sequentially washed with EtOAc (50 mL \times 2), MeOH (50 mL \times 3) and centrifuged each time. The EtOAc layer was extracted with H₂O (25 mL \times 2), and the aqueous layer combined with the MeOH layer and was concentrated and subjected to HPLC purification (Nacalai tesque® 5C18-PAQ column). HPLC condition: 20-35% B, 0-20 min (A: 0.1 M TEAA in water; B: acetonitrile, pH 7.0). The product was identified by ESI-MS (negative mode), collected and immersed in ammonia (28 % NH₄OH in water, 15 mL) at 40 °C for overnight. The crude product was concentrated and then re-dissolved in water (5 mL), purified by HPLC (Nacalai tesque 5C18-PAQ column), HPLC condition: 1 \rightarrow 13% B, 0 \rightarrow 17 min (A: 0.1 M TEAA in water; B: acetonitrile, pH 7.0), concentrated at a reduced pressure, and washed with acetone (2 mL \times 5) to remove the excess of TEAA buffer. To extensively remove TEAA, the product was collected and washed with cation exchange resin, DOWEX®, Na⁺ form. 100 mg product of **2.2** and **2.3** were collected with estimated yield of 10%. 2'-F-c-di-GMP and 2'-H-c-di-GMP were firstly synthesized and characterized by Dr. Jingxin Wang as the TEA salt in his PhD dissertation.³ However, the counter anion of c-di-

GMP affects binding to biological receptors so I spent some time designing protocols to remove the TEA cation and replacing with sodium cation. The ^1H NMR spectrum for the c-di-GMP analogs with Na cation compounds were similar to that obtained by Dr. Wang,³ the only difference being that there were no peaks related to TEA. COSY and DOSY NMR were further used to determine the coupling constant between H_1' and H_2' presented in **Table 2.3** in Chapter 2.



2'-F-c-di-GMP
2.2

2'-F-c-di-GMP sodium salt (2.2) ^1H NMR (600 MHz, D_2O , water suppression) δ 8.31 (s, 2H), 6.56 (d, $J_{\text{H-F}}^3 = 19$ Hz, 2H), 5.85 (d, $J_{\text{H-F}}^1 = 51$, 2H), 5.32 – 5.28 (m, 2H), 4.43-4.40 (m, 2H).



2'-H-c-di-GMP
2.3

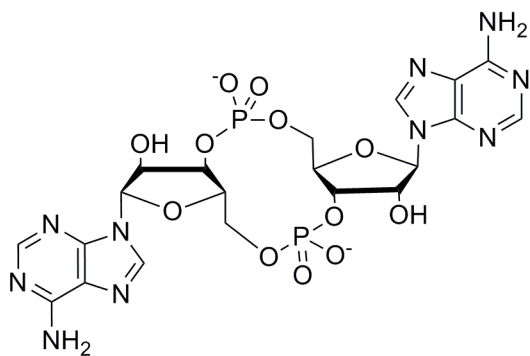
2'-H-c-di-GMP sodium salt (2.3) ^1H NMR (400 MHz, D_2O , water suppression, 60 °C) δ 8.36 (s, 2H), 6.62 (m, 2H), 5.39 (s, 2H), 4.58 (s, 2H), 4.46-4.40 (m, 4H), 3.28 (s, 2H), 3.07-3.04 (m, 2H).

6.2.2 Synthesis of endo-S-c-di-GMP analogs in Chapter 3

Synthesis of endo-S-c-di-GMP analogs (**3.3** to **3.5**) is summarized in **Scheme 3.1**. They were synthesized and characterized by Dr. Jingxin Wang and I together. The characterizations of endo-S-c-di-GMP analogs (**3.3** to **3.5**) can be found in Dr. Jingxin Wang's PhD dissertation.³ The DOSY NMR and binding studies with RNA riboswitch were performed by me.

6.2.3 Synthesis of c-di-AMP in Chapter 4

C-di-AMP was synthesized by adopting literature procedures with slight modifications.² Two portion of adenosine phosphoramidites (2 g) were used for the steps and reaction mixture was concentrated and then re-dissolved in water (5 mL), purified by HPLC (Merck Purospher® STAR RP-18 column) with HPLC condition: 5 \rightarrow 20% B, 0 \rightarrow 16 min (A: 0.1 M TEAA in water; B: acetonitrile, pH 7.0), concentrated at a reduced pressure, and washed with acetone (2 mL \times 5) to remove the excess of TEAA buffer.



c-di-AMP
4.1

C-di-AMP (4.1) $^1\text{H NMR}$ (600 MHz, D_2O , water suppression) δ 8.21 (s, 2H), 7.88 (s, 2H), 5.97 (s, 2H), 4.41 – 4.36 (m, 2H), 4.04-4.02 (m, 4H). $^{31}\text{P NMR}$ (202 MHz, D_2O) δ -0.8. ESI $^-$ /MS for $[\text{C}_{20}\text{H}_{23}\text{N}_{10}\text{O}_{12}\text{P}_2]^-$: calculated 657.0978, found 657.1017.

6.3 Computational data

All of the calculations were performed with the Gaussian 03/09 program.⁴

Calculations of the radii of 2'-modified c-di-GMP analogs (**2.2** and **2.3**) in their different aggregation states were reported in **Table 2.1** and **2.3** in Chapter 2.

Computed energy differences between “open” and “closed” forms of c-di-GMP (**3.1**) and endo-S-c-di-GMP analogs (**3.2** to **3.5**) were reported in **Table 3.1** in Chapter 3.

6.4 Biophysical data

6.4.1 Sample preparation for spectrometric and optical measurements in

Chapter 2

C-di-GMP or c-di-GMP analogs, water and 50 mM tris-HCl buffer solution (pH 7.5) containing 250 mM KCl were mixed, heated and kept at 95 °C for 5 min, cooled back to room temperature and then incubated in refrigerator for 12 h for spectrometric and optical measurements.

6.4.2 Sample preparation for spectrometric and optical measurements in

Chapter 3

C-di-GMP or analogs and DFHBI concentrations were determined via UV absorbance measurements (c-di-GMP at 253 nm and DFHBI at 405 nm) and 28,600 $M^{-1}cm^{-1}$ (c-di-GMP), 11,864 $M^{-1}cm^{-1}$ (DFHBI) were used as extinction coefficients to calculate concentrations. RNA in buffer solution was heated to 80 °C for 5 min and cooled down to room temperature in 15 min. Then $MgCl_2$ and c-di-GMP were added and the sample was kept for 12 h at room temperature. DFHBI was added to samples and fluorescence was monitored by excitation at 496 nm and emission at 501 nm.

6.4.3 Sample preparation for spectrometric and optical measurements in

Chapter 4

C-di-AMP or pApA, water, buffer solution (Tris-HCl or Tris- H_3PO_4), and metal solution (KCl, KBr or KI) were mixed, heated, kept at 95 °C for 5 min, and cooled back to room temperature, and coralyne was added. The samples were then incubated at 4 °C for 12 h. The concentration of c-di-AMP or pApA was determined by

measuring the absorbance at 259 nm using $27,000 \text{ M}^{-1}\text{cm}^{-1}$ as a molar extinction coefficient for both compounds. Fluorescence measurements and Circular dichroism (CD) experiments were carried out at 10 °C, with $\lambda_{\text{ex}} = 420 \text{ nm}$ (slit 5 nm) and $\lambda_{\text{em}} = 430\text{--}700 \text{ nm}$ (slit 5 nm). The concentration of c-di-AMP or pApA was 40 μM ; coralyne was 10 μM , and buffer was 50 mM Tris- H_3PO_4 (pH 4.5, 7.5, or 9.2) containing 250 mM KBr.

6.5 Biological data

6.5.1 Enzymatic Assay in Chapter 2

(Ms. Sarah Watt from the Lee group is acknowledged for contributing to the experimental section related to the assay to determine binding to DGC and PDE proteins).

Determination of half maximal inhibitory concentration (IC₅₀)

IC₅₀ for each compound was determined by adding 0.8 nM of the ³²P-c-di-GMP to 2 μL of unlabeled c-di-GMP analogs at varying concentrations. Compounds were tested at concentrations ranging from 200 μM to 0 μM made through 2-fold serial dilutions. The proteins Alg44 at 2.5 μM and WspR at 10 μM were added to each probe and competitor mixture in a buffer containing 10 mM Tris pH 8.0, 100 mM NaCl, and 5 mM MgCl₂. The protein RocR at 2.5 μM was added to each probe and competitor mixture in a buffer containing 10 mM Tris pH 8.0, 100 mM NaCl, and 5 mM CaCl₂ to prevent hydrolysis. These reactions were incubated for five minutes and then spotted on nitrocellulose paper.⁵ Once dry, these spots were exposed to a phosphorimager film for 10 minutes before being examined by a FLA7100 Fujifilm Life Science PhosphorImager and quantified using Fujifilm Multi Gauge software v3.0. The IC₅₀ was determined by the inhibitor vs. response equation in the Prism 5 software.

Inhibition of diguanylate cyclase activity

The activities of diguanylate cyclases WspR and PA1107 were monitored by thin layer chromatography as described.⁶ ^{32}P -GTP was added to a mixture of the inhibitor at the indicated concentration and 9 μM WspR in 10 mM Tris, pH 8.0, 100 mM NaCl and 5 mM MgCl_2 and incubated for 120 minutes at 30°C. One microliter of the mixture is spotted on cellulose thin layer plate and separated in a chamber with a buffer containing 1.5 volume of 1.5 M K_2HPO_4 and 1 volume of saturated $(\text{NH}_4)_2\text{SO}_4$. The polyethylenimine-modified (PEI) cellulose TLC plate was dried, exposed to phosphorimager screen, examined using FLA7100 Fujifilm Life Science PhosphorImager and quantified using Fujifilm Multi Gauge software v3.0.

Inhibition of phosphodiesterase activity

The activity of the phosphodiesterases RocR and PvrR were monitored by thin layer chromatography as described.⁶ ^{32}P -c-di-GMP was added to a mixture of the inhibitor at the indicated concentration and 4.5 μM RocR in 10 mM Tris, pH 8.0, 100 mM NaCl and 5 mM MgCl_2 and incubated for 120 minutes at 22 °C. One microliter of the mixture is spotted on cellulose thin layer plate and separated in a chamber with buffer containing 1.5 volume of 1.5 M K_2HPO_4 and 1 volume of saturated $(\text{NH}_4)_2\text{SO}_4$. The PEI cellulose TLC plate was dried, exposed to phosphorimager screen, examined using FLA7100 Fujifilm Life Science PhosphorImager and quantified using Fujifilm Multi Gauge software v3.0.

Effect of inhibitor on diguanylate cyclase activity

For the WspR diguanylate cyclase activity, mixtures of ^{32}P -GTP and the unlabeled GTP were used as the substrate and c-di-GMP or 2'-F-c-di-GMP was used as the inhibitor occupying the allosteric I-site. The activity of the WspR was monitored by thin layer chromatography as described above for one hour at 37°C. The initial rate of reaction (V_0) for each enzyme was determined by measuring the slope of the initial time points for each of the indicated substrate and inhibitor concentration. For each inhibitor concentration, the V_0 was plotted against the substrate concentration. The V_{max} and K_m reported in **Table 2.4** was calculated by non-linear regression analysis using Prism Graphpad software.

6.5.2 Enzymatic Assay in Chapter 4

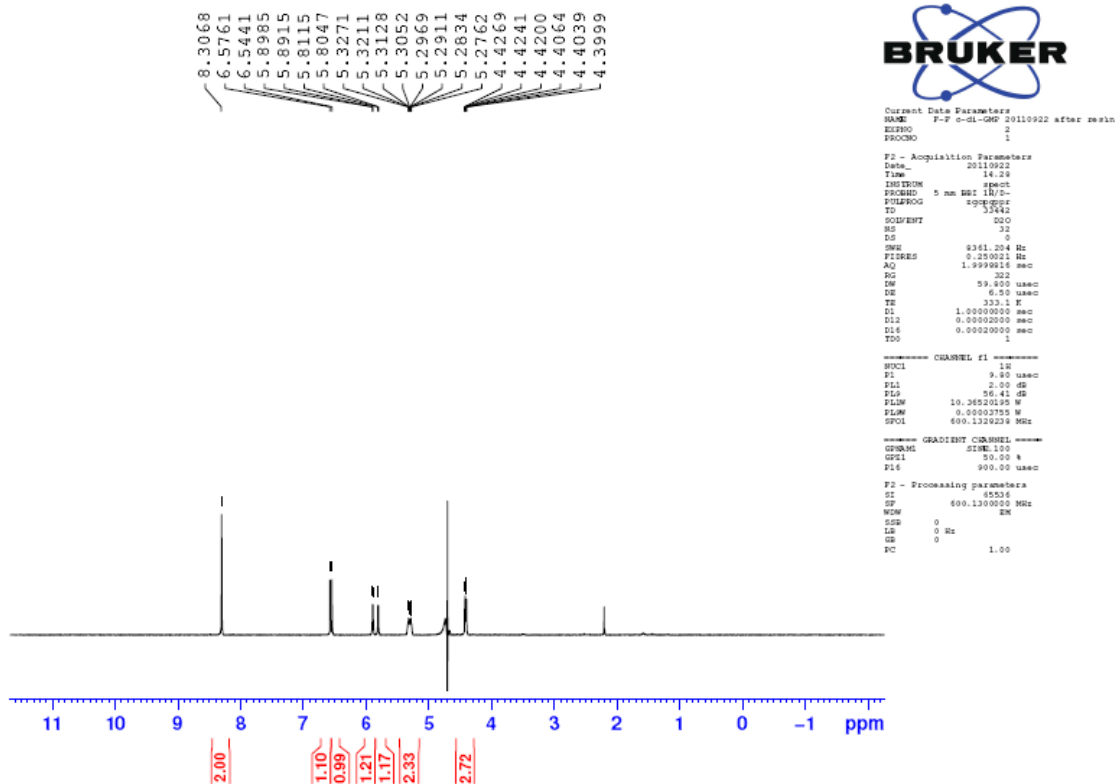
DisA and YybT were expressed in BL21(DE3) and purified by Nickel-affinity chromatography column (GE Healthcare). DisA was dialyzed into a 10 mM Tris-HCl, pH 8.0, and 100 mM NaCl solution, and YybT was dialyzed into a 50 mM Tris-HCl, pH 8.0, and 150 mM NaCl solution. Phosphodiesterase I from *Crotalus adamanteus* venom (snake venom phosphodiesterase, SVPD) was purchased from Sigma-Aldrich. For the c-di-AMP synthesis assay, DisA (10 μM) was added to 100 μM ATP in 40 mM Tris-HCl, pH 7.5, 100 mM NaCl, and 10 mM MgCl_2 at 30 °C. For the c-di-AMP cleavage assay, YybT (10 μM) in 100 mM Tris-HCl, pH 8.3, 20 mM KCl, 500 μM MnCl_2 , and 1 mM DTT17 or SVPD (1 mg/mL) in 50 mM Tris-HCl, pH 8.8, and 15 mM MgCl_2 was used to cleave c-di-AMP (100 μM) at 37 °C. Reactions were stopped by heating up to 95 °C for 5 min, and the precipitated proteins were removed by centrifugation. KBr and coralyne were added to the sample to give final

concentrations of 250 mM and 10 μ M for KBr and coralyne, respectively. The sample was incubated at 4 $^{\circ}$ C for 12 h.

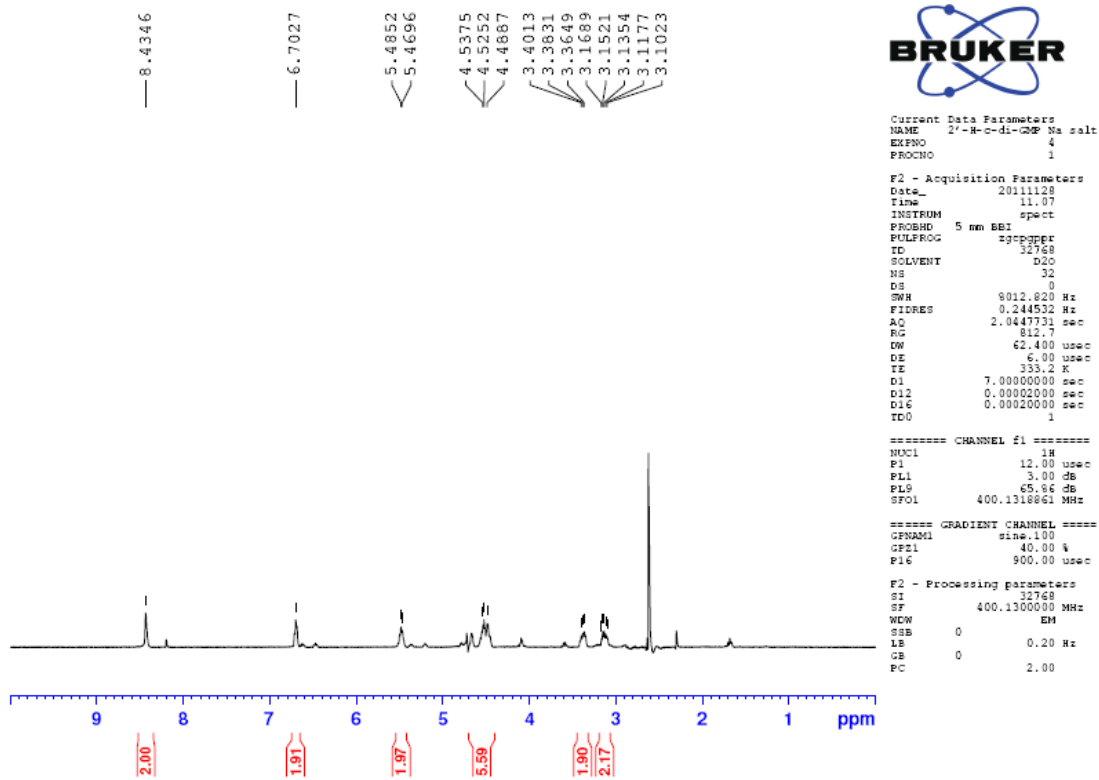
Appendices

^1H NMR of compounds 2.2 and 2.3 to show that the TEA cations were successfully removed.

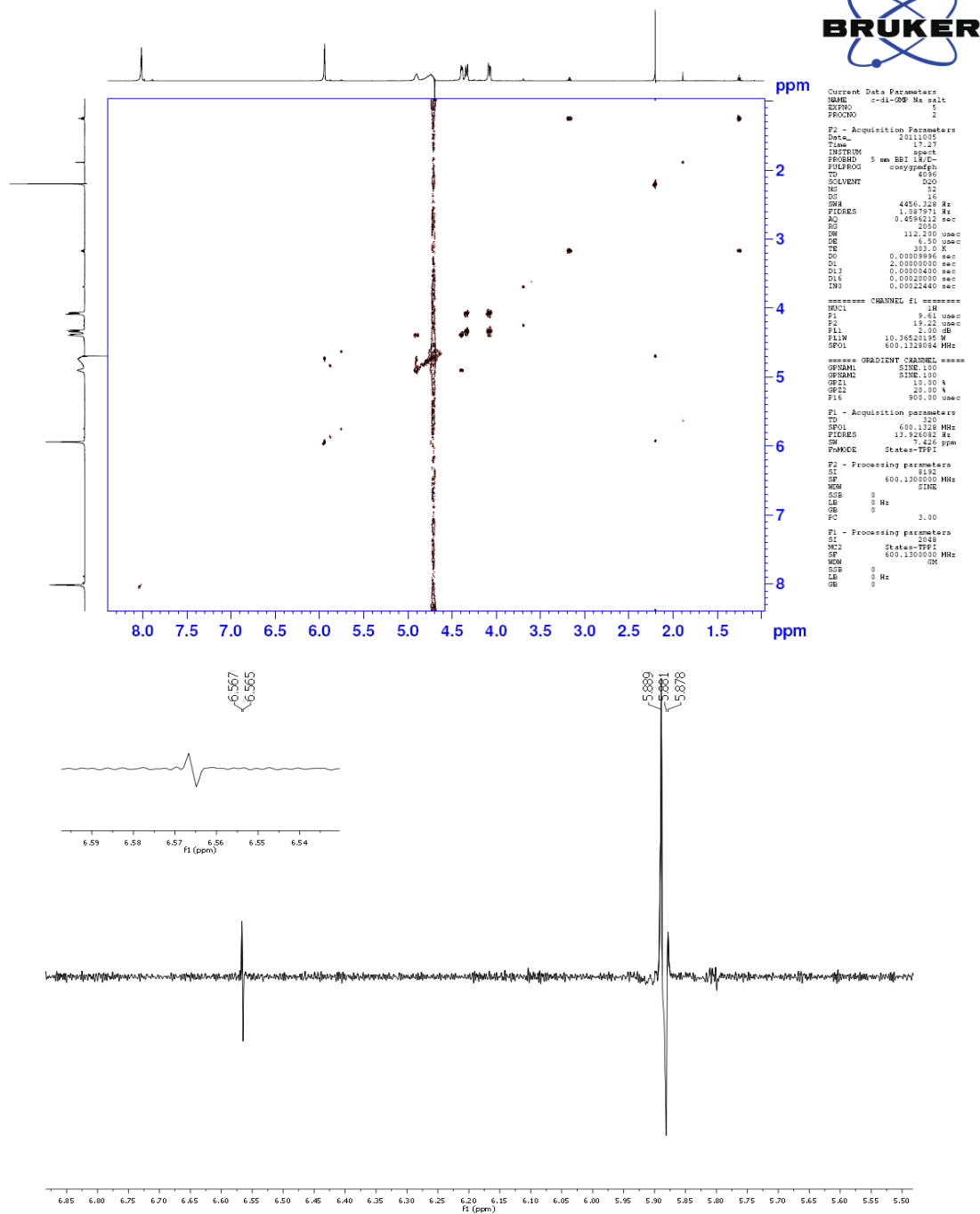
2'-F-c-di-GMP (2.2) in Na salt, ^1H NMR



2'-H-c-di-GMP (2.3) in Na salt, ¹H NMR

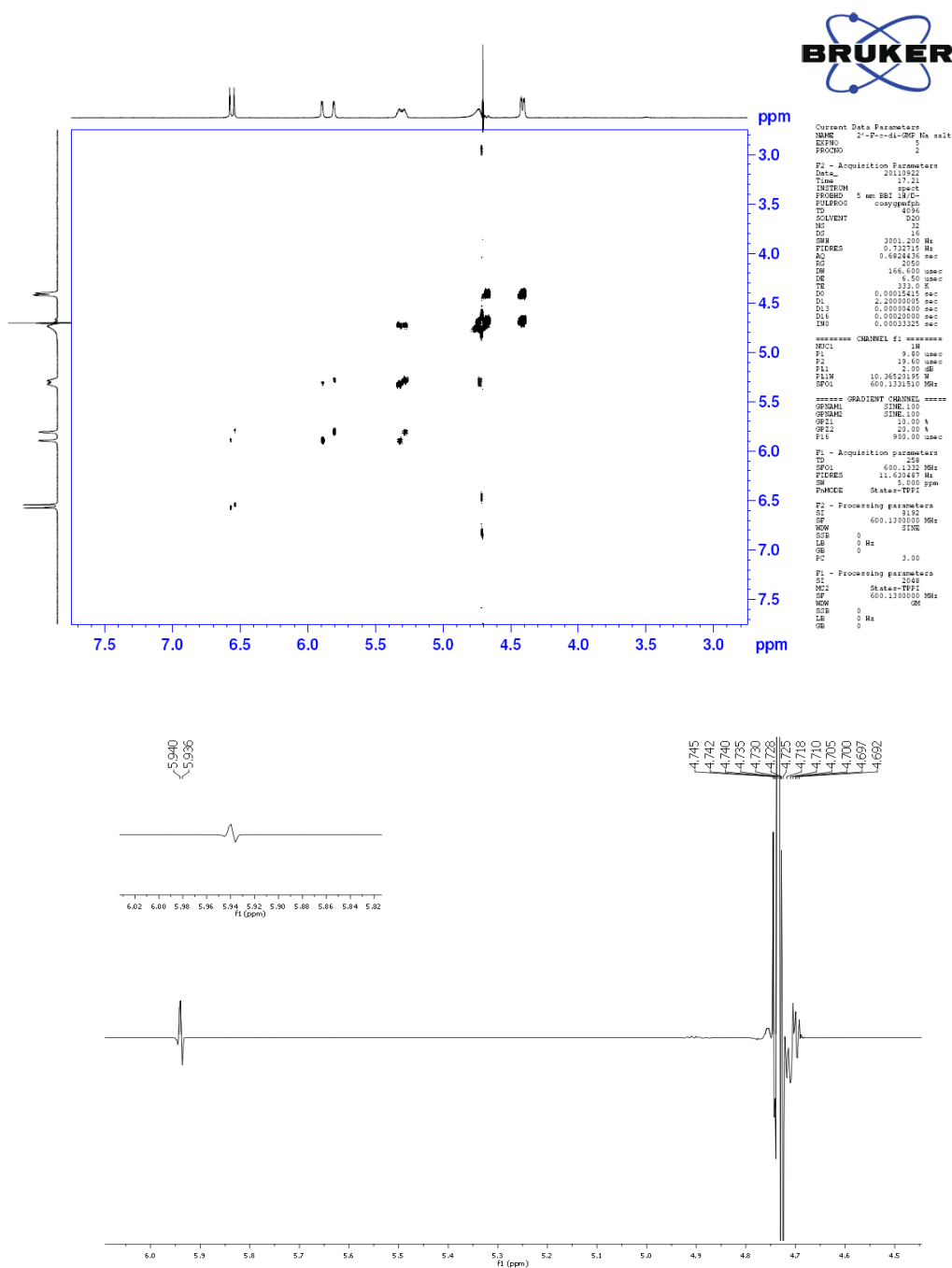


$J_{H1', H2'}$ coupling constants of c-di-GMP (2.1)



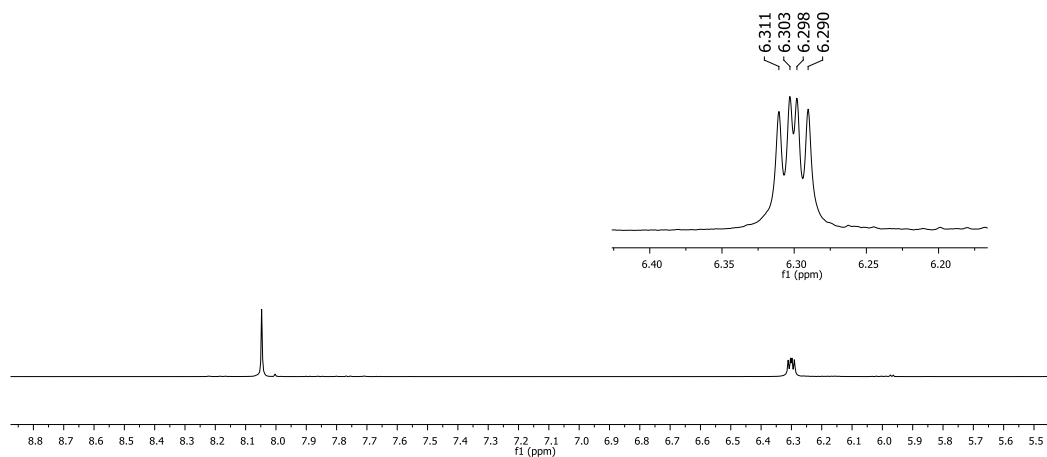
C-di-GMP (2.1), $J_{H1', H2'}$ coupling constant (~ 6.56 ppm) was extracted from COSY at 30 °C, Row 1009; the peaks (~ 5.89 ppm) are due to the auto-correlation of the peak itself. $J_{H1', H2'} = 2.2$ Hz

$J_{H1', H2'}$ coupling constants of 2'-F-c-di-GMP (2.2)



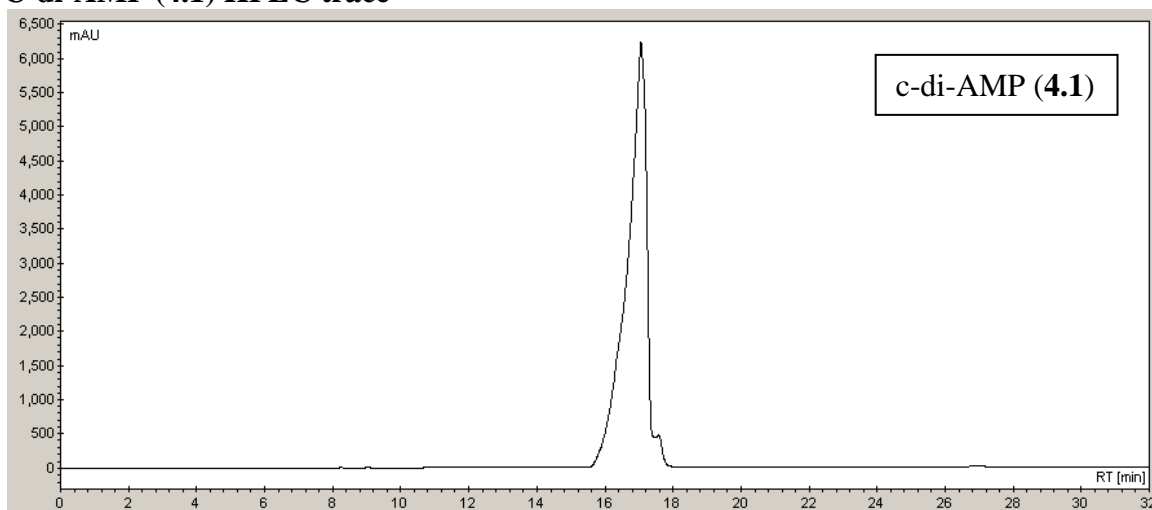
2'-F-c-di-GMP (2.2), $J_{H1', H2'}$ coupling constant (~5.94 ppm) was extracted from COSY at 30 °C, Row 768; the peaks (~4.70 ppm) are due to the auto-correlation of the peak itself. $J_{H1', H2'} = 1.1$ Hz

$J_{H1', H2'}$ coupling constants of 2'-H-c-di-GMP (2.3)



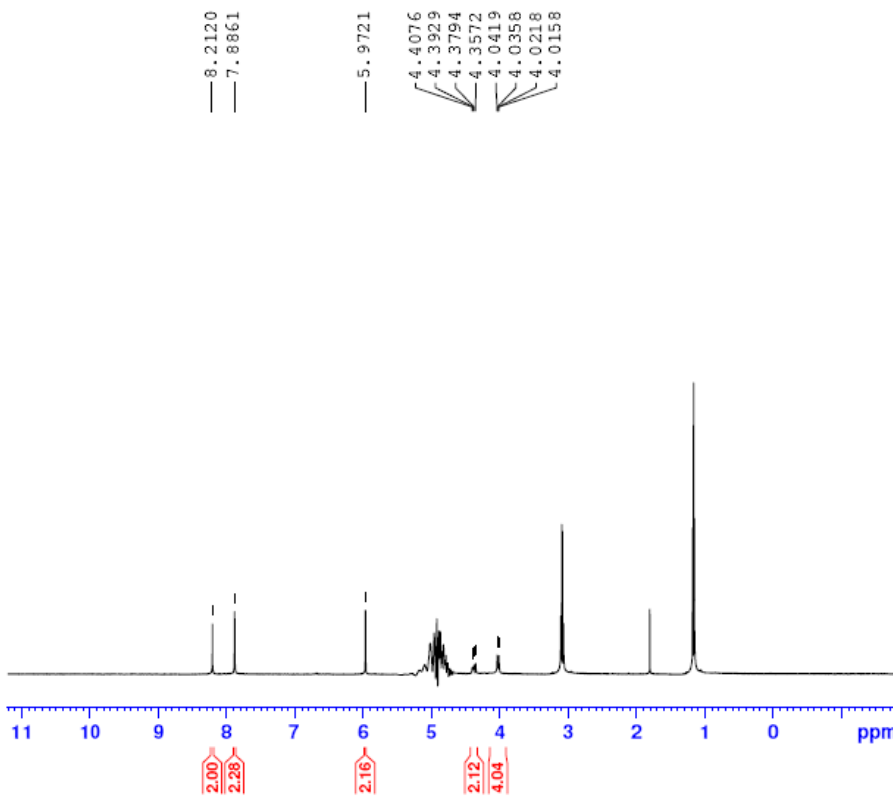
2'-H-c-di-GMP (2.3), $J_{H1', H2'}$ ($H2''$) coupling constant (~ 6.30 ppm) was extracted from DOSY at 30 °C. $J_{H1', H2'} = 4.7$ Hz and $J_{H1', H2''} = 7.5$ Hz

C-di-AMP (4.1) HPLC trace



HPLC condition: Merck Purospher® STAR RP-18 column (10 × 250 mm), eluting with 5 → 20% B at 0 → 16 min (A: 100 mM TEAA in water; B: acetonitrile, pH 7.0), rt with a UV detector.

C-di-AMP (4.1) ¹H NMR



Current Data Parameters
 NAME c-di-AMP TEAA salt
 EXPNO 2
 PROCNO 1

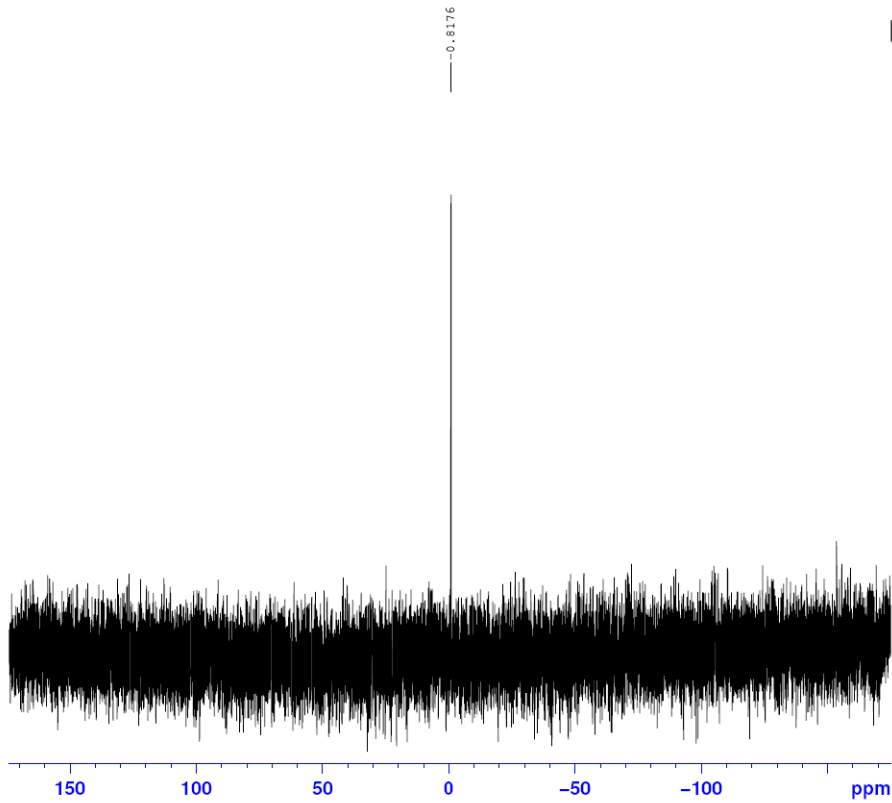
F2 - Acquisition Parameters
 Date_ 20130921
 Time_ 22.53
 INSTRUM spect
 PROCPRG 5 mm BB1 1H/D-
 PULPROG zgpg30
 ID 2768
 SOLVENT D2O
 NS 32
 DS 2
 SWH 7812.500 Hz
 FIDRES 0.238419 Hz
 AQ 2.0972021 sec
 RG 1820
 DW 64.000 usec
 DE 7.50 usec
 TE 293.8 K
 D1 2.0000000 sec
 D12 0.0002000 sec
 D16 0.0002000 sec
 TD0 1

===== CHANNEL f1 =====
 NUC1 1H
 P1 9.80 usec
 P2 19.60 usec
 F12 2000.00 usec
 FLO 120.00 dB
 FL1 2.00 dB
 PLOW 0 W
 PLLW 10.36520195 W
 SFO1 600.1328172 MHz
 SF1 62.18 dB
 SFOAL1 Sqa100.1000
 SFOAL1 0.500
 SFOFFS1 0 Hz

===== GRADIENT CHANNEL =====
 GPNAM1 SINE.100
 GPNAM2 SINE.100
 GPC1 31.00 %
 GPC2 11.00 %
 P16 900.00 usec

F2 - Processing parameters
 SI 65536
 SF 600.1300000 MHz
 WW EM
 SSB 0
 LB 0.50 Hz
 GB 0
 PC 1.00

C-di-AMP (4.1) ³¹P NMR



```
Current Data Parameters
NAME      c-di-AMP 31P NMR
EXPNO     10
PROCNO    1

F2 - Acquisition Parameters
Date_     20130425
Time      20.07
INSTRUM   spect
PROBHD    5 mm QNP 1H/1
PULPROG   zgpg30
TD         85536
SOLVENT   D2O
NS         1800
DS         4
SWH        56497.176 Hz
FIDRES     0.862078 Hz
AQ         0.5800436 sec
RG         16384
DW         8.850 usec
DE         6.00 usec
TE         297.3 K
D1         0.40000001 sec
D11        0.03000000 sec
TD0        1

===== CHANNEL f1 =====
NUC1       31P
P1         9.00 usec
PL1        0 dB
SFO1       161.8134700 MHz

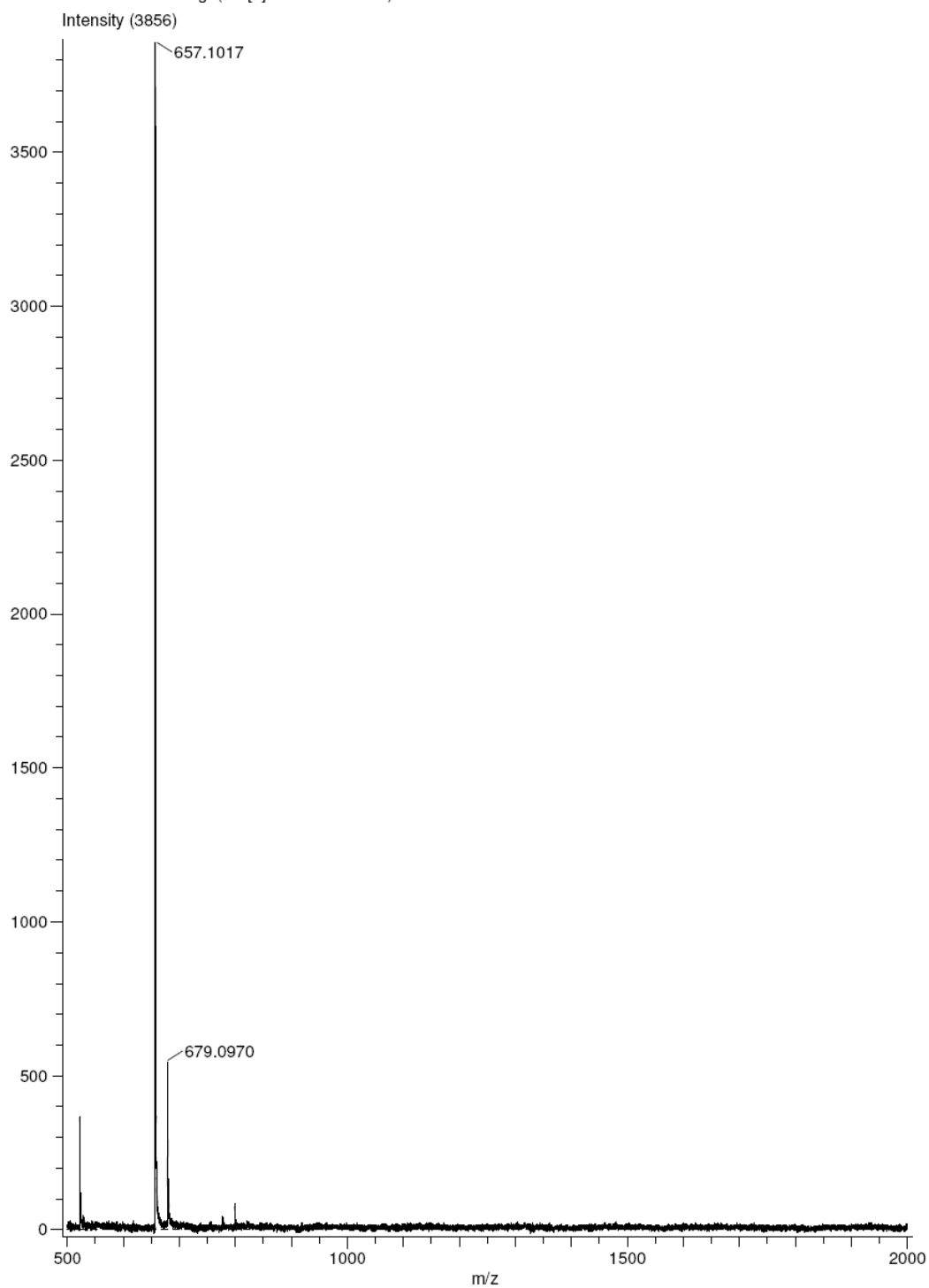
===== CHANNEL f2 =====
CPDPRG2   garp
NUC2       1H
PCPD2     96.00 usec
PL2        0 dB
PL12       18.00 dB
SFO2       399.7319986 MHz

F2 - Processing parameters
SI         85536
SF         161.8135483 MHz
WDW        EM
SSB        0
LB         2.00 Hz
GB         0
PC         1.40
```

C-di-AMP (4.1) mass spectra

Acq. Data Name: c-di-AMP
Creation Parameters: Average(MS[1] Time:1.18..1.24)

Experiment Date/Time: 6/20/2013 6:02:4...
Ionization Mode: ESI-



References and Notes

- 1 Urdea, M.; Horn, T. *Tetrahedron Lett.* **1986**, *27*, 2933.
- 2 Gaffney, B. L.; Veliath, E.; Zhao, J.; Jones, R. A. *Org. Lett.* **2010**, *12*, 3269.
- 3 Wang, J. PhD. Dissertation, University of Maryland, College Park, 2011.
- 4 Frisch, M. J.; et al. Gaussian 09, Revision A02 ed., Gaussian Inc., Wallingford, CT, 2009.
- 5 Roelofs, K. G.; Wang, J.; Sintim, H. O.; Lee, V. T. *Proc. Natl. Acad. Sci. U. S. A.* **2011**, *108*, 15528.
- 6 Wang, J.; Zhou, J.; Donaldson, G. P.; Nakayama, S.; Yan, L.; Lam, Y. F.; Lee, V. T.; Sintim, H. O. *J. Am. Chem. Soc.* **2011**, *133*, 9320.